TRANSIENTS IN SINGLE-PHASE INDUCTION MOTORS

A Study of the Transient Torque Characteristics of an Unloaded Single-phase Capacitor-start Induction Motor

by

A. Shanmugasundaram,
B.Sc., B.E., M.Sc.(Eng.), Graduate I.E.E.

Thesis presented for the degree of Doctor of Philosophy in Engineering of the University of Glasgow.

August, 1963.

CONTENTS

Figures are to be found at close of thesis.

SUMMARY

The thesis describes a study of the transient torque characteristics of an unloaded single-phase, capacitor-start induction motor. A review of published works on the study of transient torques in induction motors is made in Chapter 1. Though there have been attempts to calculate transient torque characteristics of single-phase induction motors for zero speed and constant speed conditions, there does not appear to have been any attempt at an experimental study of the problem. Experimental investigation avoids the limitations normally involved in theoretical calculations. A systematic experimental investigation necessitates the exercise of control over the point-on-wave of closing the supply to the motor and equipment to detect transient torques, under both free-rotor and blocked-rotor conditions. After an exhaustive survey of possible methods of detecting transient torques under these conditions (Appendix I), it was decided to use a d.c. excited, drag-cup, two-phase induction generator as an accelerometer in the former case and a stator reaction detecting scheme

using a precision load cell for the latter case. The calibration of the accelerometer is described in Appendix II and the design of the stator reaction detecting scheme in Appendix III.

The attempt to design and develop a p.-on-w. control and the actual one used are described in Chapter 2. The operational details and calibration of the p.-on-w. switch are also described in detail. It was found to be very important to have the accelerometer rigidly coupled to the shaft of the motor. For the stator reaction detecting scheme, it was necessary that the natural frequency of the stator suspension should be at least about 450 c/s. Results obtained simultaneously by the two detecting methods show satisfactory correspondence.

Chapter 3 deals with the investigation of transient torques with free rotor. The effect of point-on-wave of closing the supply voltage is studied in detail at a reduced terminal voltage of 140V. The results show that the initiation of the transient torques is governed by point-on-wave. The transient torques have a maximum near 0° point-on-wave

and are almost completely absent for 90°. Speed effects are discussed and it is found that speed plays an important part in determining the value of maximum peak torque. Speed also introduces dynamic braking torque which affects the mean torque pattern. Free-rotor investigations with different applied voltages are described, and their results discussed. The importance of speed effects is well demonstrated by these results. The duration of the line frequency component of the transient torque is almost entirely governed by speed except for very long run-up times. The appearance of a double line frequency pulsating torque also seems to be speed dependent. With short run-up times, the machine overspeeds before finally attaining its no-load speed. Variation in speed effects with differing acceleration and the effect of saturation on the torque peaks are discussed. Experiments to study the effect of switching on while the motor is running are reported. The results show that the dynamic braking torque assumes greater importance when re-closing is done near no-load speed and 0° point-on-wave.

Investigation of the stalled-rotor transients is presented in Chapter 4. This investigation was

carried out both by experiment and by computation. The experimental results show that the initiation of transient torques depends on the point-on-wave in much the same way as in the free-rotor case. In the absence of speed effects the magnitude of torque peaks does not show an increase over the initial value and the transient torques decay with their 'natural' electrical time constants. The principal component has a very long time constant. Transient current equations are derived based on the actual two-axes arrangement of the windings. Experimentally determined machine constants are substituted in these equations and the resulting current expressions are solved for instantaneous values using a digital computer. Instantaneous values of torque are computed from the instantaneous values of currents. The various components of the transient torque are discussed. Computed transients compare favourably with experimental results.

The approach, systems used, and results obtained are discussed in a general fashion. Blocked-rotor results and free-rotor results are compared with a view to determining the degree to which the former results can be applied to the latter condition. It is thought that the very large dynamic braking torque that can be obtained during re-closing while the rotor is rotating, may be of some practical significance.

LIST OF PRINCIPAL SYMBOLS

a = $\frac{\text{Effective turns in starting winding}}{\text{Effective turns in main winding}}$

e_{d1} = Voltage across direct axis stator winding.

e_{q1} = Voltage across quadrature axis stator winding.

i_{d1} = Direct axis stator current.

i_{d2} = Direct axis rotor current.

i_{q1} = Quadrature axis stator current.

i_{q2} = Quadrature axis rotor current.

k_{d1} = Damping factor of the direct axis stator winding.

k_{q1} = Damping factor of the quadrature axis stator winding.

k_2 = Damping factor of the equivalent rotor winding in either axis.

L_{d1} = Total inductance of the direct axis stator winding.

L_{q1} = Total inductance of the quadrature axis stator winding.

L_2 = Total inductance of the equivalent rotor winding in either axis.

M = Mutual inductance between the direct axis stator winding and the equivalent rotor winding.

P = Number of pairs of poles.

r_{d1} = Resistance of the direct axis stator winding.

r_{q1} = Resistance of the quadrature axis stator winding.

r_2 = Resistance of the equivalent rotor winding in either axis.

T = Instantaneous torque.

x_m = Magnetizing reactance of the main winding.

x_o = $x_1 + x_m$ = Open-circuit reactance of the main winding.

x_1 = Leakage reactance of the main winding.

x_2 = Leakage reactance of the equivalent rotor winding.

σ_d = Leakage coefficient of the direct axis windings.

σ_q = Leakage coefficient of the quadrature axis windings.

τ = Time constant.

Φ_d = Direct axis mutual flux.

Φ_q = Quadrature axis mutual flux.

1. INTRODUCTION

From the early days of electrical machines the behaviour of synchronous machines under transient conditions has been a matter of concern and has received extensive attention. The transient performance of induction motors, on the other hand, has received much less consideration. Furthermore, until comparatively recently, almost all the interest has been in transient voltages and currents, particularly in the over-voltages which may occur when motors are used with power-factor correction or phase splitting capacitors. Even at the present time the information available on transient torques cannot be said to be adequate.

The earliest published work on torque transients in induction motors is probably that by Wahl and Kilgore.[1] These authors have obtained approximate transient torque expressions for blocked-rotor conditions based on Stanley's equations.[2] An experimental test to support the calculated transient is also reported. Gilfillan and Kaplan have made use of a differential analyser to study Stanley's equations with special reference to transient torques during plugging.[3] Maginniss and Schultz,[4] and Weygandt and Charp[5] have made further

differential analyser studies, the former from the viewpoint of control systems and the latter with particular reference to "jogging" and "plugging". A more general study of transients in induction motors, including torque, has been made by Lyon using the method of instantaneous symmetrical components.[6] Making use of the differential equations expressed in terms of instantaneous symmetrical components as given by Lyon, Chidambara and Ganapathy have recently published expressions for transient torque in a form more suitable for studying the effects of parametric variations.[7] They have also carried out a blocked-rotor test. Takeuchi has analysed the case of starting[8] and also the changing of the power source[9] with what he describes as the 'Poly-axis Matrix Method'.

All the works reviewed above are connected only with balanced polyphase machines and are primarily, if not exclusively, analytical. The study of transient torques in single-phase motors, which normally have unbalanced windings, has received much less attention. The author is aware of only two published papers on this, both by Rao.[10,11] They deal with differential

analyser solution of torque expressions for zero speed and constant speed conditions. An experimental study of the possibility of reversing single-phase induction motors by reversing the terminal supply voltage has been reported by Das Gupta.[12] There appears to have been no attempt at an experimental study of transient torques in single-phase induction motors.

In any analytical study of transient torques simplifying assumptions are inevitable, the effects of which are difficult to estimate in the absence of direct experimental data. This is particularly so in the case of free rotor if it is assumed that no speed change occurs for the duration of the electrical transients causing transient components of torque. An experimental investigation avoids these limitations. Furthermore, such an approach is likely to lead to a better appreciation and understanding of the basic phenomena involved. It is therefore considered worth while to conduct a systematic experimental investigation of transient torques in a single-phase capacitor-start induction motor.

It would be quite natural and logical in a primarily analytical study, to begin with the assumption of zero speed, then consider speed constant but not zero and finally variable speed. These assumptions correspond in practice to blocked-rotor conditions, the case when the rotor is rotating with a substantial external inertia added and lastly the more usual case when the electrical transients are accompanied by speed changes. In an experimental study there appears to be no need to build-up to the normal 'free-rotor' conditions in such a manner. In fact, it is probably preferable to study the free-rotor condition extensively as this is the case that is most likely to bring out all the basic phenomena involved. Therefore, in this investigation the case when the motor is started from rest and allowed to accelerate freely up to its full speed will be fully investigated. Re-closing the supply to the motor while the rotor is still rotating forms another important part of the free-rotor conditions. Blocked-rotor conditions will also be examined as a first step towards correlating experimental and calculated results.

Before a systematic experimental study can be undertaken, it is necessary to consider briefly the factors affecting transient torque components so that an assessment of the apparatus required can be made. Torque in single-phase induction motors is produced by the interaction of rotor currents and fluxes in one axis with fluxes and rotor currents in the axis in quadrature. When the stator windings are switched on to the single-phase supply the transient components of the various currents and fluxes will obviously depend upon the point-on-wave of the supply voltage at the instant of switching. Therefore an essential requirement of the experimental investigation is the ability to control the point-on-wave of switching. The equipment used for this purpose and the manner of achieving satisfactory accuracy and consistency are described in Chapter 2. Throughout this thesis the term 'point-on-wave' always refers to the angular position on a sinusoidal voltage wave at the moment of closing the supply to the motor.

For the purpose of detecting transient torques for the two cases of free rotor and blocked rotor, an exhaustive survey of possible methods is carried out (Appendix I). A study of the performance of the d.c.

excited drag-cup accelerometer and the results of calibration of such a device (Appendix II) combined with its relative simplicity and reliability led to it being chosen as the torquemeter for the free-rotor case. For the blocked-rotor case a stator reaction measuring scheme is designed (Appendix III) and constructed.

It is to be noted that the purpose of the investigation is to study the transient torques immediately following an electrical switching. The transient may be purely electrical as in the case of blocked-rotor conditions or may be electro-mechanical as in the case of the free-rotor case. However, in the latter case, as soon as the electrical transients have died out, the resulting torque pattern will follow the "dynamic characteristics", the value of torque being determined solely by the rotor speed at that instant. Any purely mechanical change not associated with any electrical transient is not considered as a transient within the scope of this investigation. Also the appreciable 100-c/s pulsating torque which is normally present in a single-phase induction motor does not form a part of the transient torque being investigated.

2. APPARATUS

As the study is based mainly on direct experimental observation of the various transient phenomena being considered, a great deal of time and care has been given to developing the experimental apparatus and checking their performance and reliability. The complete experimental system can be divided into three main sections: 1. Control Equipment, 2. Detection Equipment, and 3. Recording Equipment.

2.1. Control Equipment:

The most important variable over which control should be exercised is the supply point-on-wave (p.-on-w.). It is also necessary to have control over the magnitude of the supply voltage so that the motor speed does not rise too quickly and the torque transients are thus of long enough duration to exhibit all the various components likely to be of interest.

2.1.1. Point-on-wave Control:

Since no p.-on-w. switch was available in the early stages of the investigation an attempt was made to design and develop a suitable p.-on-w. control. The

general features of the design are as follows: A series of pulses, of adjustable phase position with respect to any selected supply phase, is obtained by means of a magslip phase shifter and a peaking transformer. These pulses trigger two EN91 thyratrons which in turn trigger two reverse connected XR1 industrial thyratrons. The industrial thyratrons have high enough current capacity but unfortunately they were found to have a very high anode excitation voltage. The result was that the valves did not conduct for more than a third of the entire cycle.

High speed relays were tried as an alternative to the industrial thyratrons. In this case only one EN91 was needed. The thyratron connects the supply to the relay coil at points-on-wave selected by the phase shifter. Two relays were tried: a PQ relay and a Carpenter relay. The PQ relay was found to have a transit time of about 15.2 $\pm$ 0.5 millisecond, giving a consistency of operation within an 18° band. The Carpenter relay proved to have a transit time nearly half that of the PQ relay and a consistency of about 10°. Further tests with this relay revealed undesirable

flutter. In any case the consistency of 10° is short of that aimed at. At this stage plans were in preparation for discarding relays in favour of silicone controlled rectifiers, but by then a commercial Sequence Control Unit incorporating p.-on-w. switching became available, and attention was transferred to this control equipment.

Dekatron Sequence-Control Unit Type - 44/7/1 (Fig. 2.1.)

This unit consists of five independent channels fed by way of selector-switches from a master-control unit consisting of three cold-cathode Dekatron counting tubes.[13] The master-control unit is a three-decade unit using Dekatron-type counters giving an overall counting range of 500 cycles in steps of half-a-cycle. The pulse drive for the counters is derived from a reference three-phase supply, via a phase shifter and a pulse forming unit (Fig. 2.2.). The point-on-wave can be varied at will by the phase shifter.

It is interesting to note that as far as the p.-on-w. operation is concerned, the circuit design is much the same as that attempted by the author. The

major difference is that the peaking transformer in the author's design is replaced by a pulseforming unit.

2.1.2. Selection of Zero Degree Point-on-wave:

First, the phase sequence of the reference supply was chosen so as to advance the point-on-wave when the dial setting of the phase shifter was advanced. The dial setting to obtain 0° point-on-wave, for any selected channel and for any supply phase was determined by switching this phase voltage to a long persistence C.R.O. (Fig. 2.3a) and observing any sudden step or discontinuity. It was found that deviations of ± 2° could be easily observed (Fig. 2.3b). If the channel selected included a fine delay control, this was set at some suitable selected point. It was found that the 0° point-on-wave setting varied considerably with the warming-up time allowed. The 'drift' could be as much as 15°, but a reliable setting was obtained after a warming-up period of at least 2 hours. Provided this is done a p.-on-w. consistency of ± 2° can be expected. In view of the importance of accurate p.-on-w. selection, it was decided to make it a general rule to allow at

least 2 hours warming-up period and to check the 0° p.-on-w. setting immediately before recording any test results. This procedure also caters for any day-to-day variation in zero setting due to variations in atmospheric conditions.

2.1.3. Simultaneous Operation of Two Selected Channels:

It has already been mentioned that the Dekatron Sequence Control Unit has five independent channels - channels C to G (Fig. 2.2.). Channel C is unsuitable for supply to a motor load since it does not include a relay. Channels D, E, F and G, consist of relays having special heavy-duty, anti-bounce contacts. However, channel D has provision to select the time delay from 0 to 10 seconds, but only in steps of 10 milliseconds. Channels E, F and G have fine controls by which continuous variation of time delay is possible. In an attempt to get relays D and E to operate simultaneously, it was noticed that the fine control did not cover one complete half cycle and consequently it was not possible to make relays D and E operate simultaneously. However, it was possible to operate E and F simultaneously as they both have fine controls. Simultaneous operation of these

two relays was obtained by observing two step voltages switched through the respective contacts to a long persistence C.R.O.

2.1.4. Calibration of Fine Delay Setting for the Purpose of Non-simultaneous Operation of Two Selected Relays:

The fine delay settings are marked 10 by 1 to 20 ms. In the case of channels E and F simultaneous operation occurred with E and F fine controls set at exactly 10 and 11 ms, respectively. As this difference in setting should mean a difference of 18°, it is obviously necessary to obtain a complete calibration of one delay control. This was done in the following way. The phase-shifter dial setting for 0° point-on-wave of any selected supply phase was determined in the manner already described. To calibrate the delay of channel F with respect to E, the selected voltage was then applied through F only. The phase-shifter was turned so as to advance the point-on-wave by a certain angle, say 18°. The fine control of F was then adjusted to compensate and to bring the point-on-wave back to zero again. The fine setting of F now gives 18° delay with respect to E.

This was repeated at intervals of 18° up to the maximum delay that could be provided by the fine setting of F alone even when taken beyond the 20 ms mark. This should have been more than 162° but was found to be only 131°. Introduction of a delay of one complete half cycle together with the use of the other end of the fine delay enabled the 180° delay range to be completed but as this started at 154° a gap of 23° was unavoidable.

2.1.5. Control of Magnitude of Applied Voltage:

This was done by means of a single-phase variac auto-transformer. In spite of the small steady-state currents that would be taken by the $\frac{1}{2}$ h.p. motor under investigation, a 20-A variac was used to minimise transient regulation of supply voltage. The worst likely condition i.e., the application of rated voltage at 0° point-on-wave was examined. The recorded terminal voltage showed little regulation.

2.2. Detection Equipment:

2.2.1. Detection of Torque:

After an exhaustive survey of the various methods available for detecting transient torques under different conditions (Appendix I), it was decided to use a d.c. excited, drag-cup, two-phase induction generator as an accelerometer, i.e., torquemeter for the case of free rotor. For the study of transient torques with stalled rotor, a stator reaction scheme was chosen, using a precision load cell as the pressure sensing element.

First the performance of the two-phase induction generator as an accelerometer was examined. Preliminary tests with the device manually held against the shaft, showed that even with a selected point-on-wave and a given initial rotor position, considerable variations of torque pattern could be obtained. This was attributed mainly to the flexibility of the rubber tip, depending on the pressure exerted by the operator, and partly to mis-alignment. To avoid these effects, the motor and the accelerometer were mechanically coupled, care being taken to have a rigid connection and good alignment (Fig. 2.4.). Tests now gave repeatable patterns. To

enable the accuracy of measurements made from such transient records to be assessed, tests and calculations were undertaken (Appendix II) to determine linearity and sensitivity of the accelerometer.

The scheme for detecting the reaction of the motor stator is shown in Fig. 2.5. The stator is freely suspended on two ball bearings mounted in two rigid bakelite supports. On the shaft end of the motor, the stator is supported on a hollow shaft through which the rotor shaft passes. This avoids any bending stress on the rotor shaft itself. The whole assembly is built on two U-channels as shown in the photograph. In the absence of a suitable machined bed plate, the U-channels have again to be mounted on two other U-channels at right angles to them to avoid any rocking. A load cell is introduced under one of the motor feet and a stiffening ring under the other. The ring is designed (Appendix III) so that the system has a natural frequency of about 450 c/s. Static loading of the load cell, necessary to cater for possible negative values of torque, is provided by a

bolt-and-nut jacking arrangement. Since the stiffness of the U-channels as simply supported beams is comparable with the total stiffness of the ring and the load cell, the channels are supported by two more jacks directly under the loading points.

Calibration of the output of the load cell was not considered necessary since this system will be restricted to stalled-rotor conditions where alternating components of torque, both observed and calculated, will be expressed in terms of corresponding steady-state values. A check on linearity is, however, quite important. This was done by static mechanical loading and found to be well within the limits of accuracy required.

The quality of the results obtained by the two schemes is shown by Fig. 2.6. It is interesting to note the identity of pattern between acceleration and corresponding stator reaction. The accelerometer gives clear, noise-free signal without any filter. However, in the case of the load cell a filter was found necessary because of the very high amplification needed. In both cases screened cable was used and proper earthing was found to be important.

2.2.2. Detection of Speed:

A speed signal was sometimes required for a qualitative comparison of speed and acceleration and was obtained by means of a 400-c/s drag-cup, two-phase induction generator supplied from a J.2 oscillator. This frequency gives eight speed values for each cycle of the main, i.e. supply frequency component of transient torque or acceleration, and was found sufficient to correlate speed and corresponding acceleration.

2.3. Recording Equipment:

As the torque transients are of comparatively long duration (up to the order of a second), the recording was done by means of a C.R.O. with moving film camera. The oscillograph was calibrated on all amplifier ranges likely to be used. Where a number of related variables, e.g. currents and power, had also to be recorded, a 6-channel Duddell oscillograph with continuous paper camera was also employed.

3. INVESTIGATION OF TRANSIENT TORQUES WITH FREE ROTOR

Before undertaking a systematic experimental study of such basic phenomena as p.-on-w. effect etc., some preliminary tests were made. First with a selected initial rotor position and applied voltage, and fixed points-on-wave, varieties of acceleration records were taken in groups of six or more and compared. All the records for each group had a similar pattern but magnitude variations up to $\pm$ 5% were estimated for the amplitudes of the peaks of the mains-frequency alternating component of torque but in the majority of cases the variation was within $\pm$ 2%. It was decided to make it a general practice throughout the study to record the transients for any one selected condition at least three times.

The effect of rotor position was systematically studied. Variations of $\pm$ 7% were observed but no very conclusive pattern of variation was obtained. To avoid any variation that might be introduced by different rotor positions, the rotor was always set at one selected position before recording each starting transient. It appeared to be possible to maintain an initial rotor position setting to an accuracy of $\pm$ 0.25°.

In order that the acceleration signal can be converted to corresponding torque, for the motor being investigated (Appendix IV), the moment of inertia of the rotor was first determined by a procedure similar to that described in Appendix III, and was found to be 0.00408 kg-m^2. Since the moment of inertia of the accelerometer rotor is only 54 x 10^{-7} kg-m^2 and is thus negligible, this gives a torque sensitivity for the motor-accelerometer combination of 60 mV per N-m. Run-down tests showed that there is negligible retardation due to friction and windage.

3.1. Point-on-wave Effect:

As has been pointed out in the introduction the important basic phenomenon, in the case of single-phase induction motors, is the p.-on-w. effect. This was studied at an applied voltage of 140 volts which is 58.3% of rated value.

3.1.1. Experimental Procedure:

Allowing the necessary warming-up period for stabilizing the operation of the p.-on-w. switch, the dial setting for 0° point-on-wave was selected in the manner already described. Starting from 0° point-on-

wave, acceleration records were photographed at intervals of 30°. Six records were taken at each setting. Before each start the rotor position was set at the arbitrarily chosen zero position. Care was taken to maintain the supply voltage and the excitation of the accelerometer constant. Readings from the oscillograms were taken using a projector and screen permanently arranged to give a fixed magnification.

3.1.2. Experimental Results:

A typical set of the acceleration patterns for different points-on-wave is shown in Fig. 3.1. Fig. 3.2 shows the envelopes of the peak values of torques and the derived curves of direct and alternating components. The time scale of Fig. 3.2 is slightly distorted since the interval between peaks is taken to be constant and also the negative peaks are assumed to occur midway between positive peaks. Plotting to an exact time scale was not considered necessary for the present purpose, i.e., the study of the effect of point-on-wave on the general pattern and magnitudes of the two components.

3.1.3. Discussion of Results:

The experimental results confirm the expectation that there is an alternating component of transient torque of considerable magnitude depending on the point-on-wave of switching. Although there may be components of negligible value but of different frequencies, the main alternating component of torque appears to be of supply frequency, i.e., 50-c/s in the present case.

The initial amplitude of the alternating component of torque has a maximum value (4.0 N-m.) when the point-on-wave is indiscernable from 0°. This is as expected since the 50-c/s torque is produced by the interaction of direct and 50-c/s components of rotor currents in one axis with 50-c/s and direct components of flux respectively, in the axis in quadrature. Since the rotor circuit at standstill will have a high damping factor, the component of 50-c/s torque due to the direct current in the rotor will die out quickly. This component of torque will attain a maximum value at a point-on-wave considerably different from 0° depending on the power factor of the rotor circuit at standstill. On the other hand, the flux components are

caused by circuits which are highly inductive and therefore persist for a long time. Because of the inductive nature of this branch of the circuit, the value of direct current and therefore the corresponding 50-c/s torque will be a maximum for a point-on-wave close to zero. From the torque patterns it can be concluded that the component of 50-c/s torque due to direct current in the rotor does not affect the pattern significantly. However, it does seem to affect the magnitude of the first torque peak as shall be shown presently.

Fig. 3.3 shows the variation of the magnitude of the alternating component of torque at the first positive peak with respect to point-on-wave. If the alternating component were caused by a single function only, a sinusoidal variation could possibly be expected. It is evident from the figure that this is not so. Comparing the variation between 0° and 90° with a sine curve, it appears that the effect of the second function is to produce a small but definite component of torque which opposes the principal component for points-on-wave near 0° and adds for points-on-wave near 90°.

It can also be seen from the figure that the variation from 90° to 180° is not exactly the same as that between 0° and 90°. It does not seem to be possible to account for this difference in terms of point-on-wave as equal deviations from 90° are likely to produce similar patterns unless the second component of alternating torque is quite considerable. The comparative closeness of the actual and sinusoidal curves during the first 90° suggests that this is not so. It therefore seems that some other explanation must be sought. Results obtained at a later stage in the study seem to throw some light on this problem and reference will be made to this later in the thesis.

In Rao's[10] analytical study of switching transients in single-phase induction motors it is assumed that within the first few cycles "the rotor will not have attained any measurable speed; as such, the effect of rotation on the transient currents and fluxes may be disregarded." The results of the present investigation suggest that the validity of these two assumptions is questionable. Even with only 58.3% of normal applied voltage and therefore about 34% of the normal average torque developed, the motor

comes up to 80% of full speed in about 10 cycles. With an external inertia of about three times that of its own rotor and full voltage applied the motor will come up to speed in about the same time. In most cases under normal operation, it is likely to come up to speed in a shorter time. Furthermore, these assumptions lead one to expect that the first peak will be the largest peak. The present results (Figs. 3.1 and 3.2) however, show that the alternating component increases until about the third peak is reached and then starts decreasing. The initial increase is substantial and requires explanation. Analytical studies, where speed is assumed zero, do not reveal this phenomenon. The explanation has therefore to be sought as some effect of speed. Unsatisfactory mechanical response is ruled out in view of the fact that the system has good response to a step acceleration as in the case of 90° p.-on-w. switching.

In any induction motor, rotation of the rotor conductors in the transient direct components of flux give rise to armature reaction similar to that in any short-circuited synchronous machine. This will have an important influence on the duration of the direct components of flux and therefore on the alternating

components of torque, but can only cause an increase in the rate of decay. In the case of capacitor-start induction motors some other speed effect or effects must be causing the initial increase in magnitude of the alternating component of torque.

It is well known that in such machines the starting winding and its capacitor are designed to give a leading current at standstill[14,15]. It can also be shown from steady-state calculations that the starting winding current generally remains substantially constant up to about 80% or more of full speed. For the motor being investigated this has been experimentally checked and found to be true (Fig. 3.4). However, because of the changing power factor, the voltage across the starting winding increases appreciably with speed. This has also been verified experimentally (Fig. 3.4) and will obviously tend to increase the amplitude of the alternating component of torque. It therefore appears from the results that the effect of increased voltage across the starting winding predominates over the damping effect of speed for the first few cycles producing a net increase in the amplitude of the

alternating component of torque. Thus the initial and quite substantial rise in the alternating components of torque is a typical feature of single-phase capacitor-start induction motors.

Mean Torque Characteristics: A study of the mean torque patterns (Fig. 3.2) shows appreciable variation with point-on-wave. Whereas it can reasonably be expected that the mean torque pattern will follow that derived from steady-state equations for 90° point-on-wave, it is likely to be different for other points-on-wave for the following reason: When the rotor revolves in the decaying unidirectional flux, it is subjected to a dynamic braking torque. Obviously such a torque will oppose the mean accelerating torque and will also be a function of point-on-wave. The presence of maximum braking torque must coincide with that of maximum alternating component of torque since both originate from decaying unidirectional flux. Examination of the patterns of mean torque confirms this statement.

If it can be considered that the magnitude of the first peak of the alternating component of torque is a measure of the initial value of the decaying unidirectional flux, and the fall in the value of mean

torque between the value at the first peak and the minimum is a measure of the maximum dynamic braking torque, the relationship between these two is as shown in Fig. 3.5. The effect on the time to reach the speed at which the centrifugal switch operates (about 85% of synchronous speed) is shown by Fig. 3.6. It was verified that, for a constant applied voltage, the centrifugal switch operated with respect to speed with reasonable consistency.

3.1.4. Concluding Remarks:

The alternating components of torque are primarily dependent on the point-on-wave of the supply connection. Speed effects considerably influence the transient torque pattern. The largest value of instantaneous torque (0° point-on-wave, 3rd peak) is about 8.37 N-m compared with 0.85 N-m which is the reduced voltage torque at full-load slip.

The mean torque or the direct component is also affected by point-on-wave due to a dynamic braking effect. This has a small but definite influence on the run-up time.

3.2. Effect of Torque/Inertia Ratio:

The starting time of a motor is dependent on its own inertia and on the nature of the connected load. It is not within the scope of the present investigation to study the transient characteristics when the motor is started against a 'load'. However, since speed effects have been shown to be of importance, it is considered necessary to study the effects of different run-up times. This depends on the ratio of torque to inertia (T/J) and could be done either by maintaining a constant supply voltage and adding external inertia or by simply varying the supply voltage. The latter method is easier and more in keeping with the scope of the present work and therefore was adopted.

3.2.1. Experimental Procedure:

Different values of T/J ratio were obtained by varying the applied voltage from 120V to 240V in steps of 20V and then to 250V. In this case it was considered necessary to study the variation of the main and starting winding currents, total power and speed in addition to torque. Since the speed and acceleration signals do not have enough power associated with them to actuate Duddell

vibrators they were recorded using C.R.O.'s. Connections to the Duddell oscillograph are shown in Fig. 3.7. Acceleration and speed signals were recorded on two different C.R.O.'s and the applied voltage signal was recorded on all the three oscillographs to provide a time reference. The entire experimental set up is shown in Fig. 3.8. Two series of tests were carried out at various applied voltages, one with 0° point-on-wave and the other with 90° point-on-wave.

3.2.2. Experimental Results:

A typical set of acceleration patterns for different voltages with 0° point-on-wave is shown in Fig. 3.9 and the corresponding speed patterns are shown in Fig. 3.10. Another such pair of acceleration and speed patterns for 90° point-on-wave is shown in Figs. 3.11 and 3.12. The currents and power variations with both points-on-wave at 140 and 240 volts are shown in Fig. 3.13 (a to d.).

3.2.3. Discussion of Results:

It is evident from the results that the duration of the line frequency component of torque depends very much on the T/J ratio. As has already

been shown, the transient torque depends on the rotor speed in addition to the point-on-wave. With a selected T/J ratio and various points-on-wave, the magnitude of the line frequency component varies considerably (Fig. 3.1) but its duration remains substantially constant. In the present case, however, the duration of this component appears to vary approximately in the inverse ratio of T/J (Fig. 3.14). This is to be expected because with increased value of T/J, the motor acquires any given speed in a shorter time and therefore the 'armature reaction' effect also builds up more quickly. Consequently the line frequency transient torque vanishes earlier.

The above reasoning also suggests that the alternating component of torque should vanish at a particular speed. It has been shown analytically by T.J. Takeuchi[8] that such a 'critical' speed exists for balanced polyphase induction motors. The variation of speed at which the alternating component of torque vanishes with respect to T/J ratio is shown in Fig. 3.15. The speed remains substantially constant for values of T/J greater than about 0.4. For values less than 0.4

it decreases. It appears, therefore, that when T/J values are less than 0.4 the disappearance of the 50-c/s torque is governed partly by speed and partly by the 'natural' electrical damping of the transient flux. As the T/J ratio tends to zero, the 'critical' speed also tends to zero. The limiting condition of zero T/J ratio corresponds to the trivial case of zero applied voltage, and to the locked-rotor condition.

There is considerable scatter in Fig. 3.15. This is probably due to the fact that Figs. 3.9 and 3.10 had to be correlated to get the speed at which the 50-c/s torque vanishes.

Appearance of 100-c/s torque: A reasoning somewhat similar to that in the previous section leads one to expect that the double frequency pulsating torque might appear at a definite speed irrespective of the time involved. From Figs. 3.11 and 3.12 the speed at which this torque appears for different values of T/J was derived and plotted (Fig. 3.16). Even though there is appreciable scatter (as in Fig. 3.15), it seems that the double frequency torque appears at a speed slightly less than 600 r.p.m.

Overspeeding: It is seen from Figs. 3.11 and 3.12 that overspeeding occurs when T/J values are greater than about 0.4. It may or may not be significant that the alternating components of transient torque vanish at a definite speed of about 850 r.p.m. also for T/J values greater than about 0.4.

The fact that the transient components of flux never persist after a speed of about 850 r.p.m. is reached, indicates that the overspeeding is not associated with this flux. This conclusion is supported also by the fact that overspeeding occurs at 90° point-on-wave, when the transient direct component of flux is negligible as well as 0° point-on-wave when this component of flux is close to its maximum value. The explanation must therefore be associated with some other transient phenomenon which occurs as the machine approaches synchronous speed.

R.W. Ager[16] has offered an explanation of 'transient overspeeding' in terms of 'frequency modulation'. Briefly, the explanation is that as the motor approaches synchronous speed, the power component of current falls and the air-gap e.m.f. phasor $\bar{E}$, (Fig. 3.17) has to

'catch up' with the applied voltage phasor $\bar{V}_1$. If the ratio of torque to inertia is large enough, the rate of decrease of current and therefore the transient frequency increase will be great enough to cause appreciable overspeeding. It is interesting to note [Fig. 3.13 (c and d)] the induction generator action during the return swing.

Effects of Speed and Saturation on Peak Torques: It was seen from Fig. 3.2 that the overall effect of speed is to increase the amplitude of the alternating component of torque until about the third cycle is reached. The duration of increasing amplitude obviously cannot remain constant when the rate at which speed is acquired varies. The variation of time for which the alternating component of torque increases with respect to T/J ratio is shown in Fig. 3.18. It appears to be a reciprocal relationship. Considering the fact that the time to reach a definite speed also varies approximately as the reciprocal of T/J ratio (Fig. 3.19) it seems that for the range of T/J ratio considered, the phenomenon of increase in the amplitude of the alternating component of torque is purely a speed effect irrespective of the time involved.

The variation with respect to T/J ratio of the first, second and third peaks of the transient torque for 0° point-on-wave is shown in Fig. 3.20. The first and second peaks follow similar patterns suggesting that the effect of speed on these two peaks had been consistent within the range of T/J ratio considered. The patterns themselves are similar to that of the familiar magnetization curve. Though this is not directly due to magnetic saturation, it appears to be a secondary effect of the same. With increasing saturation, the voltage drop across the stator winding will be an increasing fraction of the applied voltage. Therefore the air-gap voltage as a proportion of the applied voltage falls as the latter increases. This appears to cause the flattening of the torque Vs. applied voltage squared curve at higher voltages.

The effect of speed on the third peak changes as the T/J ratio increases. For low values of T/J ratio, up to about 0.36, the overall speed effect causes the third peak to be greater than the second, but, for higher values the third peak is always lower

than the second. This fits in very well with Fig. 3.18 since the third peak occurs at about $2\frac{1}{2}$ cycles after switching on.

Comparison of Mean Torques: The value of mean torque corresponding to the first peak and the 'maximum dynamic braking torque' (p. 26/27) for different values of T/J ratio were derived in the manner indicated by Fig. 3.2 and are plotted against T/J ratio in Fig. 3.21. For T/J ratios above 0.7 the torque peaks were too few to allow mean torque to be established with any reliable accuracy. As would be expected the mean torque varies fairly linearly up to this limit. The dynamic braking torque also appears to vary linearly with T/J ratio in the unsaturated region. The odd point corresponding to T/J ratio of 0.7 would suggest that the distortion in the time scale is now beginning to be important.

3.2.4. Concluding Remarks:

It is seen from the dicsussion that the transient torques are as much dependent on speed as on point-on-wave. In fact the disappearance of the line frequency component is governed almost entirely by speed except for very long starting times. The maximum value of peak torque acquired

is also dependent on speed since the increase in amplitude of the alternating component of torque is dependent on speed.

There is overspeeding for values of T/J ratio greater than about 0.4 but this does not appear to be caused by the transient flux. Magnetic saturation affects the peak torques due to the increasing proportion of voltage drop across the stator windings at higher voltages.

3.3. Effect of Switching on while the Motor is Running:

It has been shown from previous sections (3.1 and 3.2) that the transient torque, both the mean and the alternating components, are very much affected by speed. Therefore, if a motor is switched on while it is still running - as can happen in practice - it is to be expected that the resulting torque characteristics will be different from those corresponding to starting from rest. Also the difference will depend on the speed at which switching is effected.

3.3.1. Experimental Procedure:

The p.-on-w. switch was short circuited by an external switch so that the motor could be started from rest, switched off, and allowed to run down without operating the p.-on-w. switch. When the motor reached a selected speed the p.-on-w. switch was triggered thus reconnecting the motor to the supply at selected point-on-wave and speed. External means of bringing the motor up to the required speed was not considered since this would necessarily involve coupling additional inertia to the rotor. A tachometer was used for speeds up to 1300 r.p.m. and a stroboscope for higher speeds.

Two series of tests were carried out for speeds from 200 to 1450 r.p.m., one with 0° point-on-wave and the other with 90° point-on-wave.

3.3.2. Experimental Results:

Torque patterns corresponding to 0° p.-on-w. switching at various speeds are shown in Fig. 3.22. A similar set corresponding to 90° p.-on-w. is shown in Fig. 3.23.

3.3.3. Discussion of Results:

From the results it is seen that at low speeds - up to about 300 r.p.m. - the general pattern of torque variation is almost indistinguishable from that for the case of starting from rest. For 0° point-on-wave (Fig. 3.22) the first peak torque is always negative even at low speeds. Except for this, the general torque pattern, for speeds up to 750 r.p.m., has features similar to those for the case of starting from rest. For example, the magnitude of the alternating component shows an increase from the initial value before starting to decrease. Also the value of the first positive peak remains substantially constant. For speeds in excess of 750 r.p.m. the pattern begins to show a marked difference. The initial negative peak torque begins to assume greater importance. For speeds over 1200 r.p.m. peaks other than the first negative peak have almost vanished.

An initial negative peak, dependent on speed is present only in the case of 0° p.-on-w. switching. Examination of Fig. 3.23 shows that it is completely absent in the case of 90° p.-on-w. switching. It is

therefore concluded that the negative torque is due to the dynamic braking action of the direct component of the transient flux. The variation of the net braking torque with respect to the speed at switching is shown in Fig. 3.24. The braking torque increases slowly with speed up to about 750 r.p.m. Between this speed and 900 r.p.m. there is discontinuity indicating a sudden rise in the braking torque. The discontinuity occurs in the speed range at which the centrifugal switch closes as the machine runs down. For speeds greater than about 1100 r.p.m. the braking torque increases more rapidly with speed.

It is well known that for a capacitor-start motor, the steady-state accelerating torque with both windings in circuit is very much greater than with the main winding only provided the speed is below about 70% of synchronous value.[14] In this speed range, therefore, the net value of the momentary braking torque will be very much influenced by whether both the windings are in circuit or only the main winding is in circuit. For the motor in question the centrifugal switch recloses during the run down at about 60%

of synchronous speed. It is therefore to be expected that as the centrifugal switch closes, there will be a sudden increase in developed accelerating torque and thus a decrease in net braking torque.

For switching at speeds approaching the no-load value, the steady-state accelerating torque is diminishing rapidly and therefore the braking torque increases rapidly and approximates more closely to the dynamic braking torque. Extrapolation of the curve shows that at synchronous speed, the dynamic braking torque reaches a value of about 16 N-m.

It is worth noting that the experiment is not complicated by any appreciable 'trapped' flux effect since even the short time taken to run down to 1450 r.p.m. is enough to reduce such flux to an insignificant value (Fig. 3.22).

3.3.4. Concluding Remarks:

Reclosing the supply while the motor is still running gives rise to distinctly different characteristics from that corresponding to starting from rest, depending on the speed at the time of reclosing. If the motor is reconnected almost immediately after the

supply is broken, it will be subjected, under the worst condition, to a momentary braking torque of about 15 N-m. as compared with the corresponding full-load torque of 0.85 N-m. This braking torque can be completely eliminated if the motor could be reconnected at 90° point-on-wave.

3.4. Other Effects:

It has now been seen that a large variety of torque/time patterns are possible. Any one pattern is determined primarily by the point-on-wave of supply connection together with the initial speed of the rotor and the rate at which further speed is acquired. During the course of the study two minor effects of a less fundamental nature were observed and to some extent explored. These were first the effect of delay in connecting one of the windings and second the effect of changing the direction of rotation. Unlike the rotor position effect, neither of these phenomena is present under normal operating conditions.

3.4.1. Delayed Connection of one of the Windings:

The machine windings were connected independent of one another through channels E and F to the supply.

Relays E and F were initially set to operate simultaneously and then the delay of F with respect to E was calibrated. Point-on-wave was selected for the relay E. First with the main winding connected through E and with the point-on-wave set at 0°, various delays were introduced in connecting the starting winding to the supply and the acceleration patterns recorded. A similar set of tests was carried out but with the point-on-wave now set at 90°. Two more sets were also carried out exactly similar to the two described but with the starting winding connected through E and the delay introduced in connecting the main winding.

Study of the oscillograms showed this to be a relatively minor effect. In any case, it is a phenomenon not possible in normal operation. For these reasons a numerical study of the results was not considered worth while. However, some general conclusions drawn from the observation of the 246 oscillograms taken will now be given.

It was found that the alternating component of torque is dependent on the point-on-wave of the

main winding connection and is almost wholly caused by the transients in the main winding. The transients in the starting winding contribute very little, if any, to the alternating component of torque and therefore this torque is practically independent of the point-on-wave of the starting winding connection. It was also noticed that the main winding transients reach an insignificant value within about 0.5 sec.

3.4.2. Directional Effects:

All the results presented and discussed so far refer to a selected direction of rotation. A representative selection of characteristics for the other direction of rotation was observed. It was concluded that there was no appreciable general effect. In the course of these observations it was noticed that the transient torque peaks for the first start in any new direction always had higher values than for the subsequent ones. This effect was present both for 0° and 90° points-on-wave but was much more pronounced in the former case. Possible causes for this such as the accelerometer having remnant magnetic effect, mechanical slackness in the coupling, magnetic orientation in the

stampings were explored with negative results. This phenomenon, therefore, seems likely to be an impact effect due to some slight slackness of the rotor assembly.

4. INVESTIGATION OF TRANSIENT TORQUES WITH STALLED ROTOR

Starting a single-phase, capacitor-start induction motor from rest, gives rise to a specific type of transient torque characteristics due to the fact that the rotor is at rest initially and thereafter changes in speed continuously. Similarly, re-closing the supply to the motor while the rotor still has appreciable velocity gives rise to another class of characteristics where the predominant features are due to the heavy initial damping imposed on the transient flux by the dynamic action and the sudden dynamic braking torque. Yet another distinctly different type of characteristic will result if the motor is switched on with its rotor stalled as there is then complete absence of speed effects. This last mentioned case will now be studied both by direct experimental methods and by analytical procedures.

4.1. Experimental Investigation:

Since acceleration is now absent, the scheme adopted for free rotor conditions is no longer applicable. For this condition, it was decided to use a precision

load cell arranged to detect stator reaction. The design and performance of this system has been discussed in Chapter 2 and Appendix II.

4.1.1. Experimental Procedure:

From preliminary tests it was estimated that the maximum pressure to which the load cell is subjected (with 58.3% of full voltage applied) is of the order of 15 lbs. Transient torque recordings taken with various amounts of static pressure showed that at least about 30 lbs must be applied before a reliable pattern is obtained; with static pressures below this value the pattern is dependent on this pressure. The value of 30 lbs is much more than is required to cater for the likely negative torques and is presumably needed to establish good mechanical contact between the various contact surfaces. Since the load cell has good performance up to many times its rated capacity it was considered desirable to work near the full-load capacity of the cell. This was done by applying a static pressure of 85 lbs on all occasions.

The rotor was blocked (Fig. 2.5) using two steel arms of cross-section $\frac{3}{4}$ in. by $\frac{1}{4}$ in. Care was taken to allow sufficient warming up time for the

p.-on-w. switch before selecting the setting for 0° point-on-wave.

With 140 volts applied, the transient torques were recorded for different points-on-wave of switching from 0° to 180° in 10° intervals. Also with the point-on-wave set first at 0° and then at 90°, two series of tests were conducted varying the applied voltage from 120 V to 240 V in steps of 20 V and then to 250 V.

4.1.2. Experimental Results:

A typical set of the torque patterns for a selection of points-on-wave is shown in Fig. 4.1. Since the value of the applied voltage appears to have little or no effect on the pattern, no selection of oscillograms is given in this case. Instead, the variation of the first positive peak, after correcting for attenuation due to the filter, is plotted to a base of voltage squared (Fig. 4.2) for the case of 0° point-on-wave. The variation of the steady state torque is also shown.

4.1.3. Discussion of Results:

As in the case of free rotor, the point-on-wave plays an important part. It can be seen from

Fig. 4.1, that the signal is subjected to an appreciable discontinuity at the origin for points-on-wave other than zero. This makes it impossible to draw any relationship connecting the amplitude of alternating component of torque and the point-on-wave. However, the general variation of the alternating component with respect to point-on-wave appears to be similar to that in the free rotor case. The main difference in this case is that there is no increase of alternating component of torque since the rotor is not free to rotate and that the alternating component of torque dies out with a decrement determined only by the electrical parameters of the motor.

For 0° point-on-wave and for each supply voltage used, the envelopes of the alternating components were plotted, using a logarithmic scale, in order to study the decrements. A representative selection is given in Fig. 4.3. The general exponential nature of the transients is confirmed but at lower voltages there appears to be a secondary component which opposes the main alternating component. The secondary component reaches an insignificant value in

about 2.5 cycles and the main component has a time constant of about 10.5 cycles or 210 ms. At higher voltages the initial decrement is faster than that corresponding to a time constant of 210 ms. This is because of the high degree of saturation during the initial period of the transient at higher voltages. After about 10 cycles from the instant of switching the decrement has a time constant of about 210 ms. for all voltages. This shows that the normal steady-state saturation does not affect the time constant very much. The direct component of the transient torque in all cases remains level.

Fig. 4.2 is drawn to a double log scale to facilitate comparison of the peak and steady-state torques. The two appear to be roughly parallel showing that they have a constant ratio. The peak torque is about 2.1 times that of the steady-state torque.

It can be seen from Fig. 4.1 that there is appreciable 50-c/s torque modulated with a 100-c/s torque. Such torques have been shown to exist in electrical machines due to unbalanced magnetic pull.[17]

4.1.4. Concluding Remarks:

The magnitude of the alternating component of the transient torque is dependent on the point-on-wave in much the same way as in the case of free rotor. However, there is no tendency for this component to show an increase over the initial value. For 0° point-on-wave, the ratio of peak torque to steady-state torque is about 2.1. The "natural" electrical decay of the alternating component is fairly long. It takes more than 30 cycles for it to reach 5% of its initial value. The initial decrement is influenced by the applied voltage.

4.2. Analytical Investigation:

For steady-state calculations the choice between the use of 'double-revolving field' theory and 'cross-field' theory is largely a matter of personal preference, though there is some reason to prefer the former for normal running conditions where the starting winding is cut out and the latter for starting conditions. For transient studies there is no obvious advantage in considering any alternative to the actual, two-axes arrangement.

In this analytical investigation, the usual simplifying assumptions shall be made.[10,14,18] Most important of these are the assumptions that the distribution of m.m.f.'s is sinusoidal and that the effect of saturation can be neglected. Though the latter assumption seriously limits the extension of the analysis to normal working voltages, the first assumption does not introduce any considerable error as the parameters used in the final calculation will be experimentally determined.

Since the rotor has a symmetrical cage winding, it can be represented by two identical windings in quadrature, each having the same number of turns as the stator main winding. Therefore, the motor will be represented by four coils in the d- and q- axes, as shown in Fig. 4.4. In any such arrangement, it can readily be shown, either by the virtual displacement method adopted by Lyon[6] or by the 'power corresponding to torque' approach as used by Adkins,[18] that the torque at any instant

$$T = PM\,(i_{d1}\, i_{q2} - a\, i_{d2}\, i_{q1}) \qquad \ldots\ldots (4.1)$$

Determination of instantaneous torque is, therefore, primarily a matter of evaluating the four currents i_{d1}, i_{d2}, i_{q1}, and i_{q2}.

4.2.1. Basic Current Equations:

Under blocked rotor conditions, the voltage equations for the two axes are

$$\left.\begin{aligned} e_{d1} &= (r_{d1} + L_{d1}p)i_{d1} + Mp\, i_{d2} \\ 0 &= Mp\, i_{d1} + (r_2 + L_2\, p)i_{d2} \end{aligned}\right\} \quad .... (4.2)$$

$$\left.\begin{aligned} 0 &= (r_2 + L_2 p)i_{q2} + aMp\, i_{q1} \\ e_{q1} &= aMp\, i_{q2} + (r_{q1} + L_{q1}p + \tfrac{1}{Cp})i_{q1} \end{aligned}\right\} \quad .... (4.3)$$

It should be noted that equations (4.2) and (4.3) are two independent sets of simultaneous equations. Also, for single-phase motors e_{d1} is always equal to e_{q1}.

If θ is the point-on-wave at which the supply is connected to the motor, then the applied voltage can be expressed as

$$v = V \sin(\omega t + \theta)$$
$$= V \cos\theta \sin \omega t + V \sin\theta \cos\omega t$$
$$= V' \sin \omega t + V'' \cos \omega t \qquad \ldots\ldots (4.4)$$

Therefore the applied voltage can be considered as the sum of two functions, one cosine and the other sine. By applying the principle of superposition, the axes currents can be calculated for these two component voltages individually and then added.

Applying Laplace Transforms to equations (4.2) the transformed equations become

$$\left.\begin{aligned} i_{d1(s)} &= \frac{e_{d1(s)}}{\sigma_d L_{d1}} \cdot \frac{s + k_2}{(s+p_1)(s+p_2)} \\ \text{and } i_{d2(s)} &= -\frac{e_{d1(s)}}{\sigma_d L_{d1} L_2} \cdot \frac{M\, s}{(s+p_1)(s+p_2)} \end{aligned}\right\} \qquad \ldots\ldots (4.5)$$

$$\text{where } p_1 = \frac{k_{d1} + k_2}{2\sigma_d} + \sqrt{\left(\frac{k_{d1} + k_2}{2\sigma_d}\right)^2 - \frac{k_{d1} k_2}{\sigma_d}}$$

$$\text{and } p_2 = \frac{k_{d1} + k_2}{2\sigma_d} - \sqrt{\left(\frac{k_{d1} + k_2}{2\sigma_d}\right)^2 - \frac{k_{d1} k_2}{\sigma_d}}$$

First taking $e_{d1(s)}$ corresponding to $V' \sin \omega t$ and then $V'' \cos \omega t$, the complete expressions for i_{d1} and i_{d2} are obtained as

$$i_{d1} = \frac{V}{\sigma_d L_{d1}} \cdot \frac{(p_1 - k_2)}{(p_2 - p_1)(p_1^2 + \omega^2)} [p_1 \sin \theta - \omega \cos \theta] e^{-p_1 t}$$

$$+ \frac{V}{\sigma_d L_{d1}} \cdot \frac{(p_2 - k_2)}{(p_1 - p_2)(p_2^2 + \omega^2)} [p_2 \sin \theta - \omega \cos \theta] e^{-p_2 t}$$

$$+ \frac{V}{\sigma_d L_{d1}} \cdot \sqrt{\frac{k_2^2 + \omega^2}{(p_1^2 + \omega^2)(p_2^2 + \omega^2)}} \cdot \sin (\omega t + \theta - \phi_{d1})$$

... ... (4.6)

where

$$\phi_{d1} = \tan^{-1} \frac{\omega}{p_1} + \tan^{-1} \frac{\omega}{p_2} - \tan^{-1} \frac{\omega}{k_2}$$

and

$$i_{d2} = \frac{VM}{\sigma_d L_{d1} L_2} \cdot \frac{p_1}{(p_1-p_2)(p_1^2+\omega^2)} [p_1 \sin\theta - \omega\cos\theta] e^{-p_1 t}$$

$$+ \frac{VM}{\sigma_d L_{d1} L_2} \cdot \frac{p_2}{(p_2-p_1)(p_2^2+\omega^2)} [p_2 \sin\theta - \omega\cos\theta] e^{-p_2 t}$$

$$- \frac{VM\omega}{\sigma_d L_{d1} L_2} \cdot \sqrt{\frac{1}{(p_1^2+\omega^2)(p_2^2+\omega^2)}} \cdot \sin(\omega t + \theta - \phi_{d2})$$

... ... (4.7)

where

$$\phi_{d2} = \tan^{-1}\frac{\omega}{p_1} + \tan^{-1}\frac{\omega}{p_2} - \pi/2$$

Applying Laplace Transforms now to equations (4.3)

$$i_{q1(s)} = \frac{e_{q1(s)}}{\sigma_q L_{q1}} \cdot \frac{s(s + k_2)}{\left[s^3 + s^2 \cdot \frac{k_{q1} + k_2}{\sigma_q} + s\left(\frac{k_{q1} k_2}{\sigma_q} + \frac{1}{CL_{q1}\sigma_q}\right) + \frac{k_2}{CL_{q1}\sigma_q}\right]}$$

... ... (4.8a)

and

$$i_{q2(s)} = -\frac{e_{q1(s)}}{\sigma_q L_{q1} L_2} \cdot \frac{M s^2}{\left[s^3 + s^2 \cdot \frac{k_{q1} + k_2}{\sigma_q} + s\left(\frac{k_{q1} k_2}{\sigma_q} + \frac{1}{CL_{q1}\sigma_q}\right) + \frac{k_2}{CL_{q1}\sigma_q}\right]}$$

... ... (4.8b)

By Viet's Formula[19] a first approximation to the real root of the denominator is obtained by taking the root of the last two terms, i.e.

$$\frac{k_{q1} k_2 + \frac{1}{CL_{q1}}}{k_2 / CL_{q1}}$$

$$\therefore \simeq k_2 \quad \text{if} \quad k_{q1} k_2 \ll \frac{1}{CL_{q1}}$$

In the present case this approximation is found to be quite valid since $k_{q1}\ k_2 = 0.0228 \times 10^4$ sec.$^{-2}$ and

$\frac{1}{CL_{q1}} = 1.56 \times 10^4$ sec.$^{-2}$ Therefore, with k_2 as the real root, the other two roots of the cubic expression become approximately

$$\left.\begin{aligned} p_1 &= \alpha + \beta \\ \text{and} \quad p_2 &= \alpha - \beta \end{aligned}\right\} \qquad \ldots\ldots (4.9)$$

where

$$\alpha = \frac{1}{2}\left(\frac{k_{q1} + k_2}{\sigma_q} - k_2\right)$$

$$\text{and} \quad \beta = \sqrt{\frac{1}{CL_{q1}\sigma_q} - \alpha^2}$$

Therefore equations (4.8) can be rewritten as

$$\left.\begin{aligned} i_{q1(s)} &= \frac{e_{q1(s)}}{\sigma_q L_{q1}} \frac{s}{(s+\alpha)^2 + \beta^2} \\ \text{and} \\ i_{q2(s)} &= -\frac{e_{q1(s)}}{\sigma_q L_{q1} L_2} \cdot \frac{Ms^2}{(s+k_2)[(s+\alpha)^2+\beta^2]} \end{aligned}\right\} \qquad \ldots\ldots (4.10)$$

As before, first taking $e_{q1(s)}$ corresponding to $V' \sin \omega t$ and then $V'' \cos \omega t$, the complete solutions for i_{q1} and i_{q2} are obtained as

$$i_{q1} = \frac{V}{\sigma_q L_{q1} \sqrt{4\alpha^2\omega^2 + (\alpha^2+\beta^2-\omega^2)^2}} \cdot$$

$$\left[\frac{1}{\beta}\sqrt{\alpha^2+\beta^2} \left\{ \cos \phi \sin (\beta t - \psi_1) + \sqrt{\alpha^2+\beta^2} \cdot \sin \phi \cos (\beta t - \psi_2) \right\} e^{-\alpha t} + \omega \sin (\omega t + \theta - \phi_{q1}) \right]$$

... ... (4.11)

where

$$\phi_{q1} = \tan^{-1} \frac{\omega^2-\alpha^2-\beta^2}{2\alpha\beta}$$

$$\psi_1 = \tan^{-1} \frac{\beta}{\alpha} - \tan^{-1} \frac{2\alpha\beta}{\alpha^2-\beta^2+\omega^2}$$

$$\psi_2 = \tan^{-1} \frac{2\alpha\beta}{\alpha^2-\beta^2} - \tan^{-1} \frac{2\alpha\beta}{\alpha^2-\beta^2+\omega^2}$$

and

$$i_{q2} = -\frac{MV}{\sigma_q L_{q1} L_2}\left[\frac{k_2^2}{(k_2^2+\omega^2)[(\alpha-k_2)^2+\beta^2]}(\omega\cos\theta - k_2\sin\theta)e^{-k_2 t}\right.$$

$$+\frac{\left\{\omega(\alpha^2+\beta^2)\cos\theta.\sin(\beta t-\psi_3)\right.}{\beta\sqrt{[(\alpha-k_2)^2+\beta^2][4\alpha^2\omega^2+(\alpha^2+\beta^2-\omega^2)^2]}}$$

$$\left.\left.+\sqrt{\alpha^2(3\beta^2-\alpha^2)^2+\beta^2(3\alpha^2-\beta^2)^2}.\sin\phi\cos(\beta t-\psi_4)\right\}e^{-\alpha t}\right.$$

$$\left.+\frac{\omega^2}{\sqrt{(k_2^2+\omega^2)[4\alpha^2\omega^2+(\alpha^2+\beta^2-\omega^2)^2}}\sin(\omega t+\theta-\phi_{q2})\right]$$

... ... (4.12)

where

$$\phi_{q2} = \tan^{-1}\frac{\omega}{k_2} + \tan^{-1}\frac{\omega^2-\alpha^2-\beta^2}{2\alpha\omega} - \pi/2$$

$$\psi_3 = \tan^{-1}\frac{2\alpha\beta}{\alpha^2-\beta^2} - \tan^{-1}\frac{k_2-\alpha}{\beta} + \tan^{-1}\frac{\alpha^2-\beta^2+\omega^2}{2\alpha\beta}$$

and

$$\psi_4 = \tan^{-1}\frac{\alpha(3\beta^2-\alpha^2)}{\beta(3\alpha^2-\beta^2)} - \tan^{-1}\frac{k_2-\alpha}{\beta} + \tan^{-1}\frac{\alpha^2-\beta^2+\omega^2}{2\alpha\beta}$$

To get a mathematical expression for torque the expressions for i_{d1}, i_{d2}, i_{q1}, and i_{q2} from equations (4.6), (4.7), (4.11) and (4.12) require to be substituted in equation (4.1). As this does not appear to lead to any mathematical simplification, it is preferable to substitute the machine constants in the expressions for the currents and then carry out the required numerical multiplication to obtain instantaneous values of torque.

4.2.2. Determination of Machine Constants:

The machine constants were determined from no-load and locked-rotor tests and resistance measurement as described by Veinott.[20] The values of the different parameters thus determined, at an applied voltage of 140 V, are

$$r_{d1} = 5.18 \text{ ohms}$$

$$r_2 = 7 \text{ ohms}$$

$$x_1 = x_2 = 8.8 \text{ ohms}$$

$$x_o = x_1 + x_m$$

$$= 231 \text{ ohms}$$

The starting winding resistance and series capacitance were measured and found to be 15.5 ohms and 93.2 μF respectively. From the winding diagram of the motor supplied by the manufacturer, the turns ratio 'a' was calculated to be 1.016.

An attempt was made to determine the total inductance of the main and starting windings directly using the method described by Prescott and El-Kharashi.[21] Because of the low values of current involved, the method did not give any accurate results but it showed that the turns ratio is almost unity as compared with the value of 1.016 calculated from winding details. A special rotor without the cage winding was obtained, and using this, the open-circuit reactances of the main and starting windings, at 50 c/s, were determined as 228 ohms and 226 ohms respectively. Therefore, in the numerical calculations the turns ratio is taken as unity and the total inductance of either winding is taken as that corresponding to the reactance of 227 ohms at 50 c/s. It is worth noting that the values determined directly and by Veinott's method are in agreement within 1.8%.

The different machine constants required for the numerical evaluation of equations (4.6), (4.7), (4.11) and (4.12) are, therefore,

r_{d1} = 5.18 ohms

r_{q1} = 15.5 ohms

r_2 = 7.00 ohms

L_{d1} = 0.722 H

L_{q1} = 0.722 H

L_2 = 0.722 H

M = 0.694 H

k_{d1} = 7.18 sec^{-1}

k_{q1} = 21.45 sec^{-1}

k_2 = 9.7 sec^{-1}

σ_d = 0.076

σ_q = 0.076

a = 1.00

C = 93.2 μF.

4.2.3. Numerical Computations:

The machine constants were substituted in equations (4.6), (4.7), (4.11) and (4.12) and the numerical expressions for the different currents were then obtained. Since the values of instantaneous torque are to be obtained as a difference of two comparatively large quantities [equation (4.1)], the current expressions had to be computed to a

greater accuracy than that with which the machine constants were determined. A desk calculator was used for this purpose. The resulting current equations are

$$i_{d1} = 0.024024\,[314.16\cos\phi - 218\sin\phi]\,e^{-218t} + 0.00094094\,[314.16\cos\phi - 4.2\sin\phi]\,e^{-4.2t} + 9.4393\sin(314.16t + \phi - 56°13') \quad \ldots\ldots (4.13)$$

$$i_{d2} = -0.024182\,[314.16\cos\phi - 218\sin\phi]\,e^{-218t} + 0.00068947\,[314.16\cos\phi - 4.2\sin\phi]\,e^{-4.2t} - 9.0733\sin(314.16t + \phi - 54°27') \quad \ldots\ldots (4.14)$$

$$i_{q1} = 0.025475\,[442\sin(394t - 30°9')\sin\phi - 314.16\sin(394t + 33°1')\cos\phi]\,e^{-200.15t} + 7.1331\,(314.16t + \phi + 37°37') \quad \ldots\ldots (4.15)$$

$$i_{q2} = -0.000017247\,[314.16\sin\phi - 9.7\cos\phi]\,e^{-9.7t} - 0.024774\,[442\sin(394t - 29°2')\sin\phi - 314.16\sin(394t + 34°1')\cos\phi]\,e^{-200.15t} - 6.8565\sin(314.16t + \phi + 39°23') \quad \ldots\ldots (4.16)$$

Correction :-
For ϕ read θ

The equation for instantaneous torque is now

$$T = 2 \times 0.694 \, (i_{d1} \, i_{q2} - i_{d2} \, i_{q1}) \qquad \ldots\ldots (4.17)$$

A Sirius Digital Computor was used to compute the instantaneous values of currents and torque. Points-on-wave from 0° to 180° in steps of 30° and also the 'salient' points-on-wave at which the two unidirectional components of current in the direct axis reach their maximum and zero values, were selected for the computation. Two programmes were drawn up, one to calculate the total torque at intervals of 0.1 ms for the first cycle and the other to calculate and print out the individual components of torque and the total torque for a period of 8 cycles from switching, at intervals of 2.5 ms. The computations were carried out for each of the selected points-on-wave.

4.2.4. Computed Results:

All the different significant components of torque for the four 'salient' points-on-wave are shown in Figures 4.5, 4.6, 4.7, and 4.8. Fig. 4.9 shows the variation of the alternating component of torque at the

first peak with respect to point-on-wave and also a Table showing the time of occurrence of the first peak against point-on-wave.

4.2.5. Discussion of Computed Results:

Examination of equations (4.13) to (4.17) shows that there are nine components of torque during the transient period. They are :

1. The steady-state torque resulting from the interaction of steady-state currents and fluxes.
2. A unidirectional component with a damping factor of 13.9 sec.$^{-1}$ (i.e. τ = 3.6 cycles).
3. Another unidirectional component with a damping factor of 227.7 sec.$^{-1}$ (i.e. τ = 0.22 cycle).
4. A line frequency alternating component with a damping factor of 4.2 sec.$^{-1}$ (i.e. τ = 11.9 cycles).
5. Another line frequency alternating component with a damping factor of 9.7 sec.$^{-1}$ (i.e. τ = 5.16 cycles).
6. A third line frequency alternating component with a damping factor of 218 sec.$^{-1}$ (i.e. τ = 0.229 cycle).
7. An alternating component with a frequency of 62.6 c/s and a damping factor of 204.2 sec.$^{-1}$ (i.e. τ = 0.245 cycle).

8. A second 62.6-c/s component with a damping factor of 418 sec.$^{-1}$ (i.e. τ = 0.12 cycle), and finally
9. An alternating component of composite nature with a damping factor of 200 sec.$^{-1}$ (i.e. τ = 0.25 cycle).

Because of the coupled nature of the circuits, the d-axis unidirectional currents and flux die out with two time constants. In the q-axis, there is a capacitor in series with the stator winding resulting in only one decaying unidirectional component of currents and flux and a decaying 62.6-c/s component. If the starting winding had no capacitor in series then the q-axis currents and flux also will have two unidirectional components. In that case instead of the last three components of transient torque, there will be two more unidirectional components and another line frequency component all decaying with time.

From the values of the different components, it is seen that the most important of them, besides the steady-state component, is the first line frequency component with a damping factor of 4.2 sec.$^{-1}$ The two unidirectional components and the second line frequency component with a damping factor of 9.7 sec.$^{-1}$ never reach any significant value. The rest of the components

all reach an insignificant value within the first cycle [Figs. 4.5 to 4.8]. However, these components do affect the magnitude of the first peak bringing it, in fact, slightly less than the second peak near 0° point-on-wave (Fig. 4.5). For points-on-wave near 90°, these components help to increase the value of the first peak and at 90° point-on-wave produce by themselves a net value of about 0.2 N-m. (Fig. 4.6).

4.2.6. Concluding Remarks:

The analytical investigation also shows the importance of point-on-wave of switching. The calculations have shown that the qualitative statement that the maximum alternating component of torque occurs for 0° point-on-wave is correct within 46 min. and that the instantaneous torque values for the exact point-on-wave for maximum alternating component, and 0° are the same. The 'secondary' alternating component has its maximum for 145° 13' or - 34° 47' p.-on-w. The net effect of all the minor alternating components is to oppose the principal component for points-on-wave near 0° and assist for points-on-wave near 90°.

The maximum value of the ratio of the first peak torque to the steady-state component is 2.51. The

principal alternating component has a damping factor of 4.2 sec.$^{-1}$ or a time constant of 11.9 cycles.

4.3. Comparative Study of the Experimental and Computed Results:

The analytical results appear to be generally in good agreement with those determined by direct experiment. Whereas the experimentally determined time constant of the main alternating component is 10.5 cycles, the corresponding analytical value is 11.9 cycles. Also the ratio of peak torque to steady-state torque for 0° point-on-wave is 2.1 as determined by experiment and 2.51 by analytical method. These two sets of results may be said to be in fair agreement but the differences lead one to suspect that the transient saturation is significant even at an applied voltage of 58.3% of normal value.

5. GENERAL DISCUSSION

5.1. Comments on Experimental Approach and Systems Used:

The experimental approach adopted in this investigation has yielded results which give a good understanding of the physical phenomena associated with transient torques in single-phase capacitor-start induction motors. It seems hardly likely that such a clear physical understanding would have resulted from the solution of the equations for the complex conditions of the free-rotor case. In any case, the solution for such a condition will generally involve simplifying assumptions. Before the permissible simplifying assumptions can be made, it is probably necessary to have some prior knowledge of the relative importance of the various physical phenomena involved.

The drag-cup accelerometer has proved to be a reliable device for observing the torque patterns which contain alternating components and sudden changes. Together with controlled switching this has enabled the effect of such basic factors as point-on-

wave and speed to be observed. The reaction detecting system, though more versatile, is slightly less satisfactory from the point of view of accuracy owing to the comparatively small output signal. Load cells which have recently become available have higher output and smaller displacement at rated capacity. With the use of such devices, it should be possible to obtain a more satisfactory signal level while maintaining the necessary system stiffness.

The Duddell records have not been of great help towards understanding the phenomena involved in the production of transient torques. However, the power trace shows that the peak values of power are fairly constant for 90° point-on-wave in which case the acceleration is also fairly uniform. For 0° point-on-wave, the peak values undergo a 50-c/s modulation corresponding to 50-c/s torque. Also when there is overspeeding, the motor actually feeds back power during the return swing.

5.2. Comparative Study of Free-Rotor and Blocked-Rotor Results:

From the results obtained for the free-rotor investigation, it was noticed that the overall effect of speed is to increase the value of peak torques up to about the third positive peak. Examination of computed results shows that for points-on-wave near zero this increase is helped by the electrical transients themselves. At 0° point-on-wave, components other than the principal line frequency component help to bring down the first peak torque by about 6.5% making it less than the second peak by about 1.5%. Since these components have a very large damping factor they do not affect the second and subsequent peaks. If, however, they happen to have a low damping factor - as for a machine with rather large rotor leakage reactance - their effect may persist long enough to affect further peaks also. In that case, an increase in the peak value may occur for a few cycles due to purely electrical reasons even with blocked rotor.

The blocked-rotor investigation does not appear to have yielded results as reliable as the free-rotor investigation. This is thought to be mainly due to the large amplification needed. The value of the first peak torque for 0° point-on-wave is about 5.8 N-m as compared with the computed value of 6.95 N-m, a difference of about 17%. This may also be due to the difficulty in estimating the value of steady-state torque since it contains large amplitudes of 50-c/s and 100-c/s torques due to unbalanced magnetic pull. It may be possible to overcome this difficulty by a direct calibration of the reaction detecting system. However, the results have given reliable values for the time constant of decay of the transient torques. The value of 210 ms for the principal time constant compares favourably with the computed value of 238 ms. The results have also demonstrated the effects of high transient magnetic saturation at higher voltages.

Investigators using purely analytical methods, have generally considered the blocked-rotor transients to be a satisfactory approximation of the actual

starting transients. This assumption appears to be satisfactory only as far as the first peak torque is concerned, as can be seen from the following Table which was obtained for 140 V and 0° point-on-wave.

TABLE

Torque in N-m / Method	First positive peak	Second positive peak	Third positive peak
Computation for Blocked Rotor conditions	6.95	7.06 (max.)	6.7
Experiment with Free Rotor	7.2	8.0	8.37 (max.)

If the computed value of this first positive peak under blocked-rotor conditions was taken as an estimate of the likely largest peak for free-rotor conditions, there would be an error of about -17%.

5.3. Explanation of the Dissimilar Variation of the Alternating Component of Torque for Equal Deviations from 90° point-on-wave:

It was noticed during the study of p.-on-w. effect with free rotor that the variation of the alternating component of torque with respect to point-on-wave between 90° and 180°, is not exactly the same as that between 0° and 90°(p.22/23). It was also pointed out at that time that it does not appear to be possible to explain this difference in terms of point-on-wave. It is now possible to account for this with the aid of information obtained from the blocked-rotor studies.

Fig. 4.9 shows the variation of the alternating component of torque at the first peak with respect to point-on-wave as obtained from computed results. The variation between 0° and 90°, and that between 90° and 180° are the same. However, examination of the accompanying Table shows that between 90° and 180° the peaks occur somewhat later than between 0° and 90°. From Fig. 3.3 it is seen that, for the free-rotor case the values between 90° and 180° are less than those between 0° and 90° for the same deviation from 90°. It appears,

therefore, that during the longer time that the torque has taken to reach its first peak, the dynamic braking torque has increased significantly enough to affect the value of the peak torque.

5.4. Practical Significance of Transient Torque:

The purpose of this investigation is primarily to attempt to fill a gap in the knowledge of the performance of single-phase capacitor-start induction motors. There is little to suggest that the magnitude of the transient torques are normally sufficient to influence design and operating considerations. When started from rest with 140 V applied, the maximum peak torque is 8.37 N-m as compared with a maximum of about 6.0 N-m just before the centrifugal switch operates. The latter value is the largest value of torque likely to be obtained from steady-state theory, if care is taken to include the 100-c/s pulsating torque. The maximum transient peak torque is, therefore, about 40% greater than that could be obtained from steady-state theory. However, if the motor is re-closed while the rotor is still running near its no-load speed, it is subjected to a severe dynamic breaking torque before

it accelerates. The magnitude of this braking torque has a maximum of about 15 to 16 N-m. This is about 150% greater than the maximum of 6 N-m for steady-state conditions, or about 18 times full-load torque. It is felt that this is an important point of some practical significance though the occurrence of such a severe dynamic braking torque may normally be rare in practice. Where a motor is to be used connected to a load of comparatively large inertia, and if re-connecting the supply while the rotor still has substantial speed is a distinct possibility, the danger of mechanical damage to the shaft may be quite significant. Under such circumstances the possibility of installing a simple p.-on-w. control system which will ensure connection at or near maximum voltage, may be worth considering.

6. CONCLUSIONS

The initiation of transient torques in single-phase capacitor-start induction motors is dependent upon the point-on-wave of applying the supply voltage. Such torques attain a maximum value for a point-on-wave near 0° and are almost completely absent for 90° point-on-wave. The instantaneous torque attains negative values when the transient component is a maximum. The maximum amplitude of the initial alternating component of torque is not much greater than the steady-state value.

Speed plays an important part in governing the duration of the transient torque and the magnitude of the largest peak. It actually helps to increase the amplitude of the alternating component for some appreciable time. This is not likely to be so in the case of 'split-phase' motors, i.e., single-phase motors which do not use series capacitance in the starting winding circuit. The duration of the alternating component is almost completely governed by speed except for very long run-up times. The run-up times are determined mainly by the T/J ratio. For large T/J

ratios the motor undergoes transient overspeeding before it finally attains its normal no-load speed.

When the motor is started from rest, the effects of speed and point-on-wave do not produce torque peaks very much in excess of the maximum torque for steady-state conditions. If it is reconnected to the supply while the rotor is still rotating near the no-load speed, these factors can produce a very considerable dynamic braking torque. This transient braking torque can reach a maximum value of about 250% of the maximum that can be predicted from steady-state calculations, even allowing for the double-frequency pulsating torque. In terms of full-load torque the maximum net braking torque is of the order of 15 to 20 times greater.

Calculations based on the assumption of zero speed give a value for the first peak torque which is reasonably close to the actual value that is obtained during normal starting conditions. However, the maximum value obtained during normal starting conditions is about 17% greater than that obtained by calculations with zero speed assumption.

7. SUGGESTIONS FOR FURTHER WORK

Since the present work is probably the first attempt at a systematic experimental study of transient torques in single-phase induction motors - indeed, induction motors in general - it follows that the study, by direct experimental methods, of transient torques in induction machines is by no means exhausted. In the case of balanced polyphase machines, in addition to an investigation similar to the present one, such phenomena as that resulting from non-simultaneous connection of phases is of particular interest. In all induction machines, the effects of different types of load could be explored. The possibilities are too numerous to detail. Therefore only a few suggestions which follow immediately from the present work will be discussed.

The effect of varying T/J ratio has been studied in the present investigation by varying the applied voltage. This necessarily brings in the effect of saturation. It would be interesting to study this effect by keeping the applied voltage constant and adding external inertia to vary the T/J ratio.

It has been shown that there can be a very large dynamic braking torque during re-closing while the rotor is revolving. In the free-rotor investigations, this torque does not act on the shaft. It would be worth studying the effect on the shaft of such large dynamic braking torques. A speed stabilizing system would be required for this purpose. This may be achieved by coupling the motor to a large d.c. machine which can be used to keep the rotor revolving at any desired speed including speeds greater than synchronous speed. Alternatively, a flywheel with a very large amount of inertia can be coupled when speeds over no-load speed are not considered. Such a system can also be used to study the transient torques at selected constant speeds.

In the study by Das Gupta,[12] of the possibility of reversing single-phase induction motors by reversing the supply, the instant of reversing the connections was at a random point on the supply voltage wave. As this possibility depends on the point-on-wave at the instant of operation, it would be much more satisfactory

to investigate this with the necessary p.-on-w. control, as could be provided by the equipment used in the present study.

Single-phase induction motors of the type employed in the present investigation, are widely used in sizes ranging from about 1/50 horse power to a few horse power. An experimental study based on the present work, is needed to ascertain the influence of size and associated parameter variations.

APPENDICES

I. REVIEW OF POSSIBLE METHODS OF DETECTING TRANSIENT TORQUE

The total torque developed by an electrical machine during a transient period is made up of three components, namely, the accelerating torque - present only when the machine speed is not constant, the transmitted torque and the friction and windage torque. The friction and windage torque is generally so small that it can be neglected. Therefore the total developed torque, also known as the air-gap or electromagnetic torque, can be taken to be approximately equal to the sum of the accelerating and transmitted torques.

Any satisfactory method of obtaining the electromagnetic or air-gap torque would meet the requirements of both phases of the present study. However, for the case of free rotor it may be preferable to consider the direct method i.e., recording of acceleration. Since the study is limited to unloaded conditions, it might appear to be unnecessary to consider transmitted torque devices. A little consideration shows that this is not necessarily true. A device for observing

transmitted torque could be used as a basis of a scheme for obtaining stalled-rotor torque. Furthermore, if the addition of external inertia together with a compensating increase in supply voltage can be considered such devices can also be used for obtaining acceleration torque. Thus, it is necessary to consider methods of detecting air-gap torque, acceleration torque, and transmitted torque.

I.1. Air-gap Torque:

The total electromagnetic torque is produced by the interaction of the air-gap flux in one axis with the rotor current in the axis in quadrature. Thus, for a two-axis machine, we have torque

$$T \propto (\phi_q \, i_{d2} - \phi_d \, i_{q2})$$

To obtain a signal corresponding to the air-gap torque, it would be necessary to locate probes in the d- and q-axes of the air-gap to obtain signals which when integrated would represent the flux along these axes. Signals proportional to the d- and q- axes rotor currents are also required, and, since these axes are fixed in space, suitable signals can be obtained only from a rotor

with a commutator winding. Alternatively, the commutator can be avoided by using signals proportional to stator currents in these axes. Though ideal in theory, the special constructional features required make this likely to be quite difficult in practice. In any case, a good approximation to the total developed torque can be readily obtained by the stator reaction torque.

Stator reaction torque is equal to the total electromagnetic torque less the friction torque and, if the rotor is free to rotate, part of the windage torque. The essential requirement of such a system is a freely suspended stator and force-sensing devices which can faithfully follow variations in pressure up to at least twice the supply frequency. It is convenient to use these force-sensing devices exclusively in compression and therefore it is essential to preload the sensors sufficiently so that possible negative torques are catered for. Certain types of pressure transducers such as load cells may be suitable for this purpose and worth considering.

I.2. Acceleration Torque:

Methods of measuring angular acceleration may be classified broadly into two types, continuous and discontinuous. Preliminary tests on the starting time of the motor showed that the motor reaches running speed in about one-third of a revolution at full voltage and about one and a half revolutions at half voltage. It therefore appears that the torque transients will be associated with little angular displacement and thus discontinuous methods, for example, those based on digital recording of shaft position are likely to be inadequate and need not be considered further.

Continuous methods may again be subdivided into direct and indirect methods. The indirect methods obtain a speed signal and differentiate it. A speed signal could be obtained from, say, a homopolar d.c. generator but minor voltage variations are liable to occur continuously, independent of speed variation. These variations, though small in themselves, can when differentiated, result in unreliable signals. Direct methods of measuring acceleration are therefore preferable.

One method of measuring acceleration directly is to use a Piezo-electric crystal.[22] The particular property of such a crystal is that, if it is subjected to force along its mechanical axis, an electrical P.D. proportional to force, is developed along its electrical axis. Therefore, if a Piezo-electric crystal is suitably attached to a rotating disc, then the output signal will be proportional to the angular acceleration. However, in order to measure and record the signal from the crystal, a slip-ring and brush-gear assembly will be necessary. This, together with the fact that the output of the crystal is small and dependent upon temperature and air-gap size, makes this technique of doubtful suitability.

A method which combines the advantages of continuous and direct measurement with the reliability of a brushless device, uses a two-phase drag-cup induction generator.[23] Such a device is normally used with a.c. excitation of a certain fixed frequency and gives an output of the same frequency but with an amplitude proportional to the speed of the drag-cup rotor. If, however, d.c. excitation is used (Fig. I.1)

the main flux Φ_d will be constant and rotation will produce e.m.f.'s which because of the negligible rotor inductance[24] will result in currents distributed at all times, as shown. These rotor currents give rise to a cross flux Φ_q dependent on speed. This flux will link the q-axis stator winding and provide a signal only when speed is changing. As drag-cup rotors have high resistance, the effect of armature reaction will be negligible and, in any case, this must effect speed signals in the same way as acceleration signals. Commercial types of drag-cup tacho-generators are designed to have speed linearities of the order of $\pm$ 0.5% and so can be expected to give, with d.c. excitation, acceleration signals of the same accuracy.

I.3. Transmitted Torque:

Commercial types of 'torquemeters' generally give transmitted or 'shaft' torque.[25,26,27] The possibility of using one such scheme or of devising a suitable system using, for example, strain gauges or capacitive displacement pick-ups, is worth considering, particularly for the stalled-rotor case.

I.4. Choice of Systems:

After a general consideration of the relative merits of the various systems in relation to their particular requirements, it was decided to adopt,

(a) a d.c. excited drag-cup induction generator for the free-rotor case, and

(b) a stator reaction measuring scheme using a precision load cell for the stalled-rotor case.

II. CALIBRATION OF THE DRAG-CUP ACCELEROMETER

The accelerometer was calibrated both by direct experimental methods and by calculation from experimentally determined speed sensitivity. At first an attempt was made to achieve constant values of acceleration of known magnitude by means of a system of falling weights. Due to the effects of viscous and aerodynamic friction, stretching of the chord, vibration, etc., no satisfactory result was achieved and attention was transferred to methods of obtaining periodically varying acceleration. Two methods were used, one employing an electromagnetic vibration generator and the other a simple link mechanism.

II.1. Calibration using an Electromagnetic Vibration Generator:

The vibration generator used, produces linear S.H.M. up to an amplitude of ± 3/16". Beyond this the motion ceases to be simple harmonic. When connected to the periphery of a small disc fitted on the shaft of the accelerometer (Fig. II.1) angular S.H.M. was obtained provided the diameter of the disc is so

chosen that the maximum angular displacement in within 15°.

The frequency of oscillation was set at exact multiples and submultiples of mains value. The linear amplitude of vibration was measured using a microscope and a stroboscope (Fig. II.1). A mark was made on the armature and the frequency of the stroboflash was adjusted to be slightly different from the frequency of vibration. The mark now appeared to move very slowly between the extremities of its travel. The distance between these two positions was measured by the microscope. The corresponding output from the accelerometer was recorded.

For an S.H.M., the equation of motion is $x = a \sin \omega t$, where 'a' is the amplitude and equals half the total travel measured by the microscope. Differentiating this twice, the linear acceleration is obtained as

$$\ddot{x} = -\omega^2 a \sin \omega t.$$

Therefore, the peak angular acceleration is

$$\ddot{\theta}_{max} = \frac{\ddot{x}_{max}}{r} = \frac{a\omega^2}{r}$$

Where 'r' is the radius of the disc attached to the accelerometer.

The results (Fig. II.2) show reasonable linearity but there is appreciable scatter. This was thought to be due to the difficulty in maintaining proper alignment.

II.2. Calibration using a Link Mechanism:

If two discs, one smaller in radius than the other are coupled by a rigid link and if the smaller disc is rotated at a constant angular velocity ω, then the larger disc will undergo angular oscillations. Oscillatory motion, not necessary sinusoidal, was achieved in this way (Fig, II.3). The design (Fig. II.4.) was chosen to simplify the associated mathematics.

For the arrangement chosen, the angular oscillations are given by the following expression:

$$l^2 = (x+r_2 \sin \phi - r_1 \sin \omega t)^2 + (r_2 \cos \phi - r_1 \cos \omega t)^2$$

... ... (II.1)

Hence,

$$\frac{d\phi}{dt} = \frac{r_1 \omega}{r_2} \frac{[-x \cos \omega t + r_2 \sin(\omega t - \phi)]}{[-x \cos \phi + r_1 \sin(\omega t - \phi)]}$$

... ... (II.2)

and

$$\frac{d^2\phi}{dt^2} = \frac{r_1 \omega}{r_2} \cdot$$

$$\cdot \left[\frac{\begin{array}{l} [-x \cos\phi + r_1 \sin(\omega t - \phi)][x\omega \sin \omega t + r_2 \cos(\omega t - \phi) \cdot (\omega - \frac{d\phi}{dt})] \\ - [-x \cos \omega t + r_2 \sin(\omega t - \phi)][x \sin\phi \frac{d\phi}{dt} + r_1 \cos(\omega t - \phi)(\omega - \frac{d\phi}{dt})] \end{array}}{[-x \cos \phi + r_1 \sin (\omega t - \phi)]^2} \right]$$

... ... (II.3)

To obtain the value of ωt corresponding to maximum acceleration, it would be necessary to differentiate again and equate $\frac{d^3\phi}{dt^3}$ to zero. As the resulting equation is going to be a function of expressions (II.1), (II.2), and (II.3), a purely analytical solution was not attempted.

By graphical means a curve relating ωt and ϕ was determined. From this displacement curve, the acceleration curve was derived by numerical double differentiation using the formula

$$a_n = \frac{\phi_{n+2} + \phi_{n-2} - 2\phi_n}{4\tau^2} \qquad \text{.... (II.4)}$$

where τ corresponds to the time interval at which the values of ϕ are measured. The acceleration curve for τ equal to unity is shown in Fig. II.5 along with the displacement curve.

Since the maximum values of acceleration obtained by grapho-numerical differentiation are not likely to be of the required order of accuracy, the values of ωt alone corresponding to peak accelerations were taken from Fig. II.5. These values were substituted in equations (II.1), (II.2), and (II.3), to obtain reliable values of acceleration at any given speed.

The driving disc was attached to the shaft of a d.c. motor (Fig. II.3), the speed of which was controlled by a Ward-Leonard system. As the output waveform

(Fig. II.6) remains independent of speed and agrees well with the theoretical form, it can be concluded that the effects of speed are negligible. The device is quite linear (Fig. II.7) and has a sensitivity of 0.24 mV per radian per sec^2.

II.3. Calculation of Acceleration Sensitivity from Experimentally Determined Speed Sensitivity.[28]

The experimental confirmation of the expected linearity of the output signal permits the calculation of an acceleration sensitivity value on the basis of a known or measured speed sensitivity.

When the generator is used with alternating current excitation,

$$\hat{\Phi}_d = k_1 \hat{i}_{d(a.c)}$$, since demagnetizing effects are negligible. Furthermore, k_1 is a constant since there is no saturation (verified experimentally).

Also $$\hat{\Phi}_q = k_2 \omega_r \hat{\Phi}_d$$

and $$\hat{e}_q = k_3 \omega \hat{\Phi}_q$$

Thus $\hat{e}_q = k_1 k_2 k_3 \omega_r \omega \hat{i}_{d(a.c)}$

or $E_q = k_1 k_2 k_3 \omega_r \omega I_{d(a.c.)}$

Let $\frac{E_q}{\omega_r} = K = k_1 k_2 k_3 \omega I_{d(a.c.)}$ (volts/rad.per sec.)

When used with direct current excitation,

$$\Phi_d = k_1 I_{d(d.c.)}$$

$$\Phi_q = k_2 \omega_r \Phi_d$$

$$= k_1 k_2 \omega_r I_{d(d.c.)}$$

Therefore $\frac{d\Phi_q}{dt} = k_1 k_2 I_{d(d.c.)} \frac{d\omega_r}{dt}$

But $E_q = k_3 \frac{d\Phi_q}{dt}$

$$= k_1 k_2 k_3 I_{d(d.c.)} \frac{d\omega_r}{dt}$$

$$= \frac{K}{\omega} \frac{d\omega_r}{dt}, \text{ if } I_{d(a.c.)} = I_{d(d.c.)}$$

Therefore $E_q \Big/ \frac{d\omega_r}{dt} = \frac{K}{\omega}$ (volts/rad.per sec.^{2})

The value of the output e.m.f. per radian per second, K_p was measured for a selected excitation (0.2 A) and was found to be 0.0785 V/rad. per sec. It was also found that the output was linear up to 3000 r.p.m., which is twice the speed of the motor being studied. Therefore the acceleration sensitivity is 0.25 mV/rad. per sec.^{2}.

II.4. Discussion of Results:

Acceleration Sensitivity mV/rad. per sec^2.	Method used
0.27	Vibration Generator
0.24	Link Mechanism
0.25	Calculation from Speed Sensitivity

The two direct experimental methods give somewhat different values and it is necessary to consider their relative merits. The first method did not give completely satisfactory result, there being appreciable scatter (Fig. II.2). In contrast with this the link

mechanism gives almost perfectly linear output (Fig. II.7). It is therefore considered that the first method is not sufficiently reliable and the value obtained from it will be ignored. Thus the final value is taken to be the average of the value obtained by calculation from speed sensitivity and that obtained by the link mechanism, i.e. 0.245 mV/rad. per sec.^{2} The accuracy of this value can be expected to be $\pm$ 2%.

III. DESIGN OF STATOR REACTION DETECTING SYSTEM

The main design feature of the stator reaction system is the choice of the natural frequency for the system so that it has a satisfactory response up to at least 100 c/s. Let the system have a natural frequency of oscillation of 'fn' and consider it to be subjected to forced vibrations by a disturbing force of frequency 'fd'. The ratio of the amplitude under a periodically varying disturbing force to the statical deflection is called the 'magnification factor' and it is given by[29]

$$\beta = \frac{1}{1 - \frac{fd^2}{fn^2}} \qquad \text{.... (III.1)}$$

when damping is negligible.

It is reasonable to assume that the damping of the system shown in Fig. 2.5 is negligible. Even if damping is present, its effect is only to bring the magnification factor nearer unity since in that case the magnification factor is given by

$$\beta = \frac{1}{\sqrt{\left(1 - \frac{fd^2}{fn^2}\right)^2 + \frac{fd^2 r^2}{fn^2}}} \qquad \text{.... (III.2)}$$

where 'r' is a factor proportional to damping. To get a magnification factor as near unity as possible up to 100c/s, 'fn' should be made as high as possible.

The natural frequency of Torsional oscillations is given as

$$fn = \frac{1}{2\pi}\sqrt{\frac{T}{J}} \qquad \text{.... (III.3)}$$

where 'T' is the torque per unit twist and 'J' is the mass moment of inertia about the axis of oscillation. To obtain a high value for 'fn', 'J' must be made as small as possible and 'T' must be made as large as possible. The only possible reduction in the moment of inertia of the stator was by removal of the starting-winding capacitor from the stator frame. With the capacitor removed, the moment of inertia of the stator was determined as follows. In place of the load cell and the ring shown in Fig. 2.5, two light springs of known spring constants were introduced. The system was then made to oscillate freely and the oscillation was recorded with the aid of the

accelerometer, A, and compared with a 50-c/s timing wave. From the frequency of oscillation (9.03 c/s) and the torque per unit twist (167.5 N-m), the moment of inertia was calculated to be 0.052 kg-m^2.

The maximum displacement for the 100 lb. load cell used, is quoted by the manufacturer as 0.015 inch. The stiffness of the load cell is therefore 1.17×10^6 N/m. If the whole of the restoring torque is provided only by the load cell, then the natural frequency will be 66 c/s. It is therefore necessary that the system stiffness be increased many times. But as the total stiffness is increased the load taken by the load cell decreases. In other words the sensitivity of the system decreases. As the output of the load cell is already small (16 mV at its rated capacity), the total stiffness should not be increased more than is absolutely necessary. A natural frequency of 450 c/s at least is required in order to get a magnification factor of 1.01 at 50 c/s and 1.05 at 100 c/s. To obtain this order of natural frequency, the total stiffness has to be about $(450/66)^2$ or 47 times that of the load cell. As any type of stiffening column will be too thin to be used

in compression, a ring design was adopted.

The displacement in the direction of load for a thin ring is given by Timoshenko[30] as

$$\delta = 0.149 \frac{PR^3}{EI} \quad \text{.... (III.4)}$$

where 'P' is the load, 'R' the mean radius, 'E' the elastic modulus and 'I' is the moment of inertia of the section of the ring. The design dimensions of the steel ring are shown in Fig. III.1. The deflection of this ring at a load of 100 lbs was calculated using equation(III.4) and it is 0.322×10^{-3} inch. This gives a stiffness for the ring of 46.6 times that of the load cell. With this ring as the required stiffener, the natural frequency of the system is raised to about ($\sqrt{47.7} \times 66$) i.e. 456 c/s.

An estimation of the deflection of the U-channels treating them as eccentrically loaded simply-supported beams, shows that their effective stiffness is comparable with that of the rest of the system. As this will bring down the natural frequency if allowed to be present, the channels were supported

by jacks directly under the points of loading.

Electrical connections to the load cell are as shown in Fig. III.2. The precision potentiometer is introduced to enable measurements of static load to be made and also to help maintain the trace on the oscillograph screen.

IV. NAME PLATE DETAILS OF THE MOTOR

CP. 344

GRYPHON (Brook Motors Ltd.)

No. C1447 OZ

50 ~, Type - PROT.

240 volts

Continuous Rating

1 phase, RPM 1420

3.4 F.L. Amps

0.5 H.P., 50°C Rise

B.S. 170 39 233

ACKNOWLEDGEMENTS

The author wishes to express his sincere gratitude to Professor F.M. Bruce for his encouragement and for providing the facilities of the department.

Thanks are due to the members of staff of the Department of Electrical Engineering, Royal College of Science and Technology for their interest in the work. The author is greatly indebted to Mr. W.S. Wood for his guidance and for many hours of useful discussion.

Appreciation is also due to Mr. J. Brown, Senior Laboratory Technician, Mr. W. McAdam, Photographic Technician, and the workshop staff for their valuable services. Permission by the Department of Mathematics to use the Digital Computer is gratefully acknowledged.

The opportunity of doing this work was provided by the award of a Commonwealth Scholarship and the author is sincerely grateful to the Commonwealth Scholarship Commission in U.K. for this. The author is particularly and deeply grateful for the warmth and sympathy shown by all the members of staff at the time of his personal bereavement.

REFERENCES

1. Wahl, A.M. and Kilgore, L.A.: "Transient Starting Torques in Induction Motors", Transactions of the American I.E.E., 1940, Vol. 59, p.603.

2. Stanley, H.C.: "An Analysis of the Induction Machine", ibid., 1938, Vol. 57, p.751.

3. Gilfillan, Jr., E.S. and Kaplan, E.L.: "Transient Torques in Squirrel-Cage Induction Motors with Special Reference to Plugging", ibid., 1941, Vol. 60, p.1200.

4. Maginniss, F.J. and Schultz, N.R.: "Transient Performance of Induction Motors", ibid., 1944, Vol. 63, p.641.

5. Weygandt, C.N. and Charp, S.: "Electromechanical Transient Performance of Induction Motors", ibid., 1946, Vol. 65, p.1000.

6. Lyon, W.V.: "Transient Analysis of Alternating-Current Machinery" (The Technology Press of Massachusetts Institute of Technology, 1954).

7. Chidambara, M.R. and Ganapathy, S.: "Transient Torques in 3-phase Induction Motors During Switching Operations", Transactions of the American I.E.E., April 1962, No. 59, p.47.

8. Takeuchi, T.J.: "Starting Transient Torque of Squirrel Cage Induction Motor", Electrotechnical Journal of Japan, 1961, Vol. 6, No. 3/4, p.120.

9. Takeuchi, T.J.: "Transient Phenomena at Instant of Changing Power Source of Induction Motor while it is Running", ibid., 1960, Vol. 6, No.1, p.3.

10. Rao, P. Venkata.: "Switching Transients in Single-phase Induction Motors", Transactions of the American I.E.E., 1956, Vol. 75, pt.III, p.1023.

11. Rao, P. Venkata.: "Switching Transients in Single-phase Induction Motors with Constant Speed", ibid., 1959, Vol. 78, pt.III A, p.713.

12. Das Gupta, A.K.: "Possibility of Reversing Single-phase Squirrel Cage Induction Motors by Reversing the Terminal Supply Voltage", ibid., 1960, Vol. 79, pt. III, p.679.

13. Reyrolle and Co.Ltd.: "Description and Operation Recommendations for Dekatron Sequence-Control Unit Type-444/7/1" - IOMS 690/10-60.

14. Veinott, C.G.: "Theory and Design of Small Induction Motors", (McGraw-Hill Book Company Inc., New York, 1959).

15. Wood, W.S.: "Theory of Electrical Machines", (Butterworths Scientific Publications, London, 1958).

16. Ager, R.W.: "Transient Overspeeding of Induction Motors", Transactions of the American I.E.E., 1941, Vol. 60, p.1030.

17. Robinson, R.C.: "Line-Frequency Magnetic Vibration of A-C Machines", Transactions of the American I.E.E., February, 1963, No. 64, p.675.

18. Adkins, B.: "The General Theory of Electrical Machines" (Chapman and Hall, London, 1959).

19. Zaguskin, V.I.: "Handbook of Numerical Methods for the Solution of Algebric and Transcendental Equations" (Pergamon Press, London, 1961).

20. Veinott, C.G.: "Segregation of Losses in Single Phase Induction Motors", Transactions of the American I.E.E., 1935, Vol. 54, p.1302.

21. Prescott, J.C. and El-Kharashi, A.K.: "A Method of Measuring Self-Inductances Applicable to Large Electrical Machines", Proceedings I.E.E., Paper No. 2871 M, April 1959, Vol. 106, Part A, p.169.

22. Brüel, Per V.: "Modern Accelerometers", Technical Review (Denmark), April 1952, No. 2, p.2.

23. Wood, W.S. and McNaull, I.: "A Simple Method of Recording Angular Acceleration", The Engineer, March 30, 1962, Vol. 213, No. 5540, p.569.

24. Laeroux, Gérard : "The Asynchronous Motor with a Drag Cup Rotor", L'Électricien, December, 1960, Vol. 88, p.235.

25. General Electric Co.: "Electromagnetic Torque Meter", Pamphlet GEA 4441 B.

26. ..... : "Capteurs de Torsion", Pamphlet VM 314-F, Fribourg/Switzerland.

27. Orvar Dahle, Research Laboratories: "The Ring Torductor - A Torque-Gauge, Without Slip Rings, for Industrial Measurement and Control", A S E A Journal, 1960, Vol. 33, No.3, p.23.

28. Wood, W.S., and Shanmugasundaram, A.: "Performance of a Type E-5-A/1 2" Induction Generator as an Angular Accelerometer": Muirhead Technique (In Print).

29. Timoshenko, S. - "Vibration Problems in Engineering", (D. Van Nostrand Co.Inc., 1928).

30. Timoshenko, S.: "Strength of Materials", Part II, (D. Van Nostrand Co.Inc., 1941).

ILLUSTRATIONS

FIG.2.1. DEKATRON CONTROL UNIT INCORPORATING POINT-ON-WAVE SWITCHING

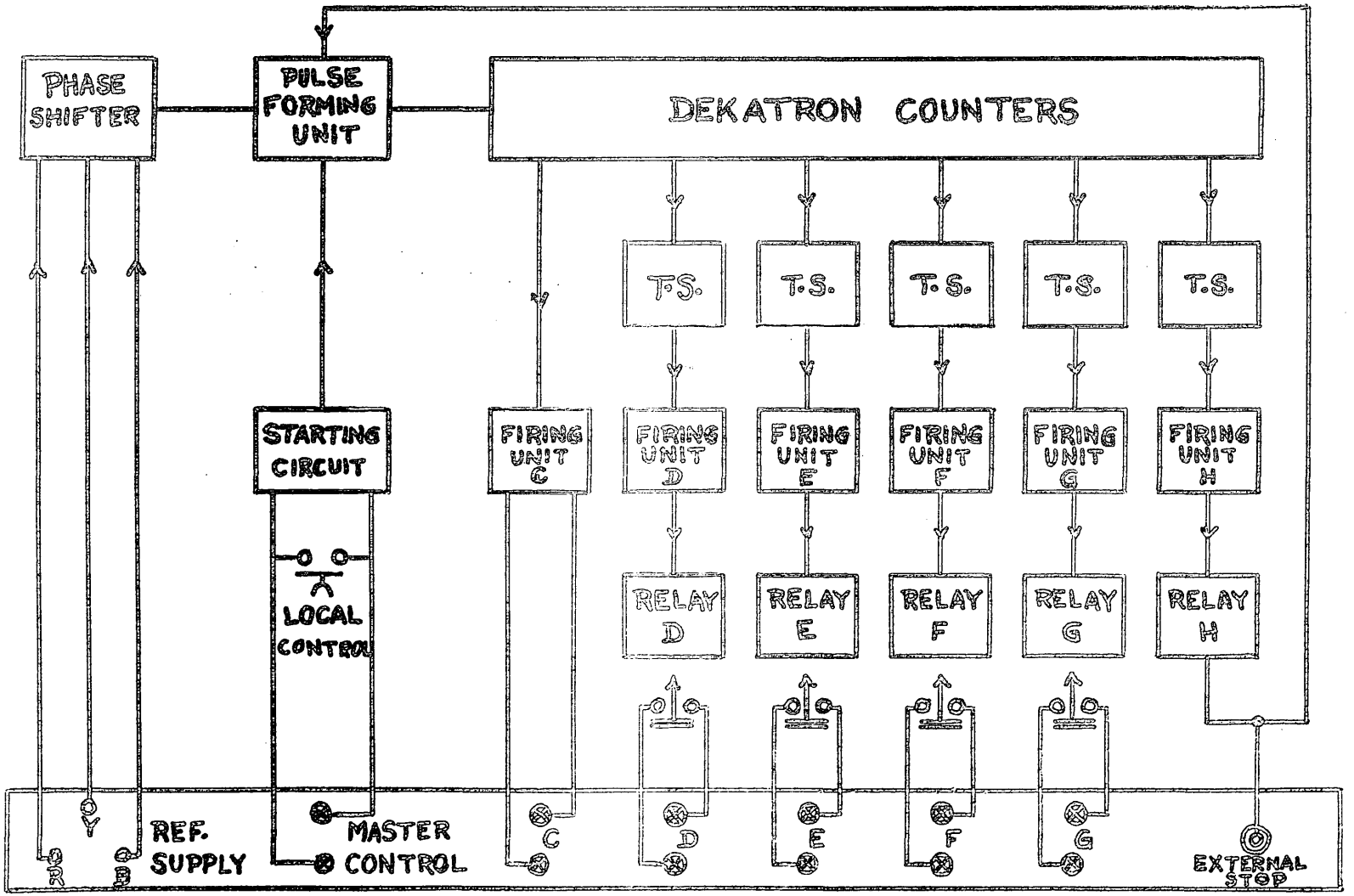

FIG. 2.2. BLOCK DIAGRAM OF THE CONTROL UNIT

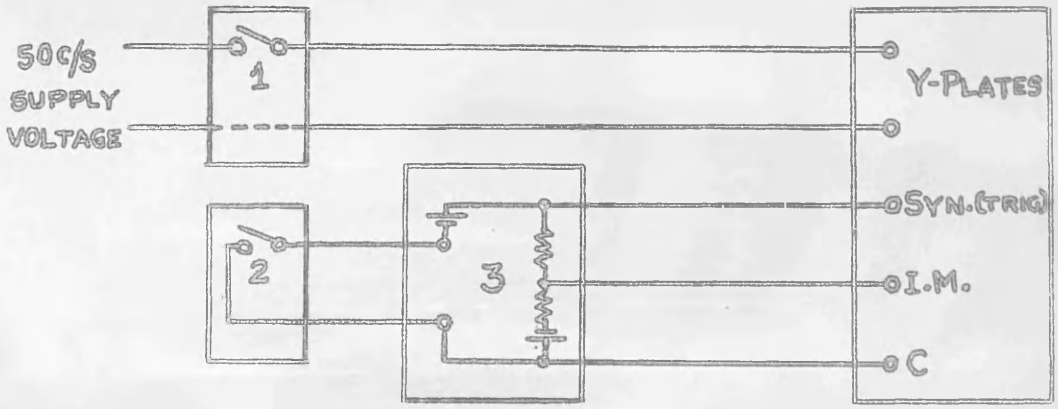

1. CHANNEL E WITH INTEGRAL $\frac{1}{2}$ CYCLE DELAY
2. CHANNEL D WITH NO DELAY
3. TRIGGERING AND BRIGHTENING CIRCUIT

FIG. 2.3a. CIRCUIT FOR OBSERVING POINT-ON-WAVE

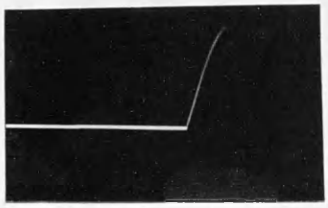

0° p.-on-w.

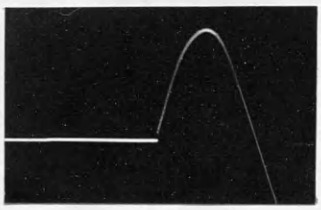

+ 2° p.-on-w.

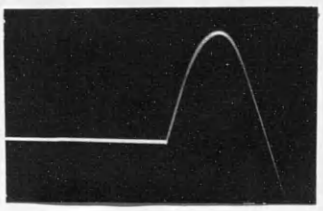

- 2° p.-on-w.

FIG. 2.3b. ACCURACY OF SELECTION OF 0° P.-ON-W.

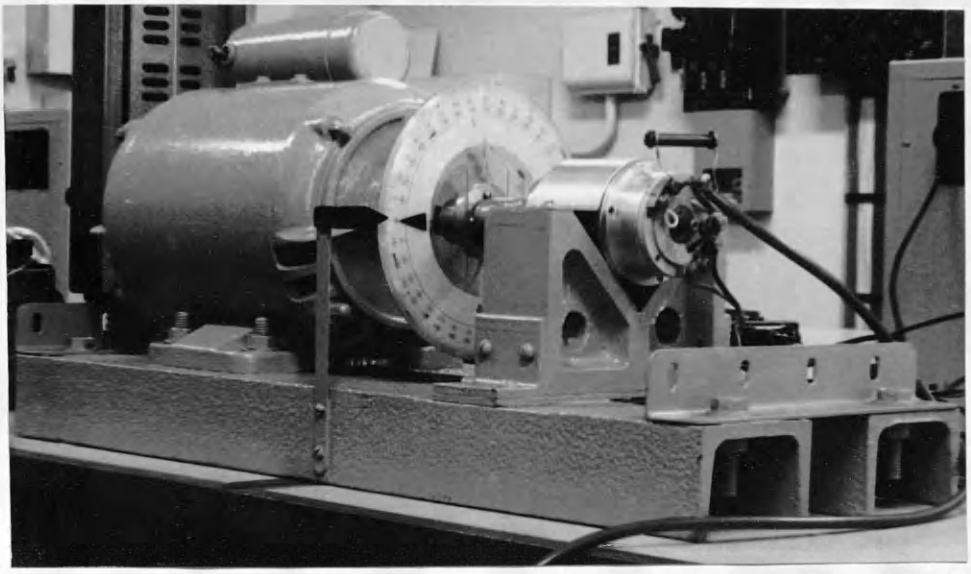

FIG.2.4. MOTOR WITH ACCELEROMETER RIGIDLY COUPLED

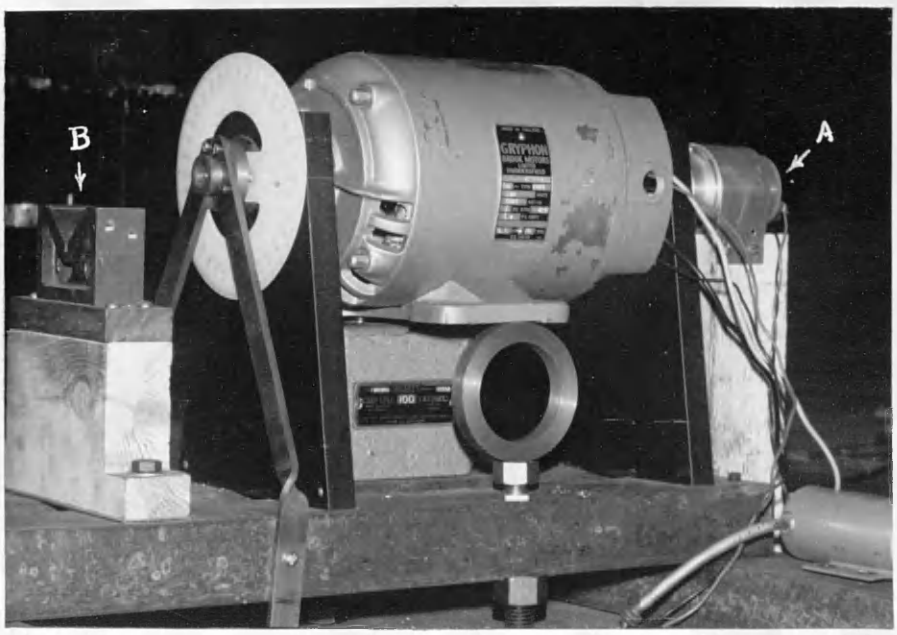

FIG.2.5. SCHEME FOR STUDYING TRANSIENT TORQUES WITH ROTOR BLOCKED

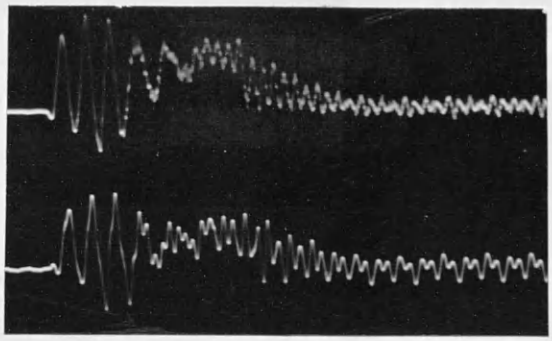

FIG. 2.6 a. SIMULTANEOUS RECORDING OF AN ACCELERATION AND CORRESPONDING STATOR REACTION SIGNALS

(Blocking arms of Fig. 2.5 are removed and an accelerometer, on the V-block B, coupled to the free shaft.)

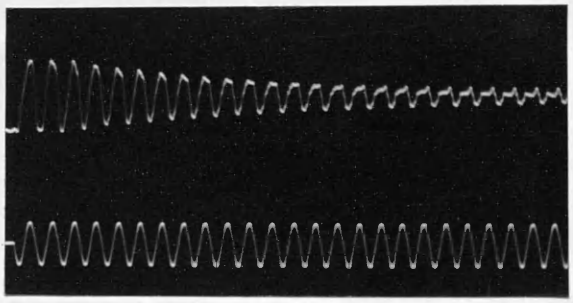

FIG. 2.6 b. A TYPICAL STATOR REACTION PATTERN FOR BLOCKED-ROTOR CONDITIONS

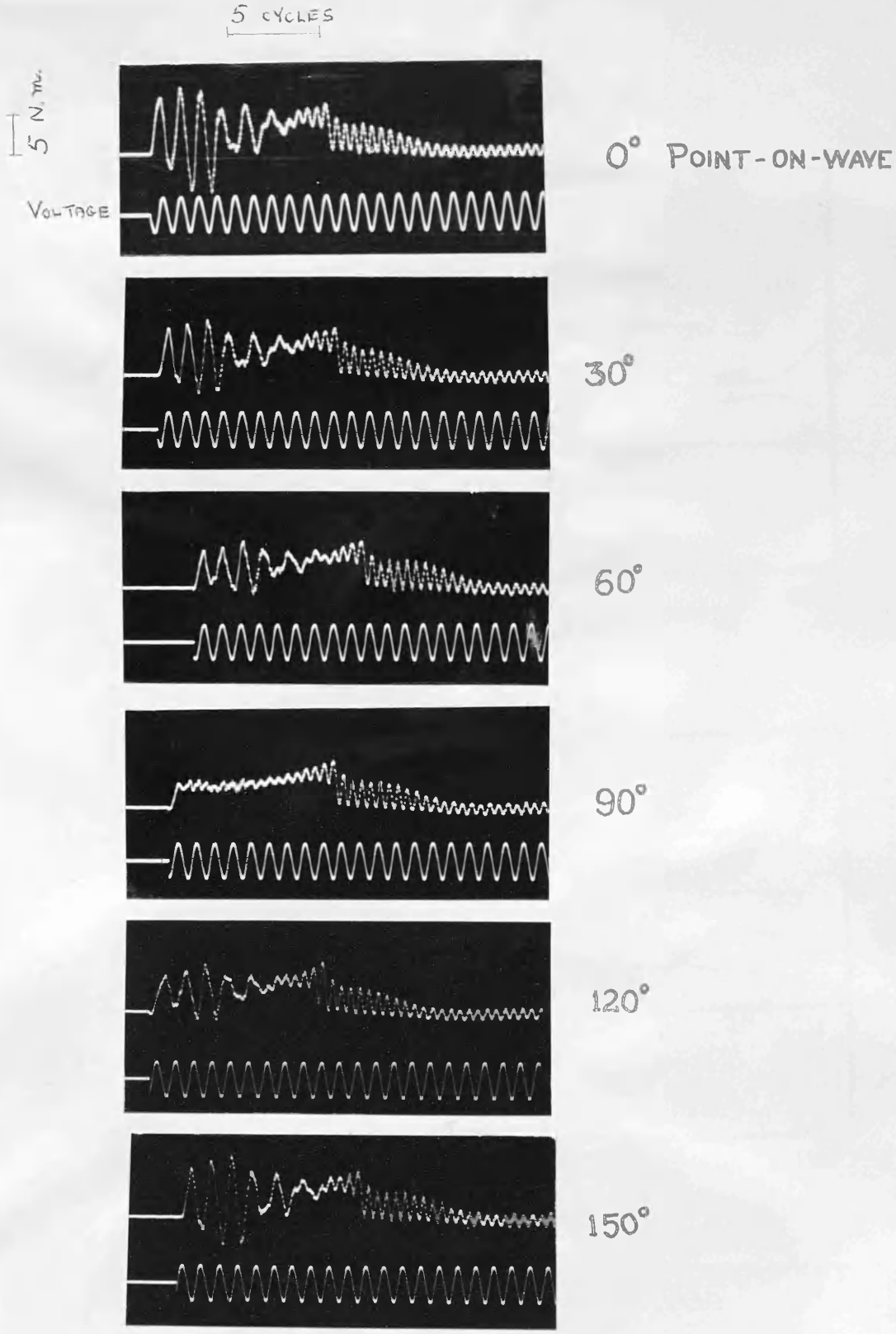

FIG. 3.1. POINT-ON-WAVE EFFECT WITH FREE ROTOR (140V)

(NOTE: the point-on-wave of switching is indicated by the voltage wave)

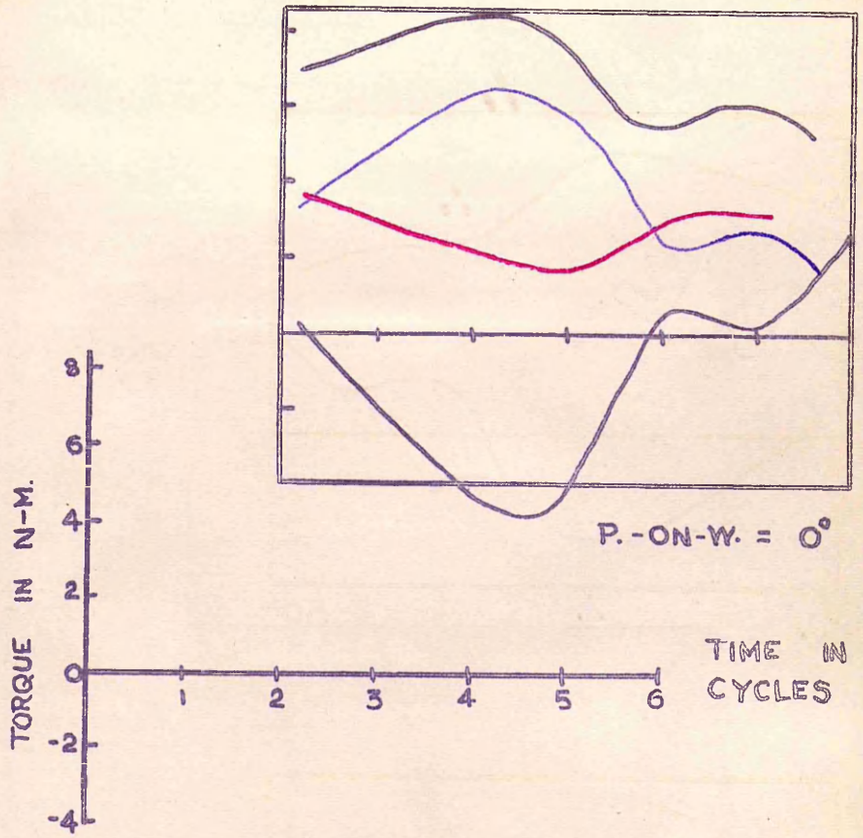

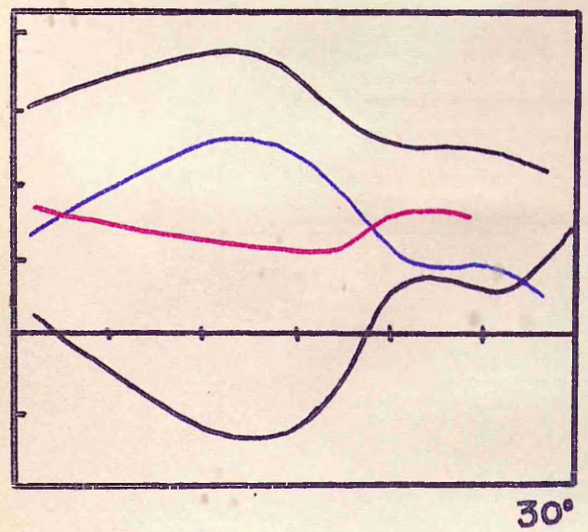

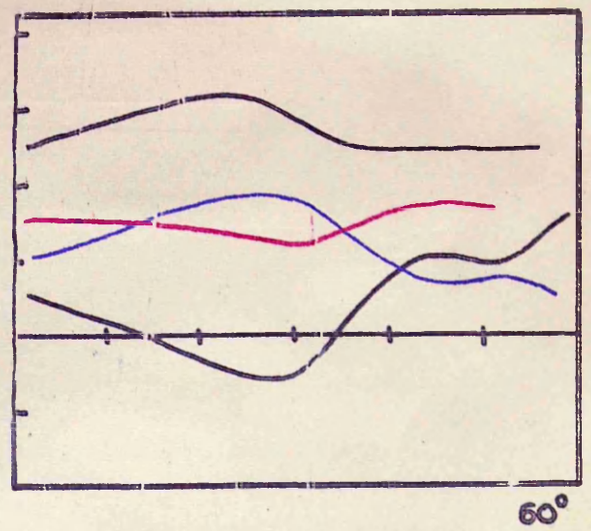

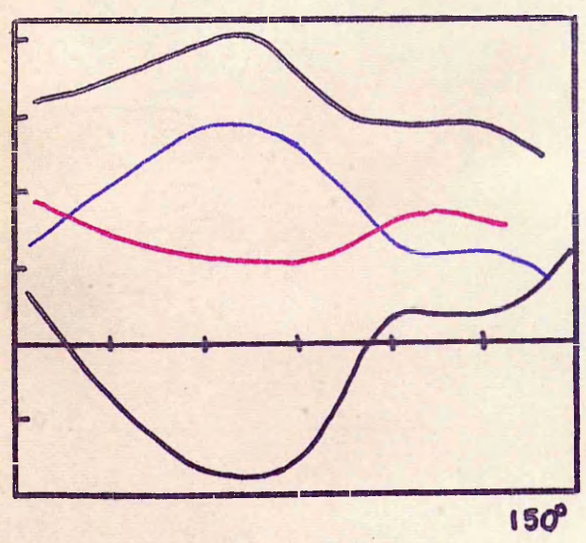

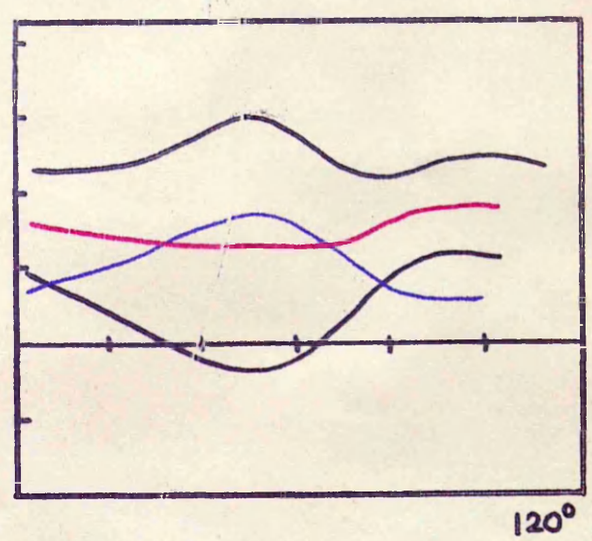

FIG.3.2. P.-ON-W. EFFECT – ENVELOPE, MEAN AND ALTERNATING COMPONENTS OF TRANSIENT TORQUE (140 V)

FIG.3.2

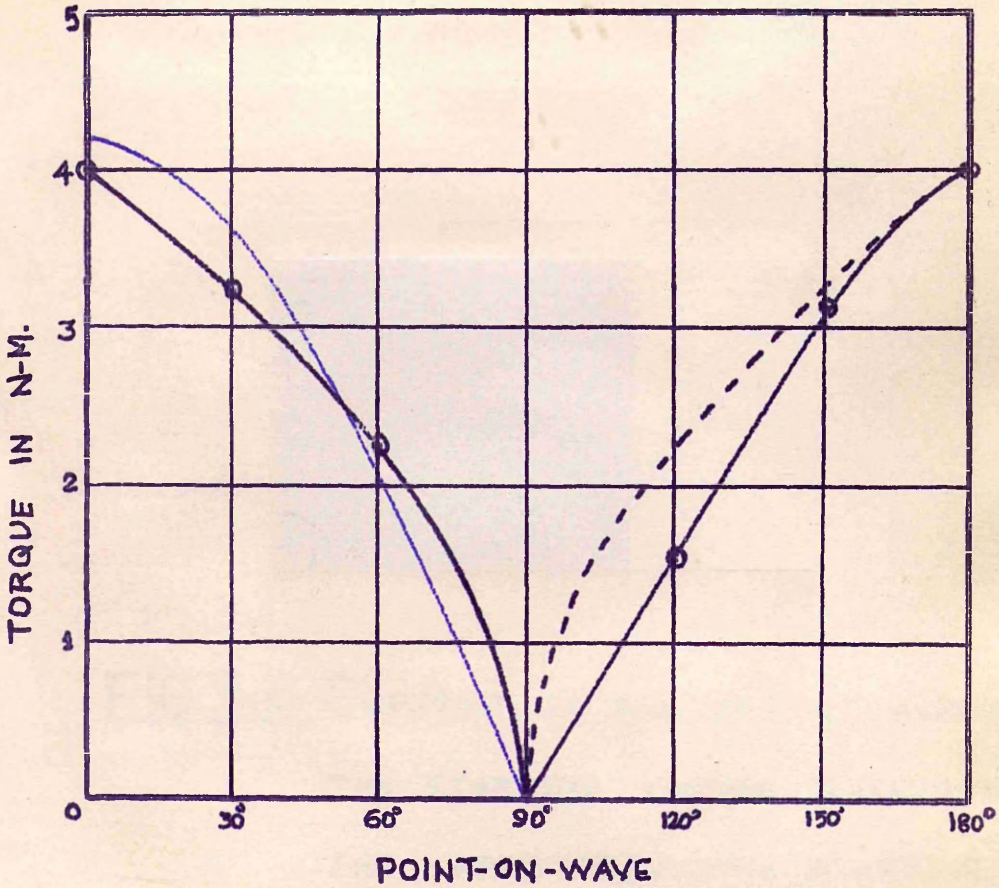

FIG. 3.3. P.-ON-W. EFFECT - ALTERNATING COMPONENT OF TRANSIENT TORQUE AT THE FIRST POSITIVE PEAK (140 V)

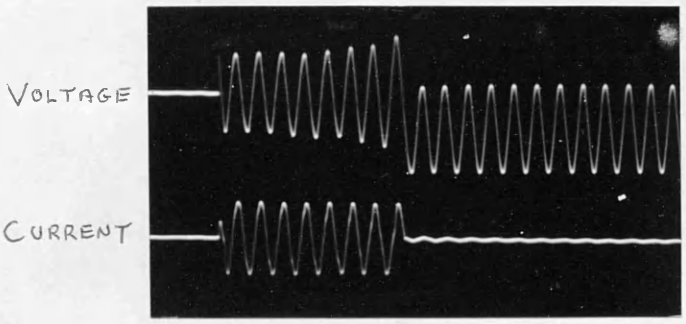

FIG.3.4. CURRENT IN AND VOLTAGE ACROSS THE STARTING WINDING (EXCLUDING THE CAPACITOR) DURING STARTING

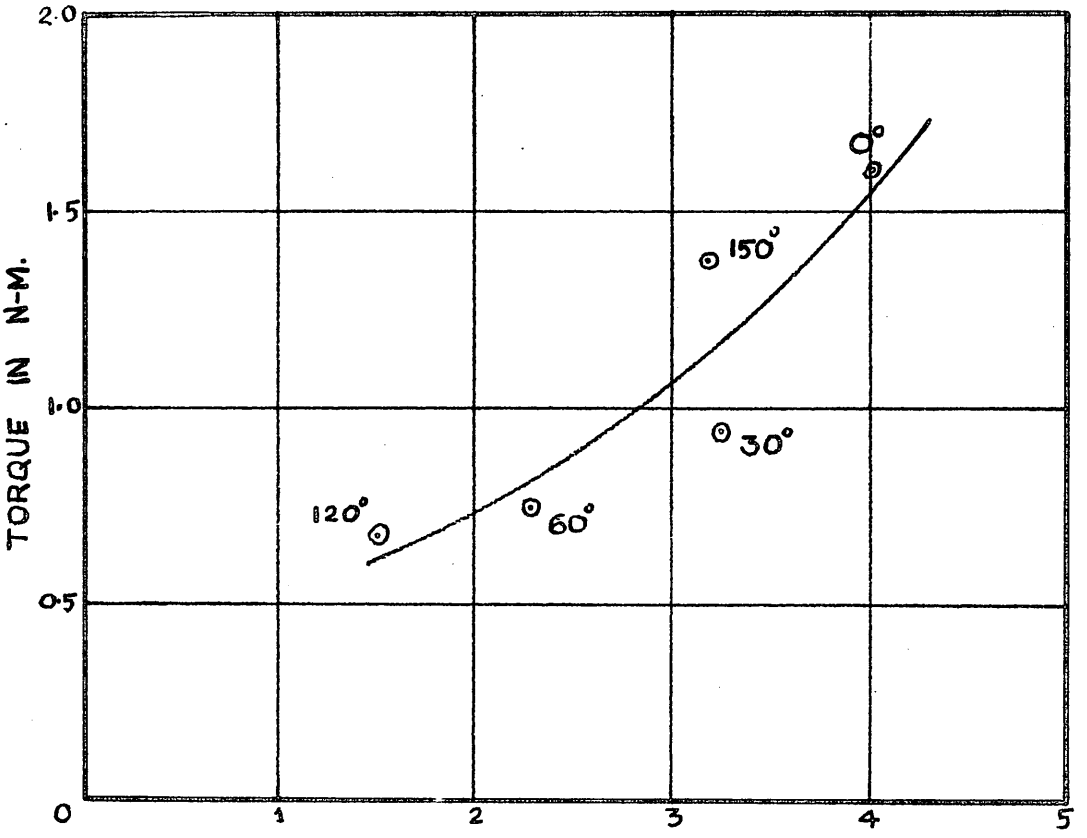

FIG. 3.5. 'MAXIMUM DYNAMIC BRAKING TORQUE' WITH RESPECT TO 'INITIAL VALUE OF UNIDIRECTIONAL FLUX' (140 V)

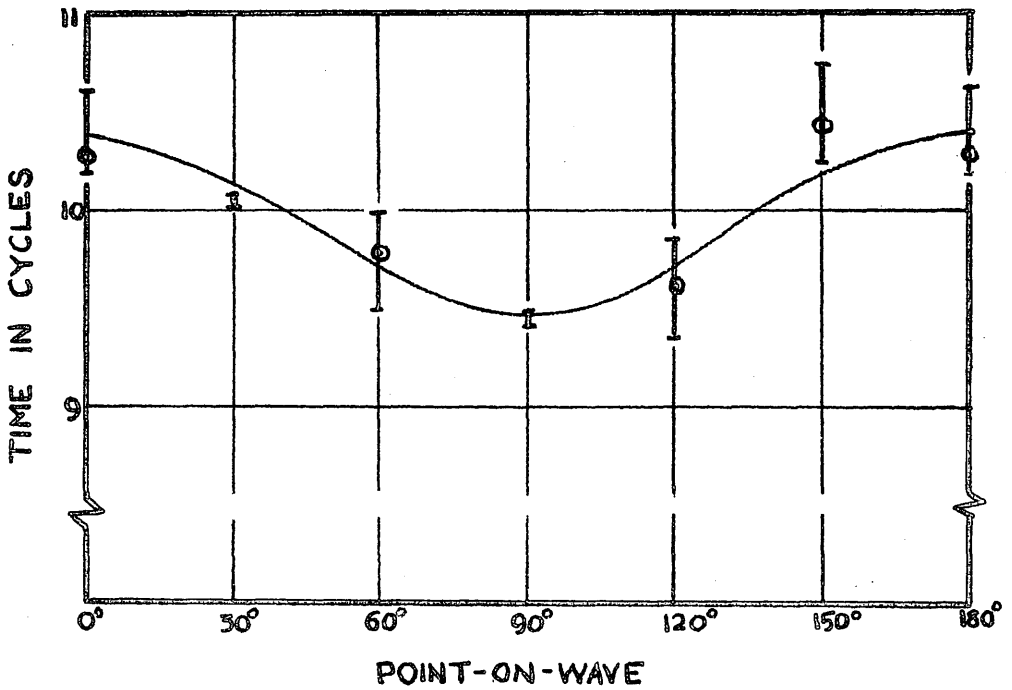

FIG.3.6. TIME FOR CENTRIFUGAL SWITCH TO OPEN

(140V)

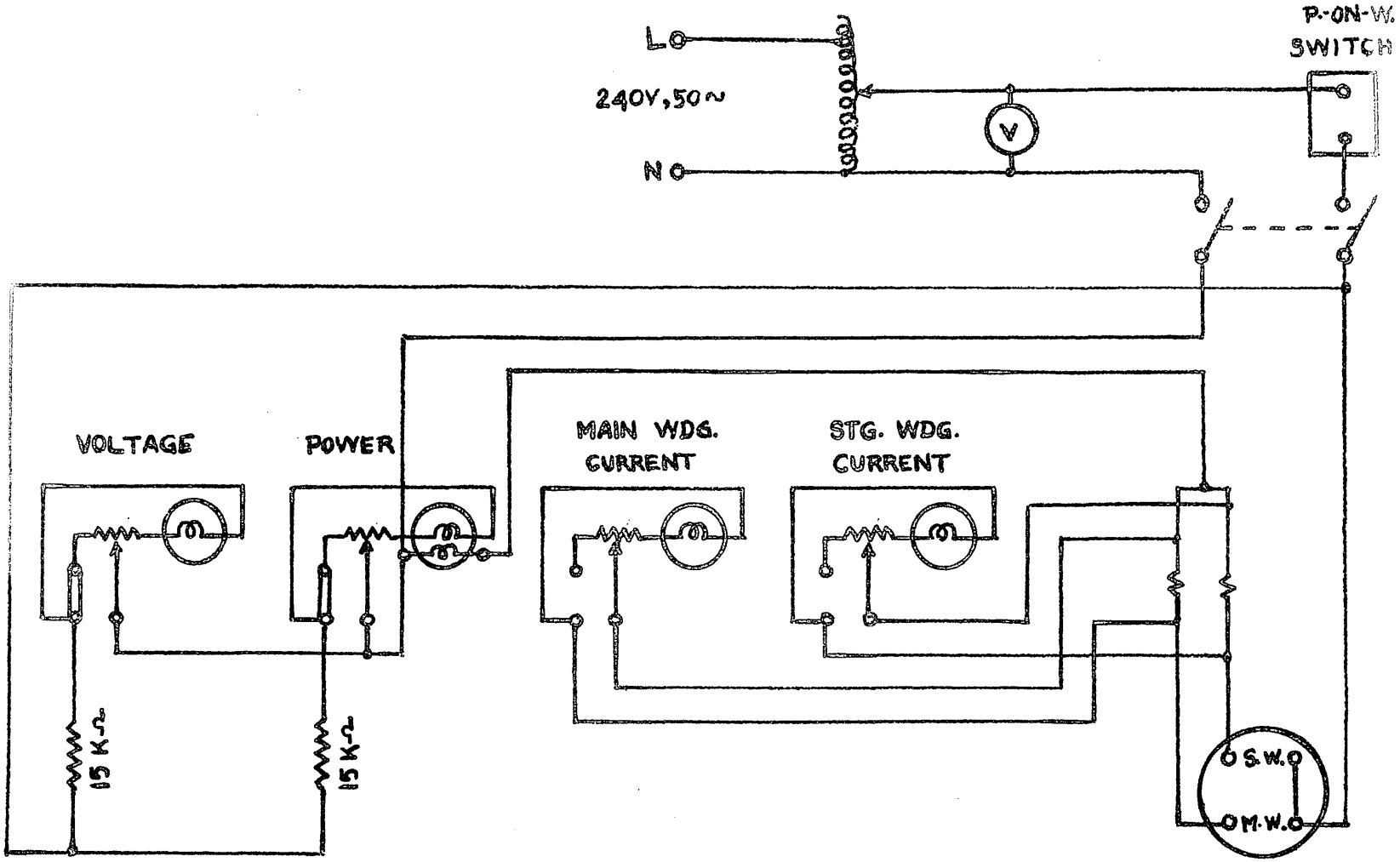

FIG. 3.7. CONNECTIONS TO DUDDELL OSCILLOGRAPH

FIG.3.8. COMPLETE SET-UP FOR STUDYING THE EFFECTS OF VARIATION OF T/J RATIO

FIGS. 3.9 & 3.10

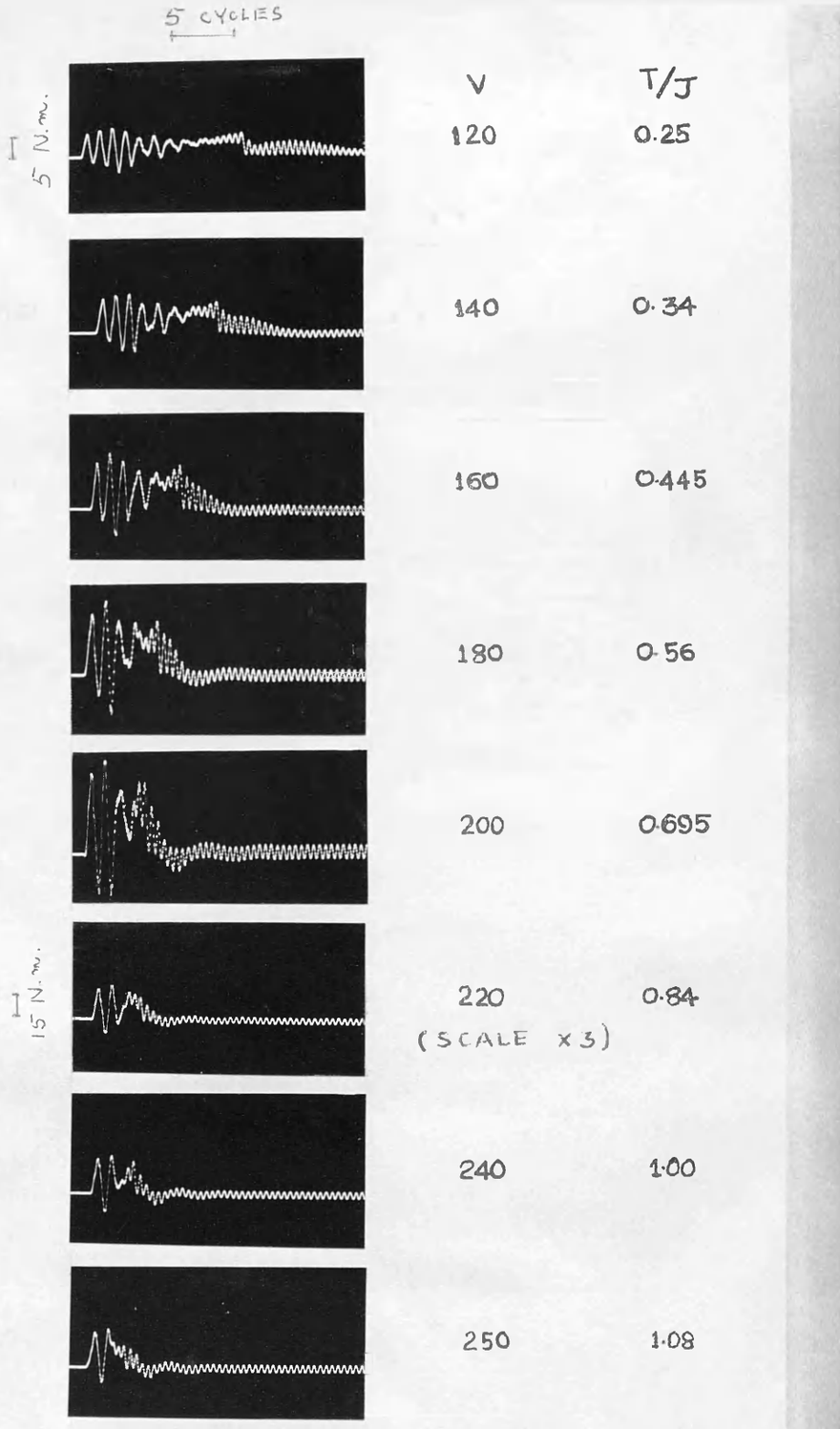

V	T/J
120	0.25
140	0.34
160	0.445
180	0.56
200	0.695
220 (SCALE x3)	0.84
240	1.00
250	1.08

FIG. 3.9. EFFECT OF T/J RATIO – ACCELERATION PATTERNS FOR 0° POINT-ON-WAVE

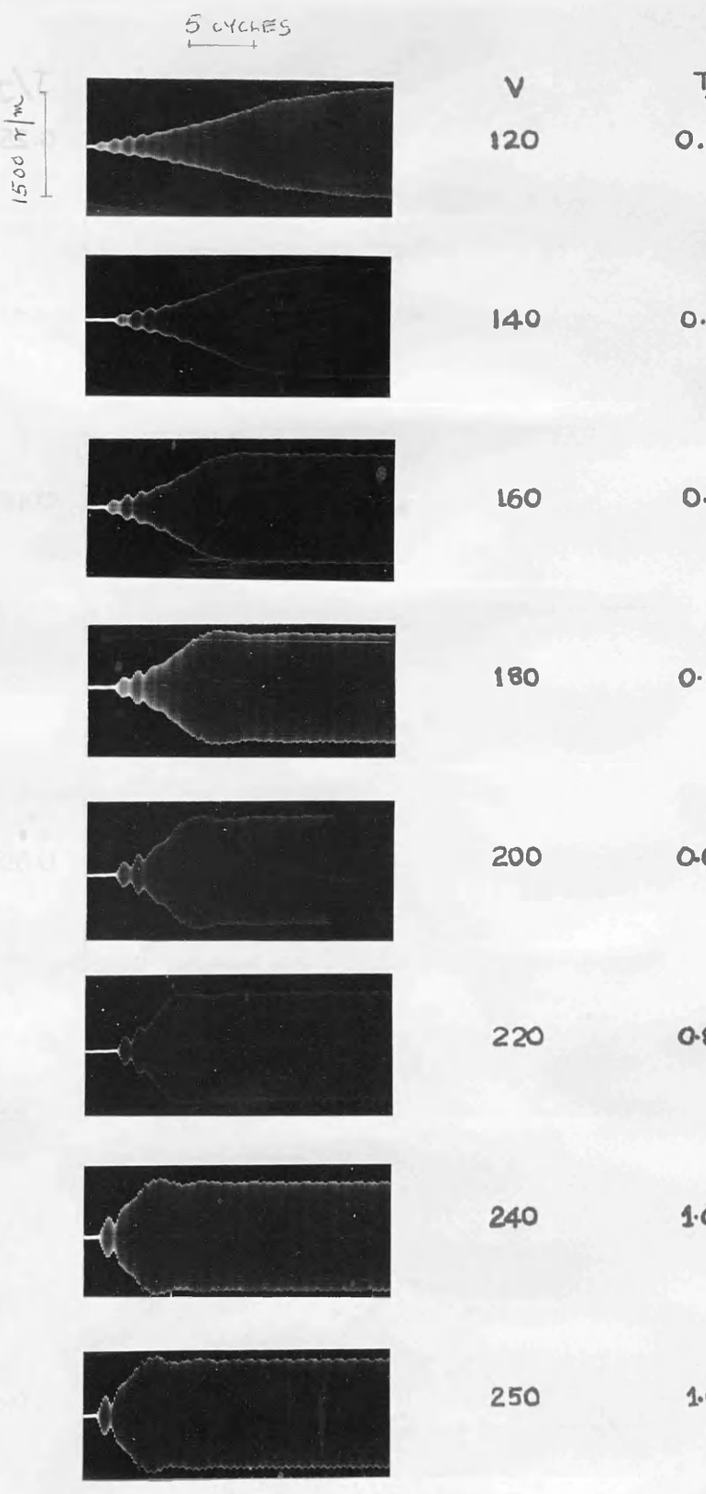

V	T/J
120	0.25
140	0.34
160	0.445
180	0.56
200	0.695
220	0.84
240	1.00
250	1.08

FIG. 3.10. SPEED PATTERNS CORRESPONDING TO ACCELARATION PATTERNS SHOWN IN FIG. 3.9.

FIGS.3.11&3.12

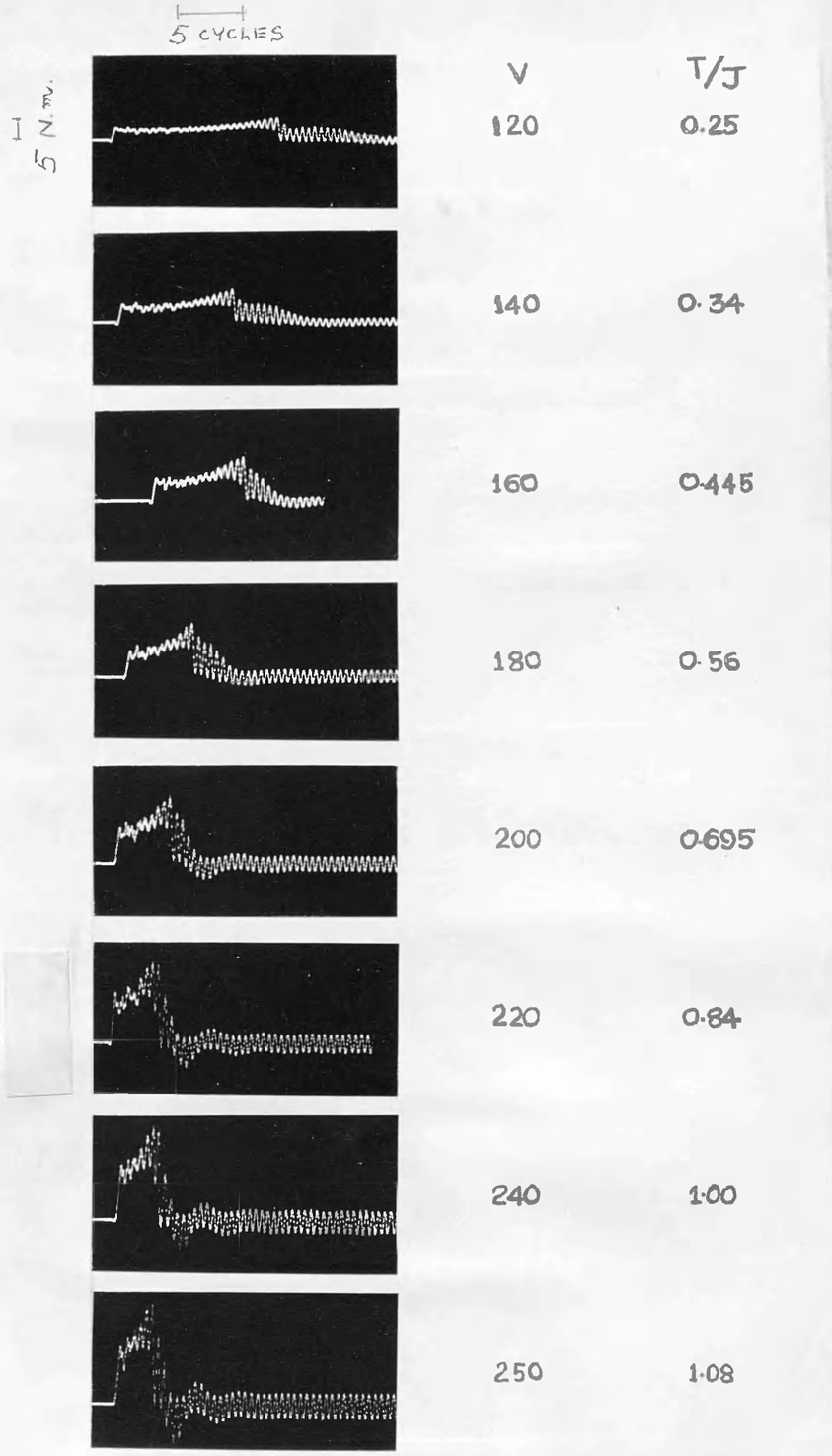

FIG. 3.11. EFFECT OF T/J RATIO – ACCELERATION PATTERNS FOR 90° POINT-ON-WAVE.

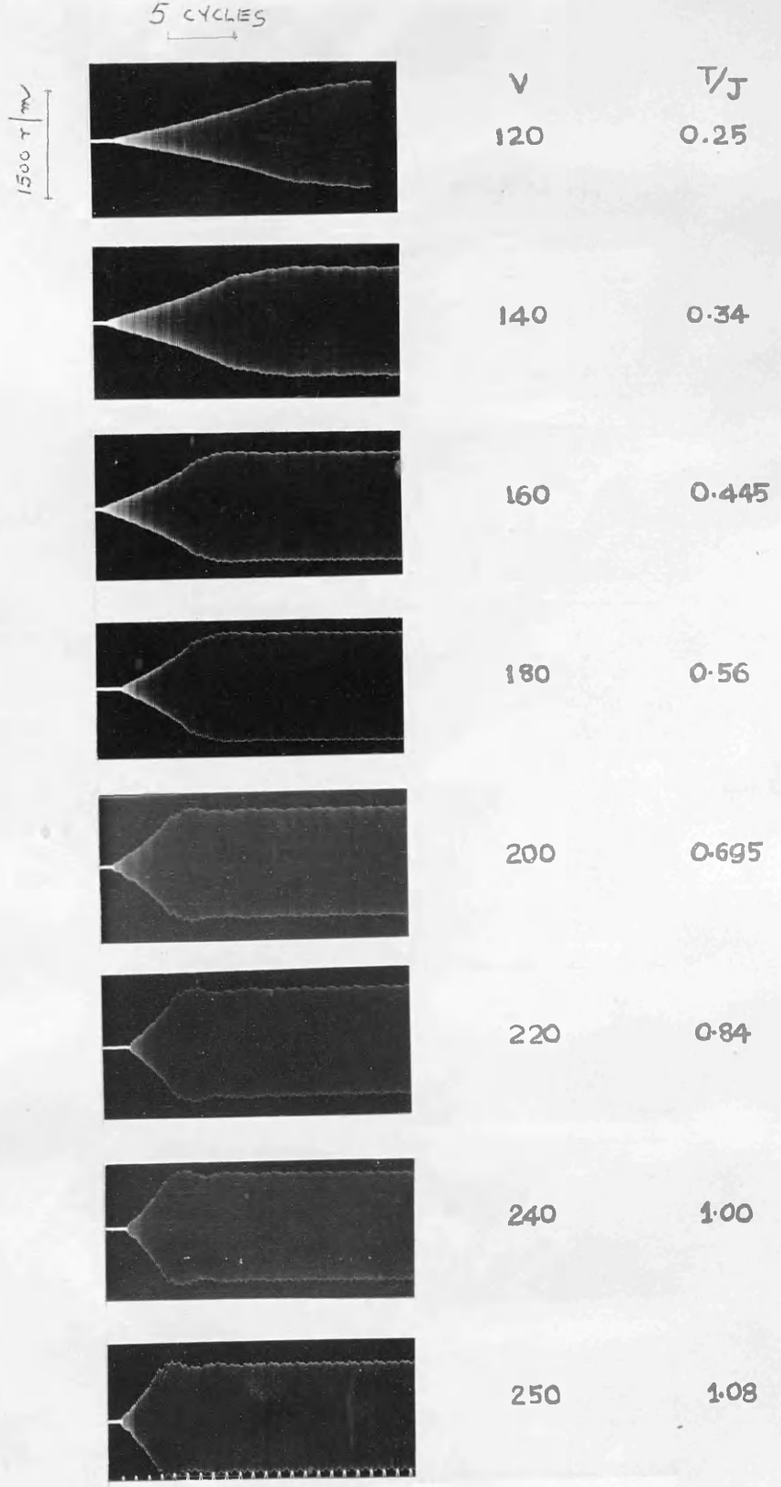

FIG. 3.12. SPEED PATTERNS CORRESPONDING TO ACCELARATION PATTERNS SHOWN IN FIG. 3.11.

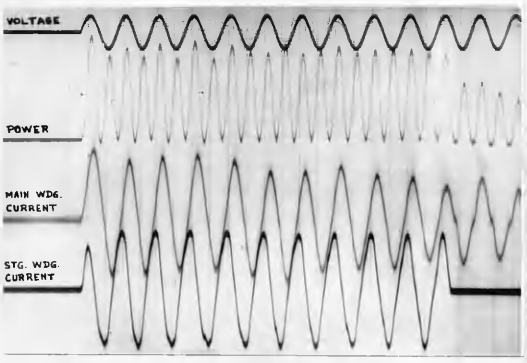

a) 140 V , 0° P.-ON-W.

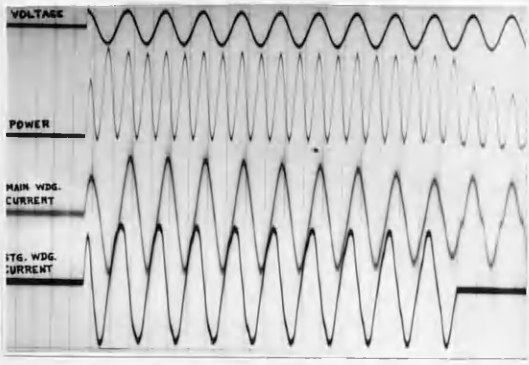

b) 140 V , 90° P.-ON-W.

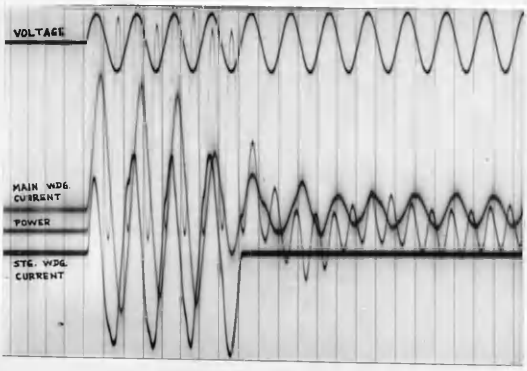

c) 240 V, 0° P.-ON-W.

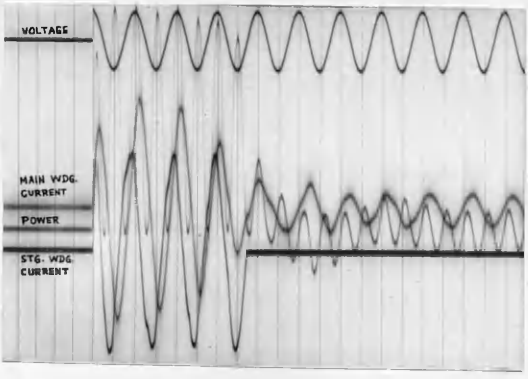

d) 240V, 90° P.-ON-W.

FIG. 3.13. DUDDELL OSCILLOGRAMS

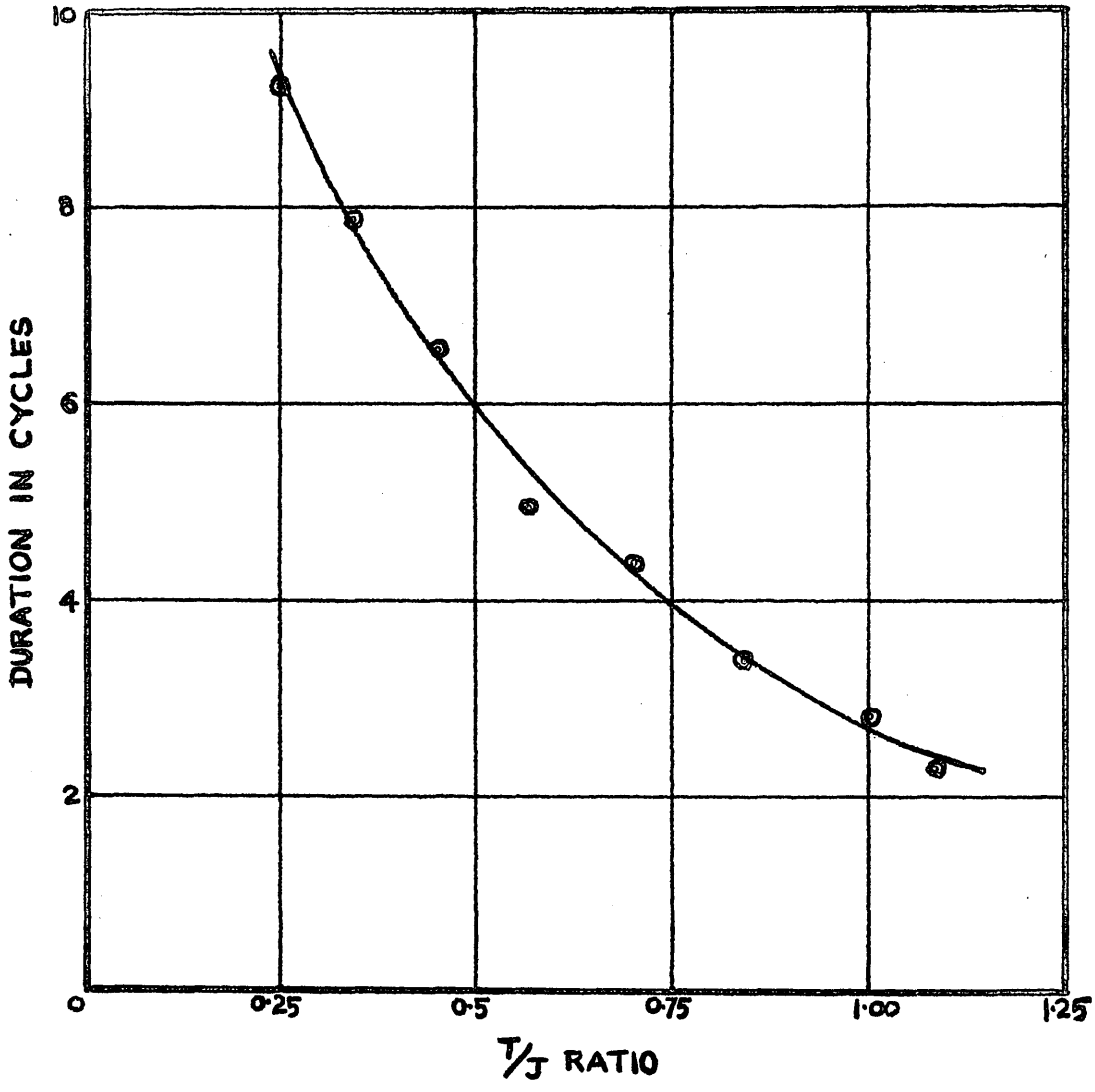

FIG.3.14. DURATION OF LINE FREQUENCY COMPONENT OF TRANSIENT TORQUE FOR 0° POINT-ON-WAVE.

(T/J = 1 AT 240V WITH FREE ROTOR)

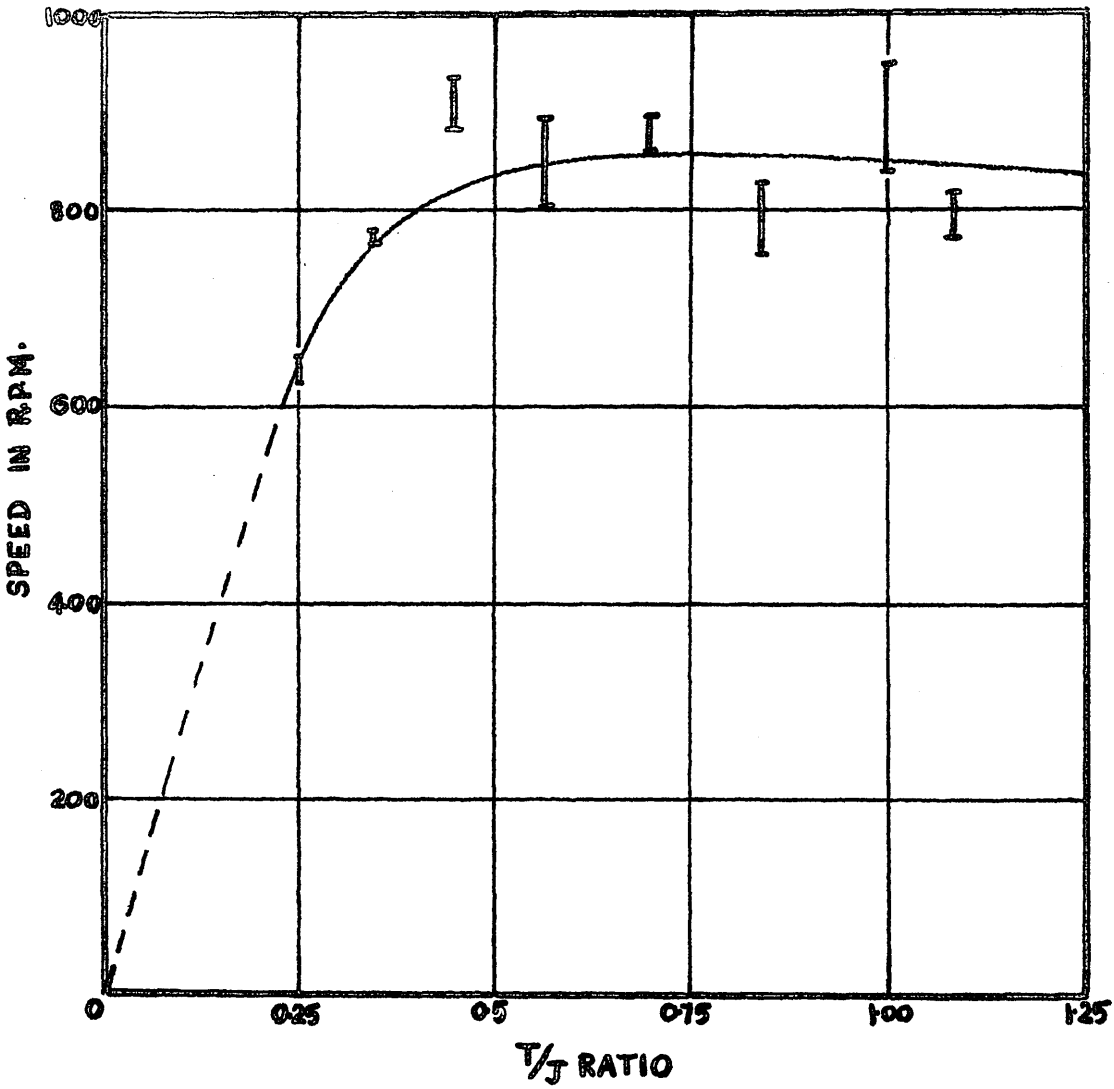

FIG.3.15. SPEED AT WHICH LINE FREQUENCY COMPONENT OF TRANSIET TORQUE VANISHES FOR 0° POINT-ON-WAVE.

(THE SPREAD IS CAUSED MAINLY BY THE METHOD OF MEASUREMENT, I.E. CO-RELATION OF THE SPEED AND ACCELERATION OSCILLOGRAMS.)

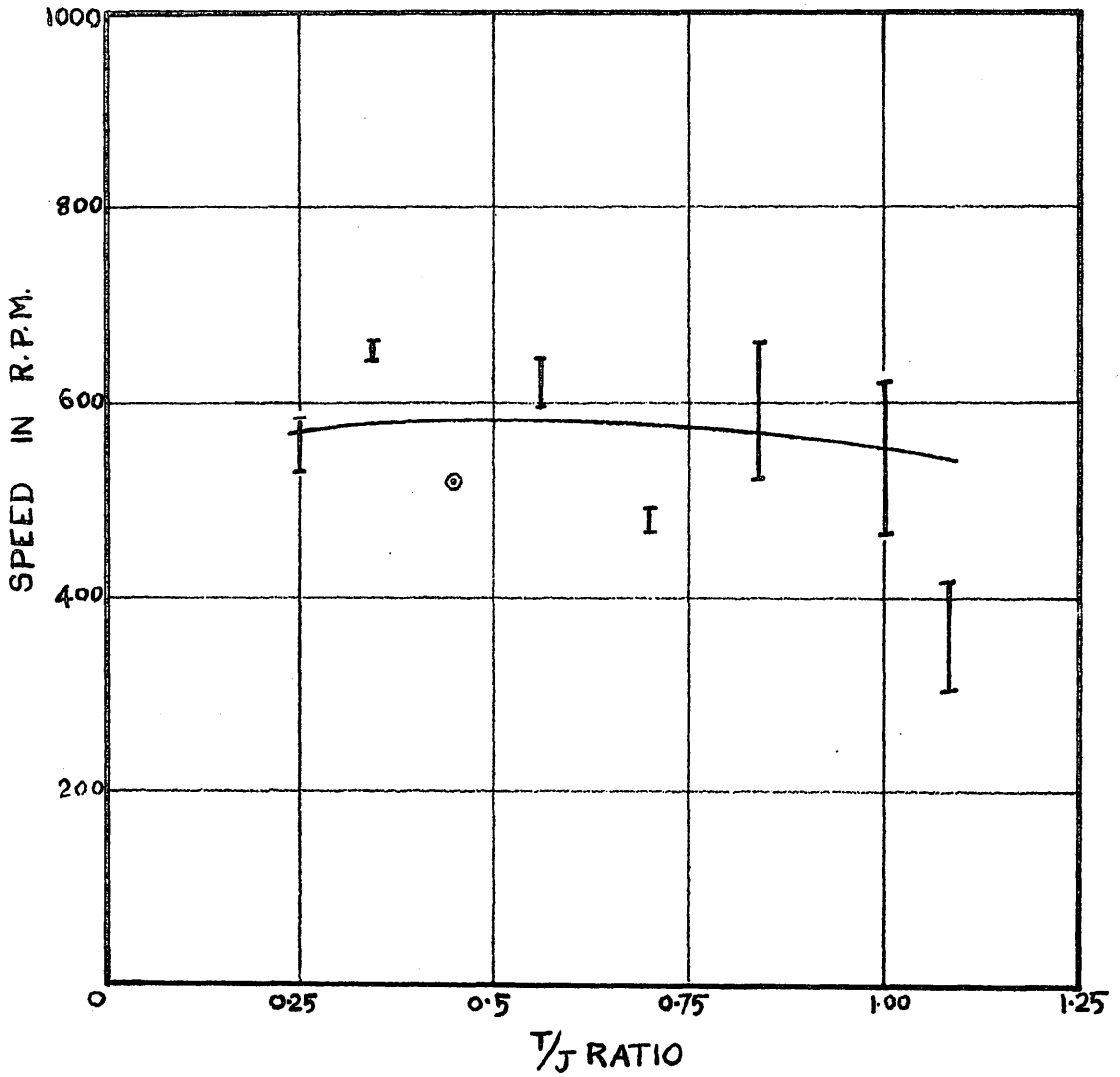

FIG. 3.16. SPEED AT WHICH DOUBLE LINE FREQUENCY TORQUE APPEARS FOR 0° POINT-ON-WAVE.

(THE SPREAD IS CAUSED MAINLY BY THE METHOD OF MEASUREMENT, I.e. CO-RELATION BETWEEN THE SPEED AND ACCELERATION OSCILLOGRAMS.)

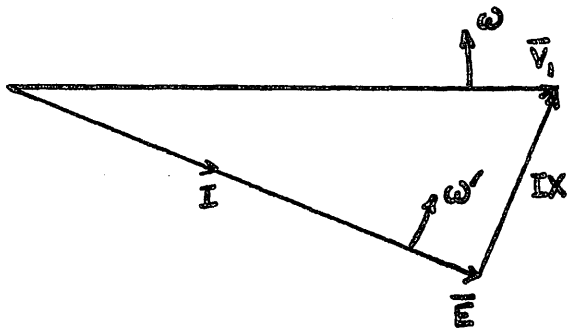

FIG.3.17. APPROXIMATE PHASOR DIAGRAM FOR INDUCTION MOTORS

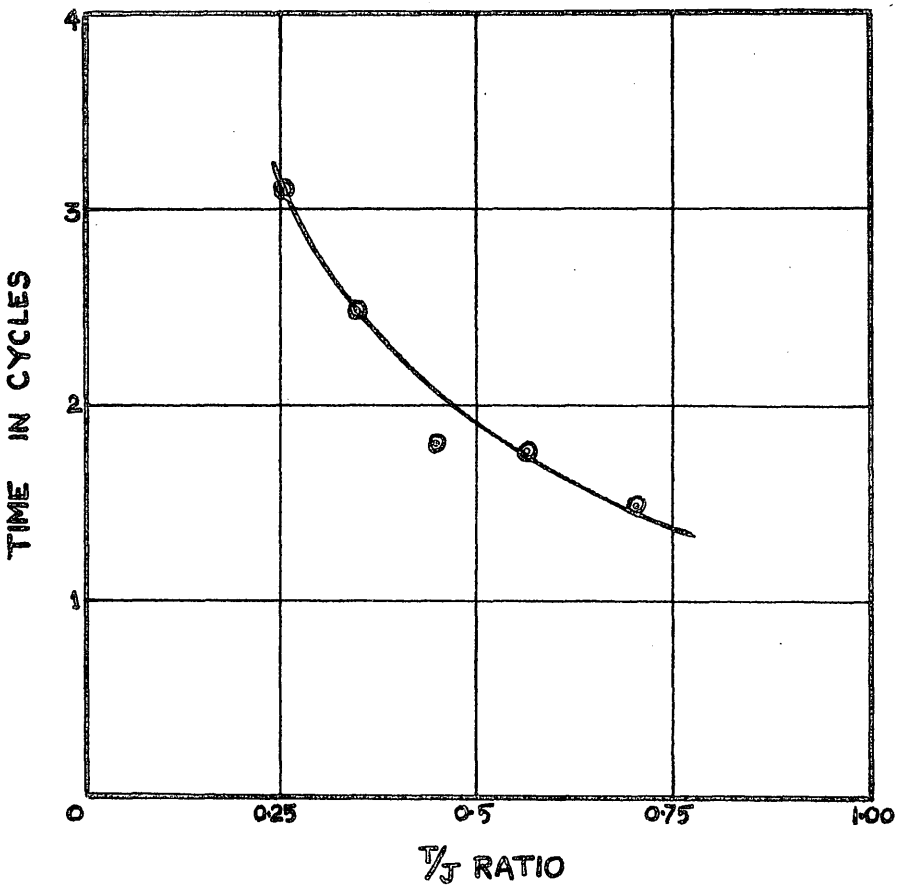

FIG. 3.18. TIME FOR WHICH ALTERNATING COMPONENT OF TRANSIENT TORQUE INCREASES FOR 0° POINT-ON-WAVE

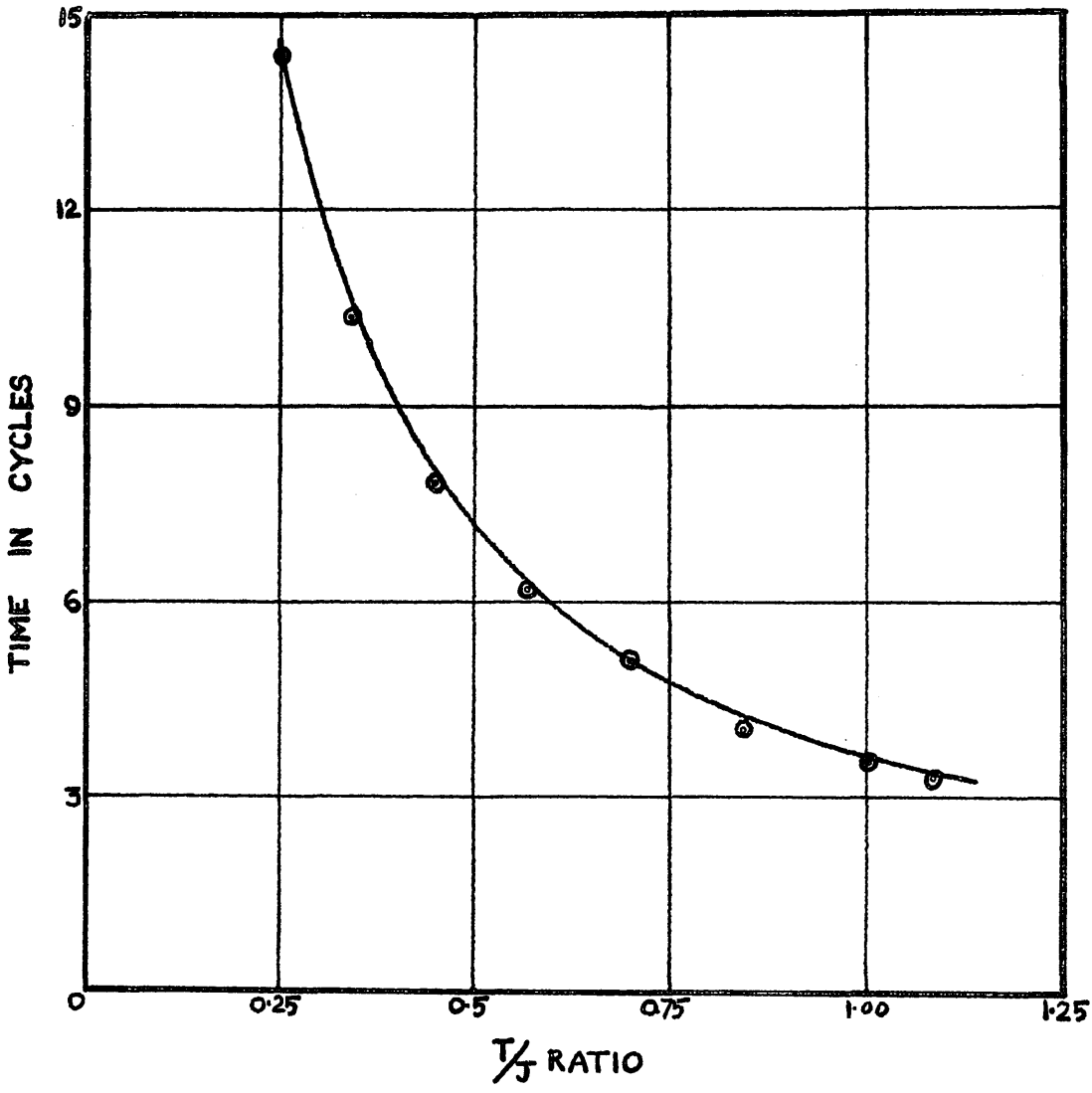

FIG.3.19. TIME TO ATTAIN 80% NO-LOAD SPEED FOR σ P.-ON-W. SWITCHING

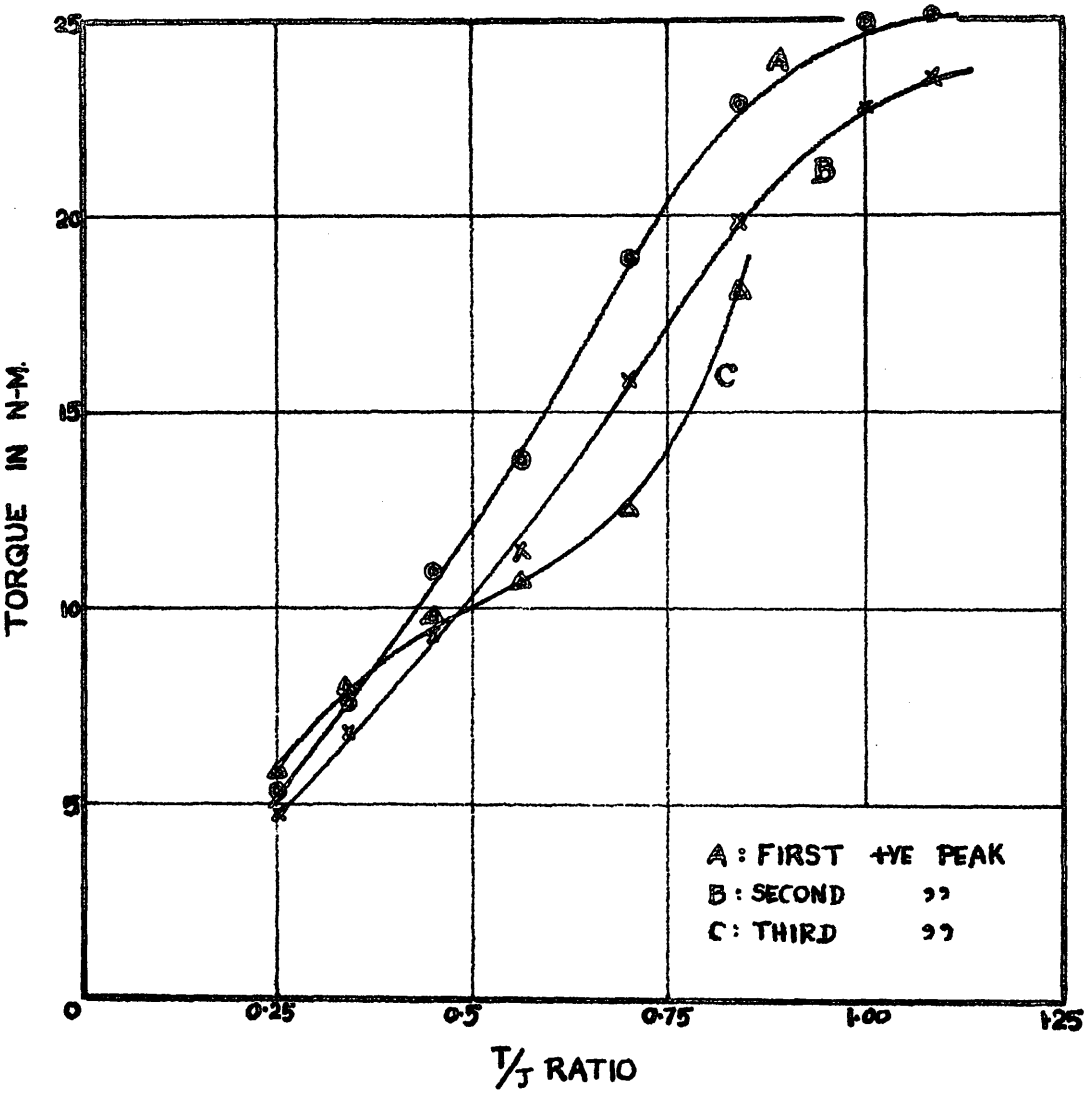

FIG.3.20. PEAK TORQUES FOR 0° POINT-ON-WAVE

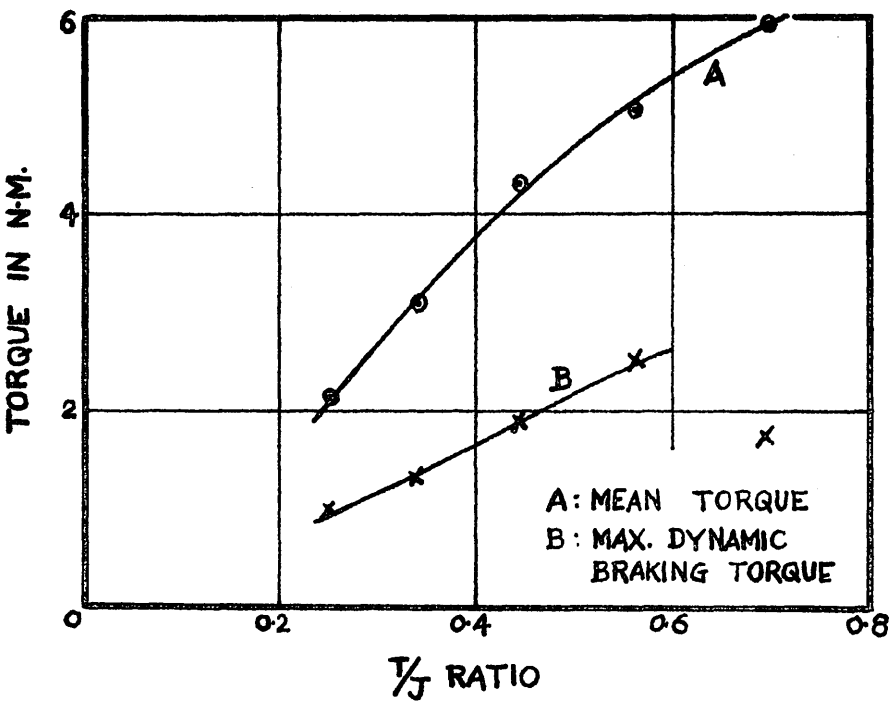

FIG.3.21. MEAN TORQUE AND 'MAXIMUM DYNAMIC BRAKING TORQUE' FOR 0° POINT-ON-WAVE

FIG. 3.22

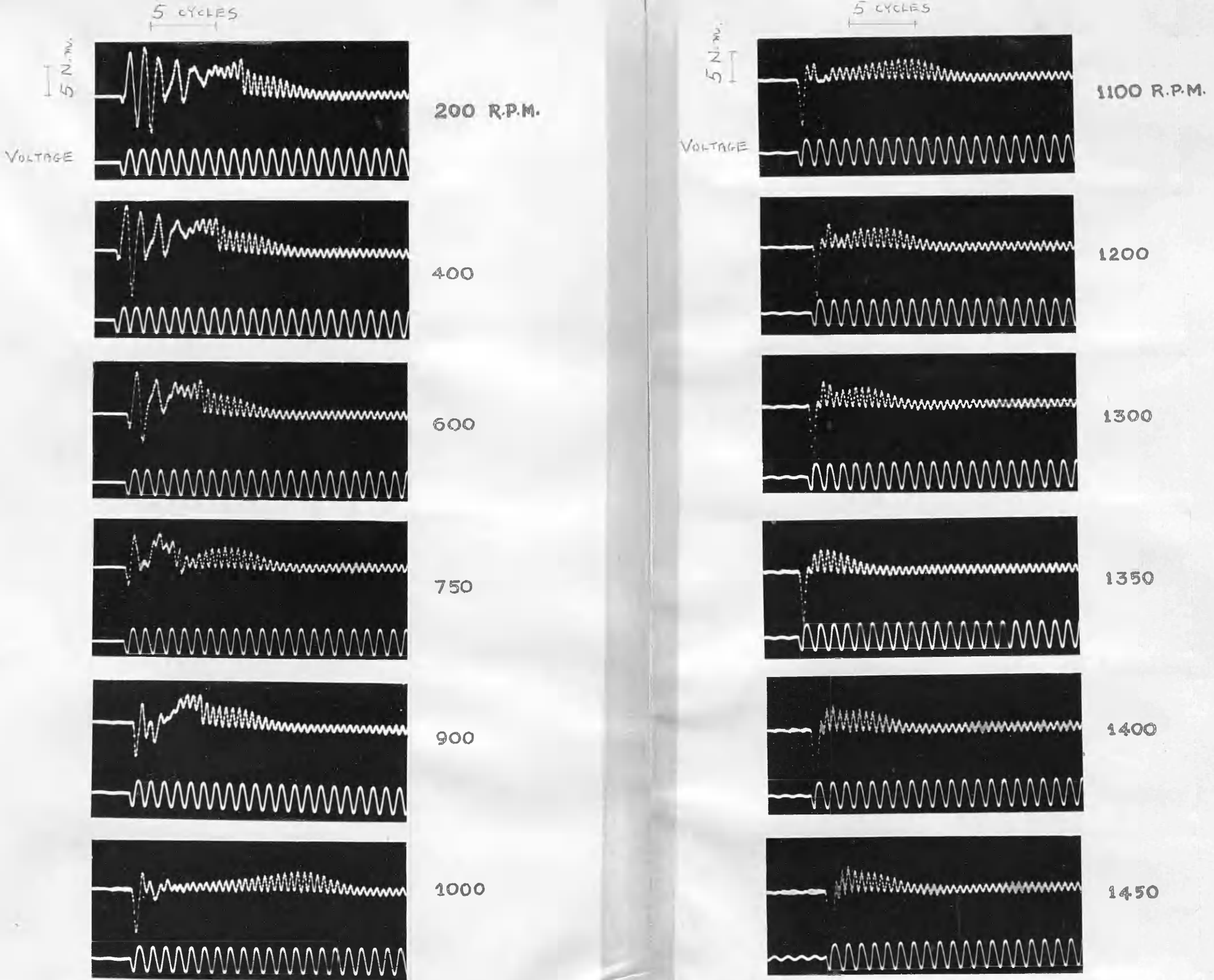

FIG.3.22. SWITCHING ON AT SPEEDS WITH 0° POINT-ON-WAVE (140V)

FIG.3.23

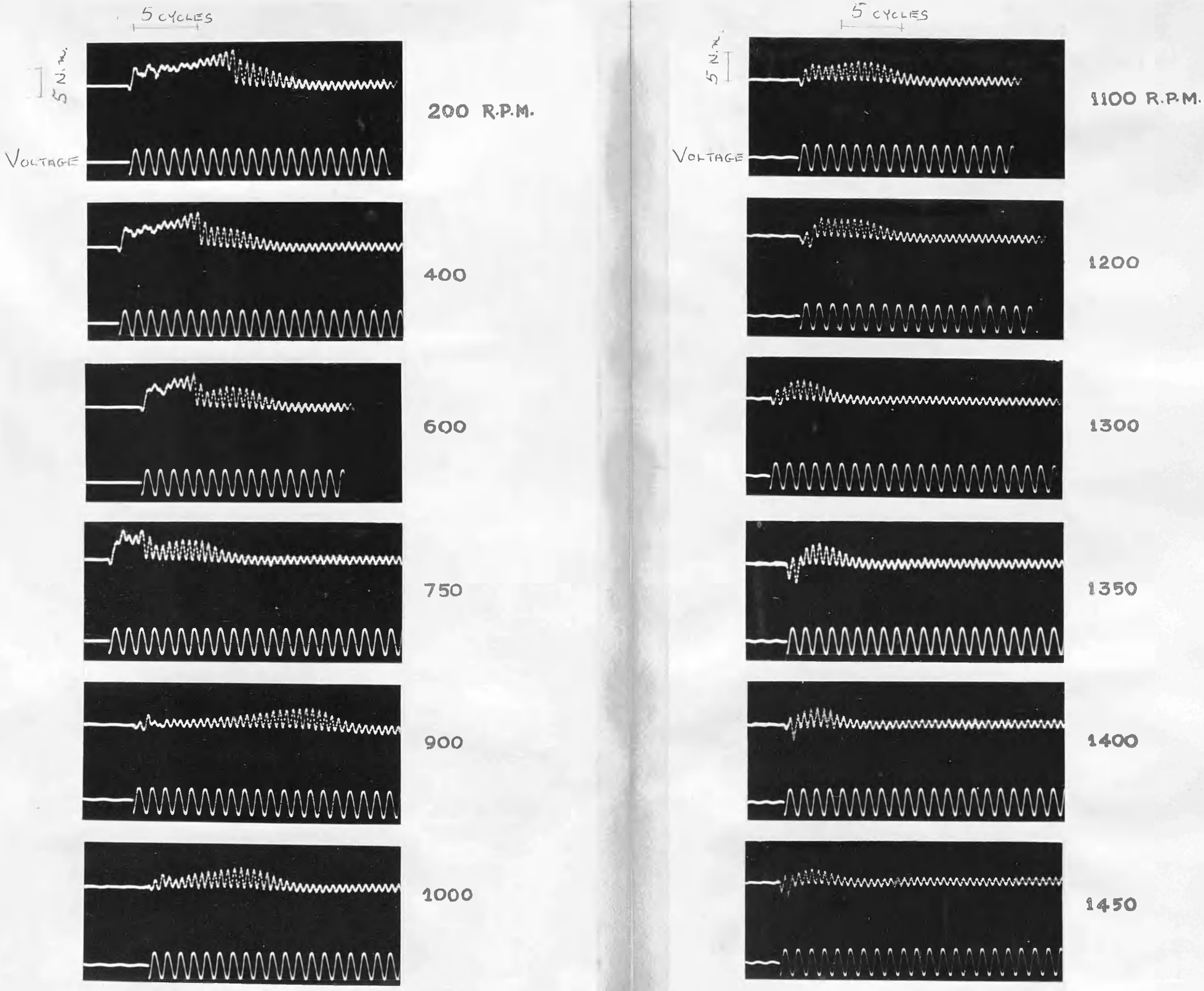

FIG.3.23. SWITCHING ON AT SPEEDS WITH 90° POINT-ON-WAVE (140V)

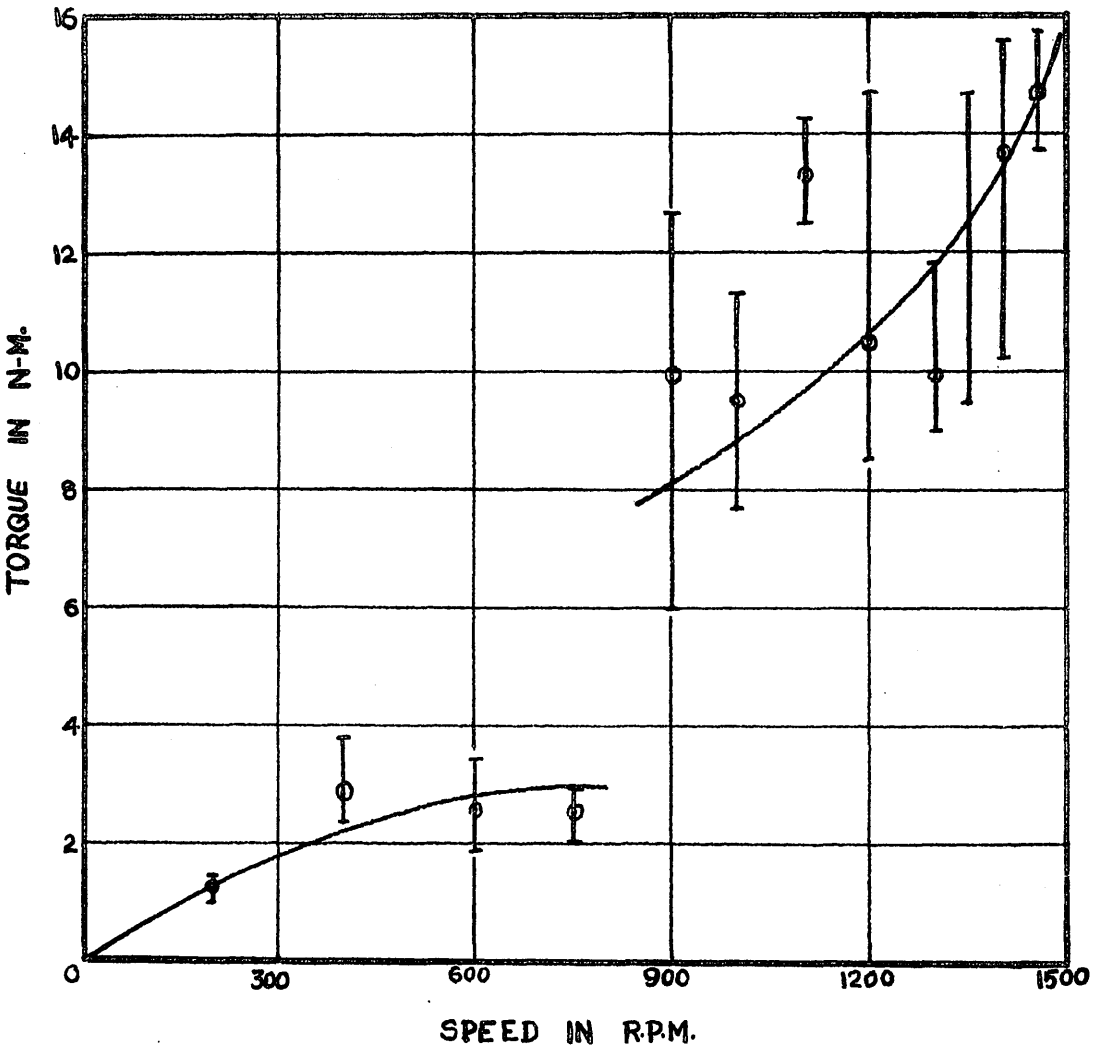

FIG.3.24. SWITCHING ON AT SPEEDS - NET BRAKING TORQUE FOR 0° POINT-ON-WAVE (140V)

THE DISCONTINUITY CORRESPONDS TO THE RE-CLOSING OF THE CENTRIFUGAL SWITCH AS THE MACHINE RUNS DOWN.

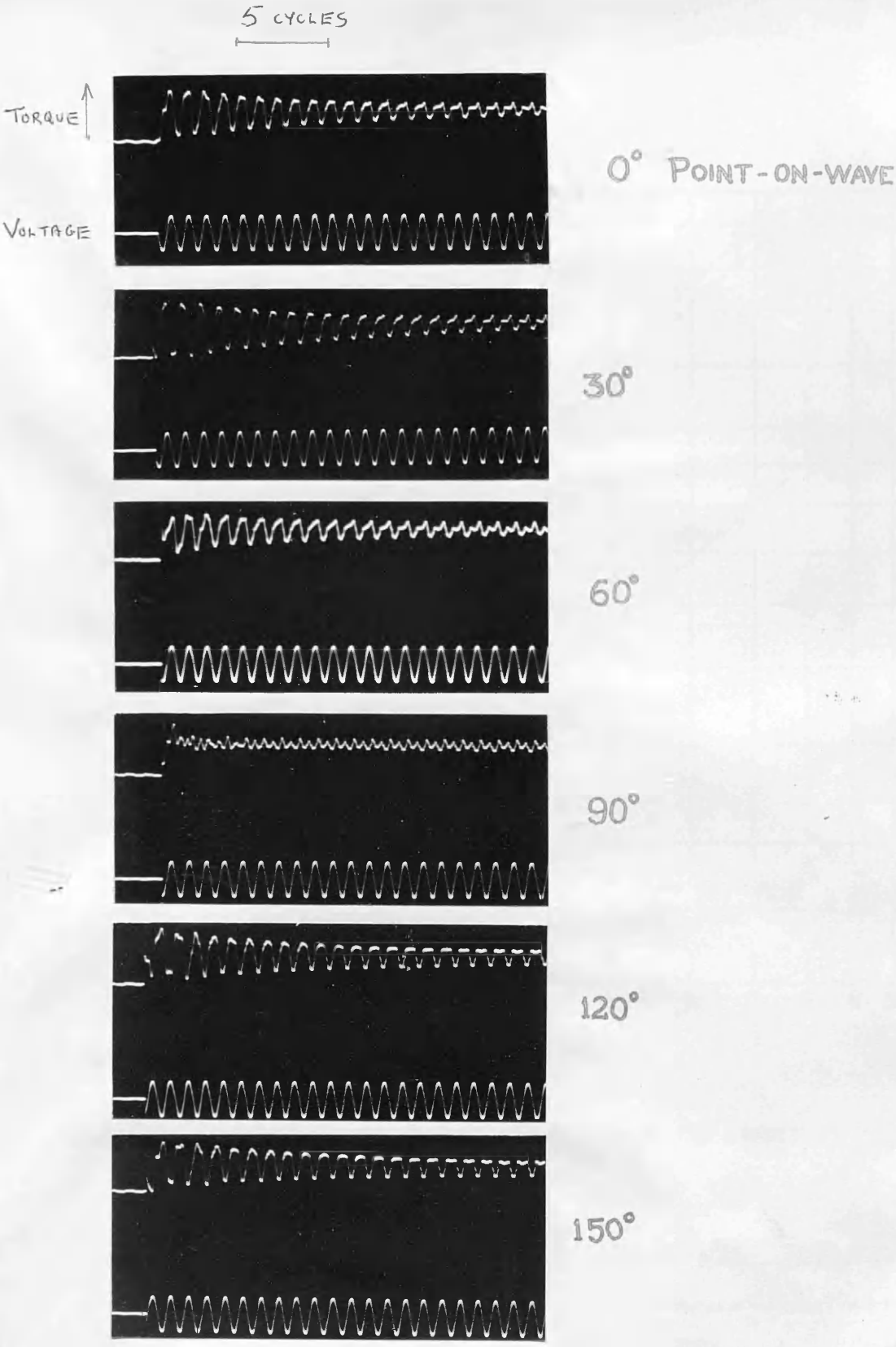

FIG. 4.1. POINT-ON-WAVE EFFECT WITH BLOCKED ROTOR (140 V)

(NOTE: THE POINT-OF-WAVE OF SWITCHING IS INDICATED BY THE VOLTAGE WAVE)

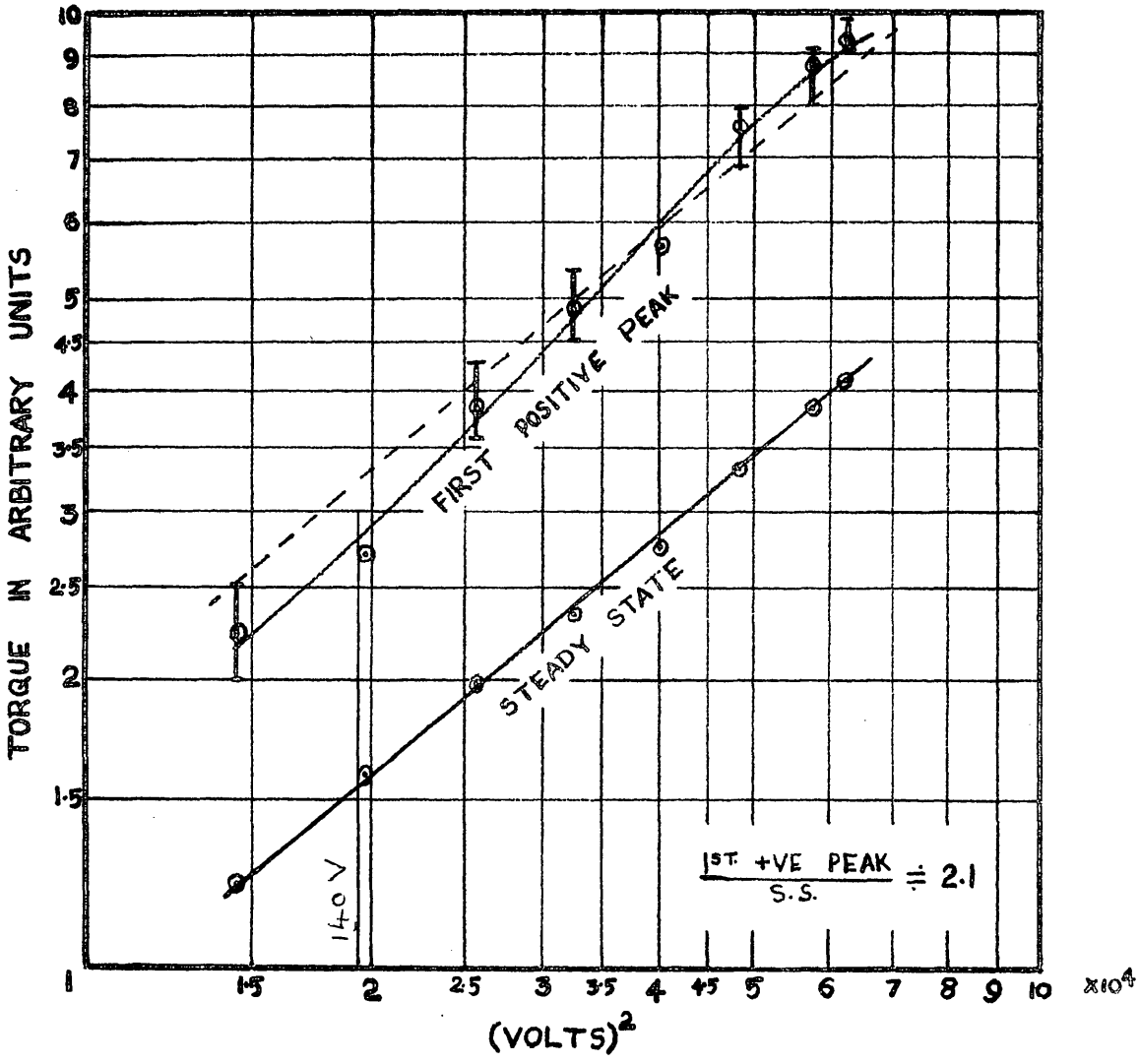

FIG.4.2. FIRST POSITIVE PEAK FOR 0° POINT-ON-WAVE AND STEADY-STATE TORQUE

THE DOTTED LINE IS A PARALLEL TO THE STEADY-STATE CHARACTERISTIC AND GIVES AN APPROXIMATELY CONSTANT RATIO OF ABOUT 2·1. (THE SPREAD HERE IS MAINLY DUE TO THE SLIGHT INCONSISTENCY IN THE OPERATION OF THE P.-ON-W. SWITCH.)

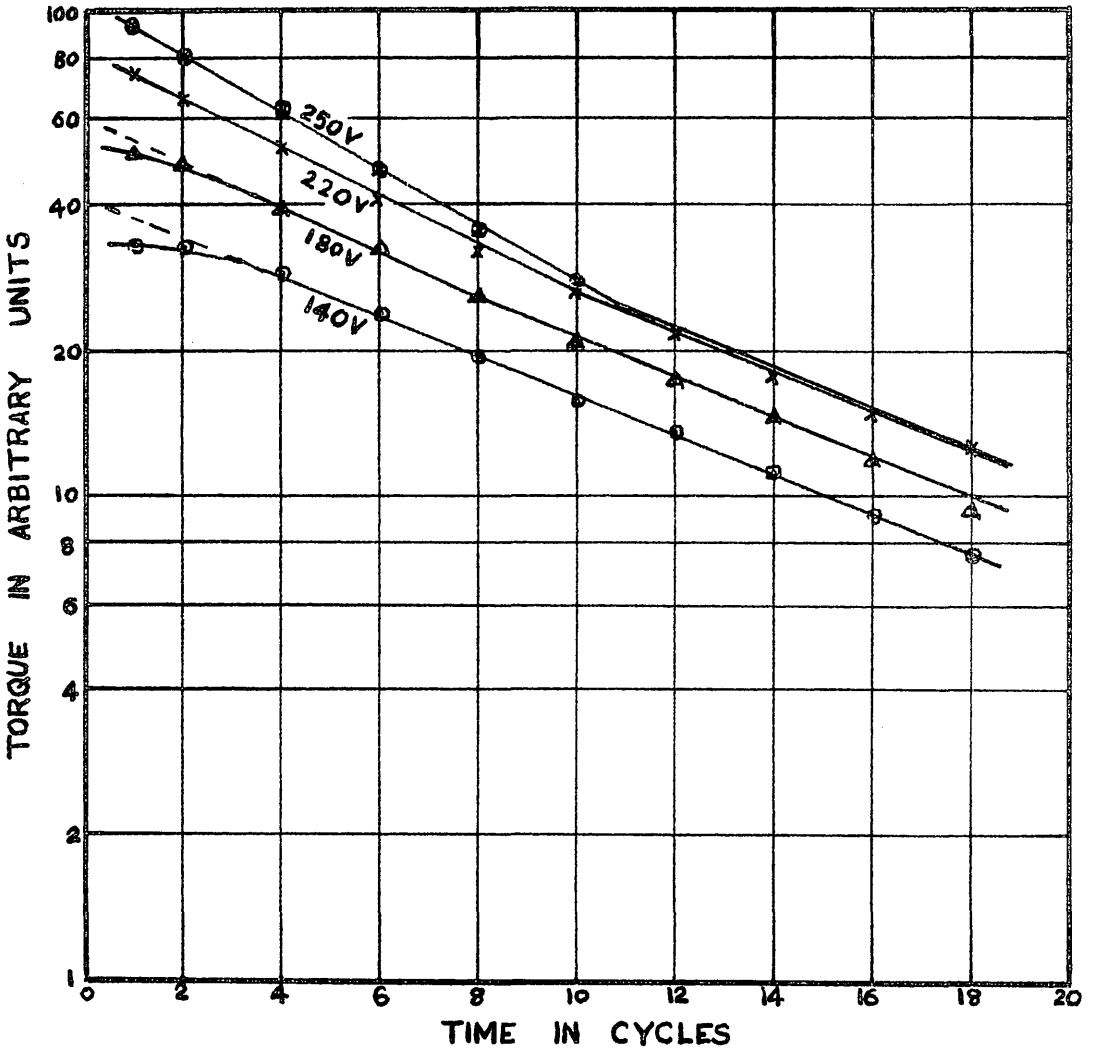

FIG. 4.3. SEMILOG PLOT OF THE ALTERNATING COMPONENT TO DETERMINE TIME CONSTANTS (0° POINT-ON-WAVE).

NOTE THE INITIAL INCREASED RATE OF DECAY AT HIGHER VOLTAGES DUE TO TRANSIENT SATURATION.

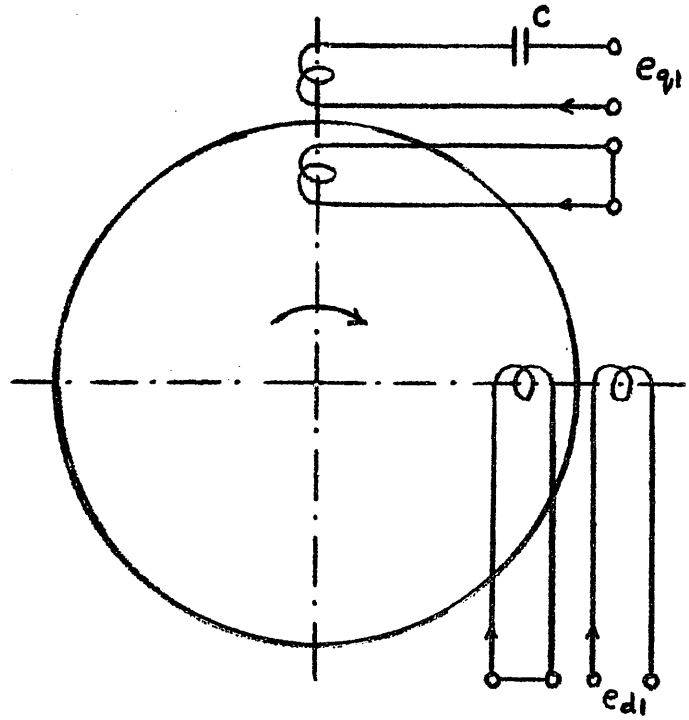

FIG.4.4. TWO-AXES REPRESENTATION OF THE MACHINE

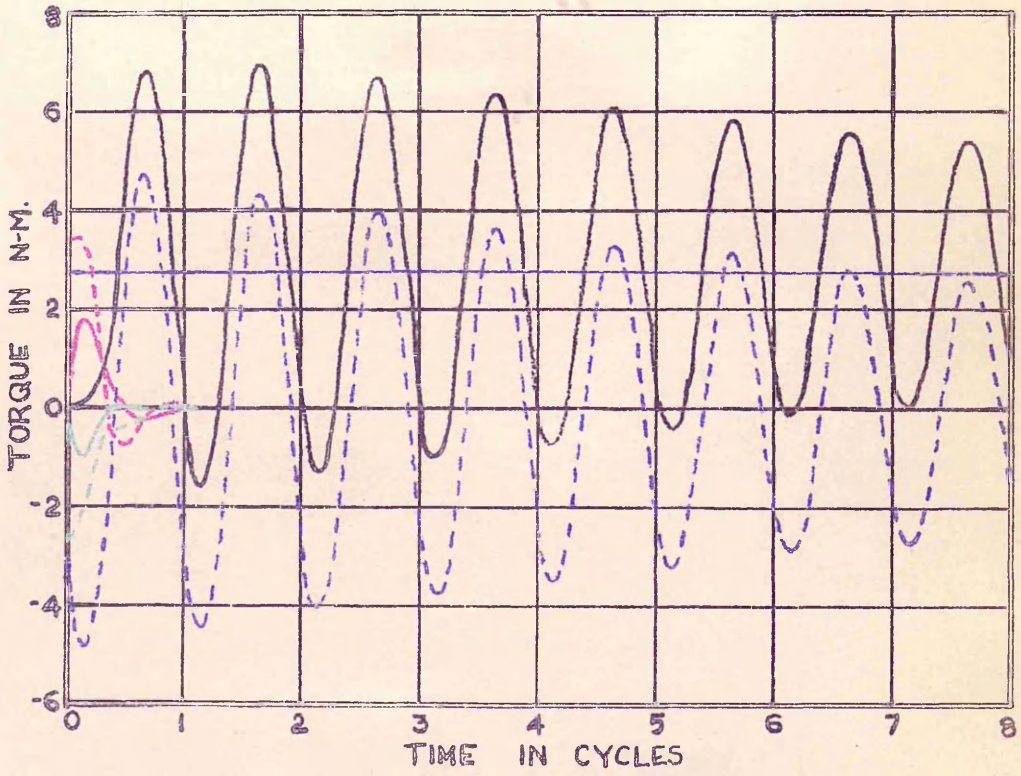

FIG. 4.5. COMPUTED CHARACTERISTICS FOR 179°14' POINT-ON-WAVE WHEN THE PRINCIPAL LINE FREQUENCY COMPONENT IS A MAXIMUM (140 V)

THE CHARACTERISTIC FOR 0° POINT-ON-WAVE IS INDISTINGUISHABLE FROM THAT FOR 179°14' POINT-ON-WAVE.

[COMPARE TOTAL CHARACTERISTIC HERE WITH FIG. 4.1, (0° POINT-ON-WAVE)]

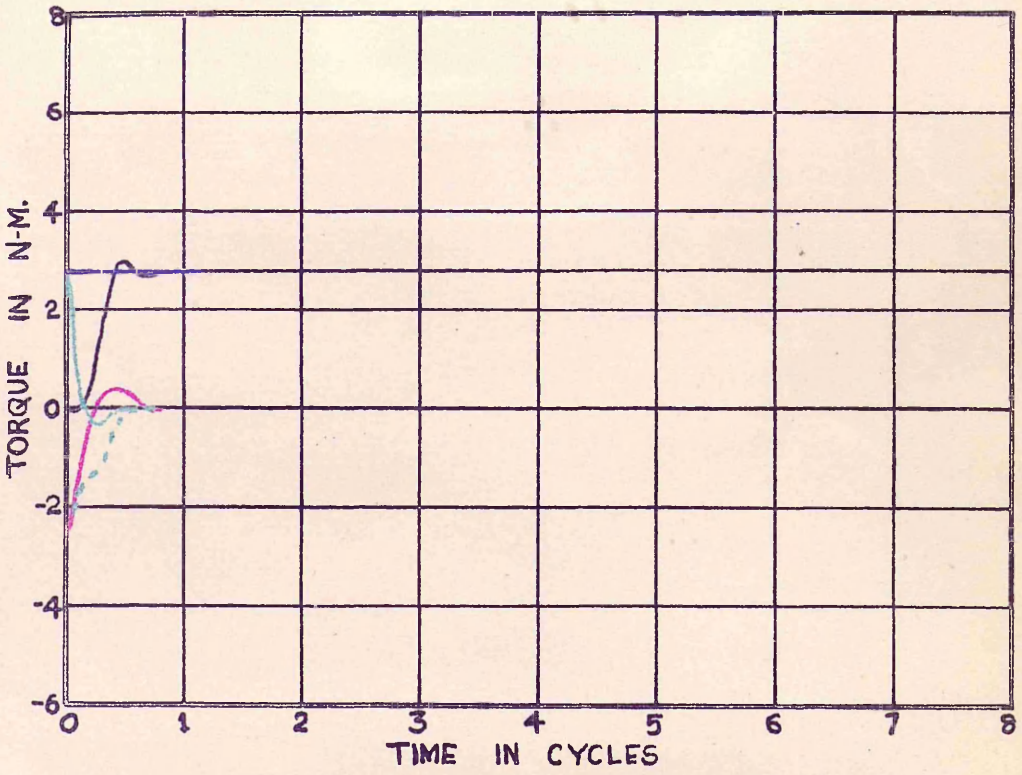

FIG. 4.6. COMPUTED CHARACTERISTICS FOR 89°14′ POINT-ON-WAVE WHEN THE PRINCIPAL LINE FREQUENCY COMPONENT IS ABSENT (140V)

[COMPARE WITH FIG. 4.1 (90° POINT-ON-WAVE)].

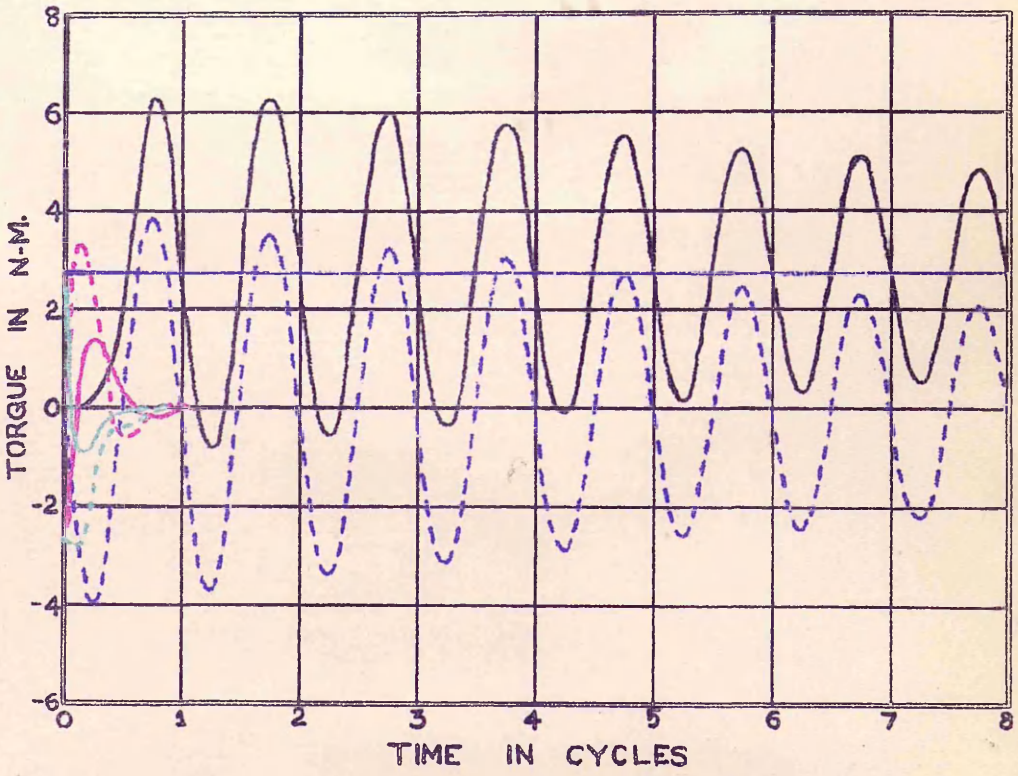

FIG.4.7. COMPUTED CHARACTERISTICS FOR 145°13' POINT-ON-WAVE WHEN THE 'SECONDARY' LINE FREQUENCY COMPONENT IS A MAXIMUM (140V)

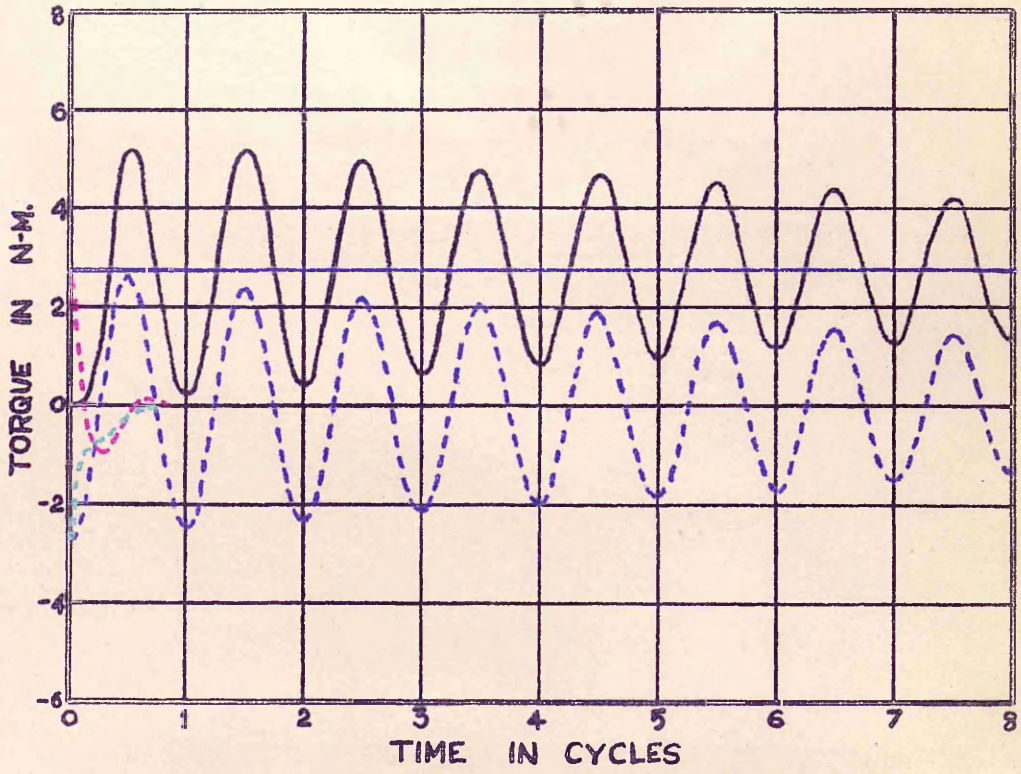

FIG.4.8. COMPUTED CHARACTERISTICS FOR 55°13' POINT-ON-WAVE WHEN THE 'SECONDARY' LINE FREQUENCY COMPONENT IS ABSENT (140 V)

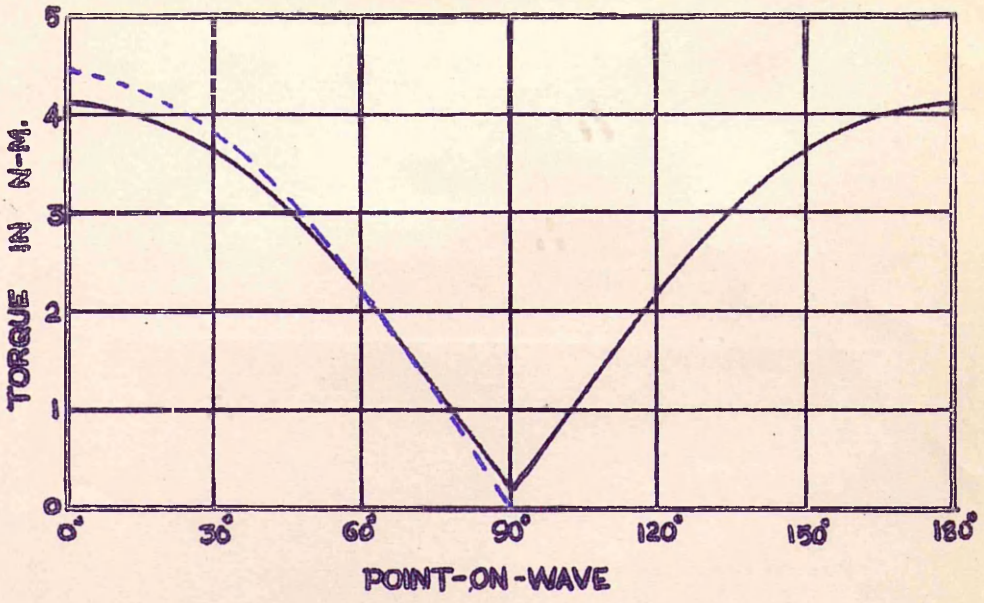

FIG.4.9. TRANSIENT COMPONENTS AT THE FIRST POSITIVE PEAK FROM COMPUTED RESULTS (140 V)

TABLE

POINT-ON-WAVE	TIME OF OCCURENCE OF FIRST POSITIVE PEAK
0°	13.3 MILLISEC.
30°	11.7
60°	10.4
90°	10.0
120°	16.5
150°	14.9
180°	13.3

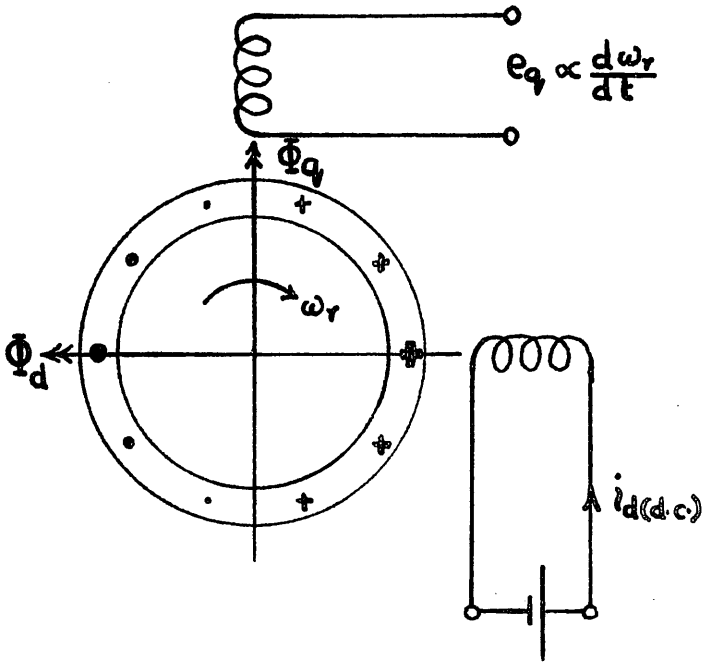

FIG.I.1. D.C. EXCITED DRAG-CUP INDUCTION GENERATOR

FIG. II.1. VIBRATION GENERATOR COUPLED TO ACCE-LEROMETER FOR CALIBRATION PURPOSES

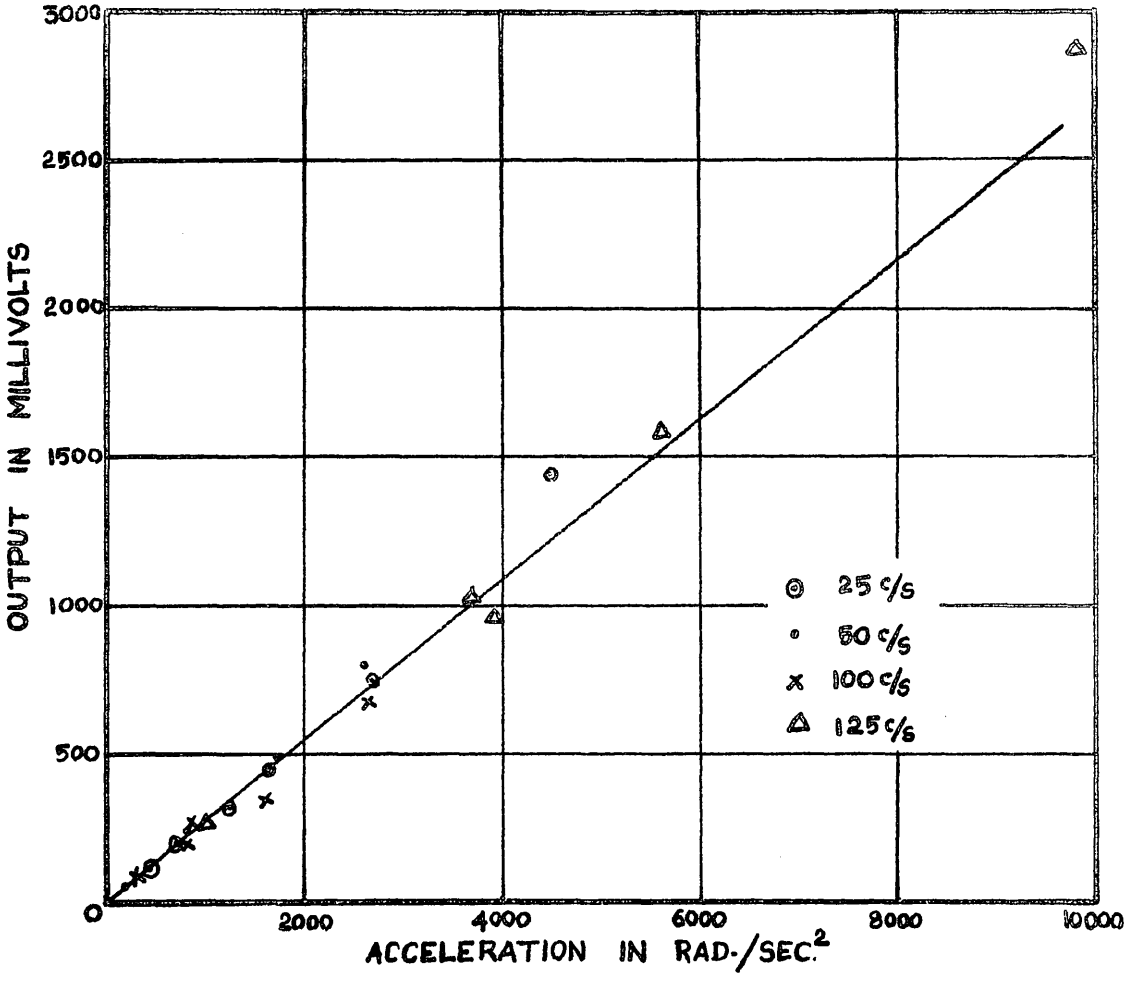

FIG. II.2. CALIBRATION OF THE ACCELEROMETER USING VIBRATION GENERATOR

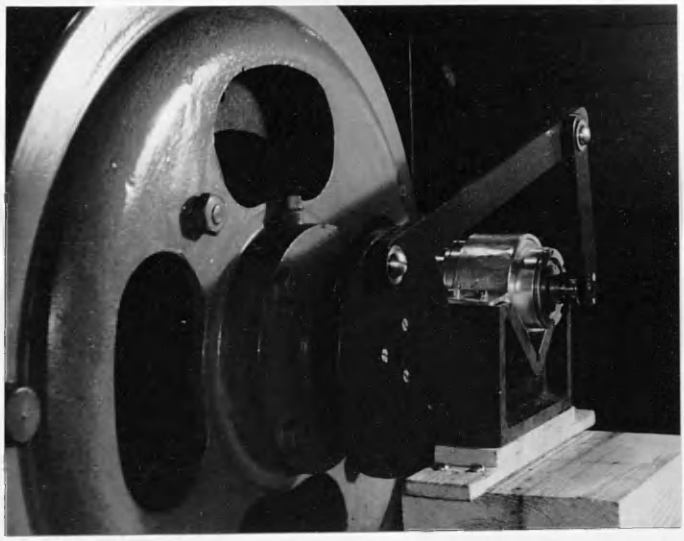

FIG. II.3. LINK MECHANISM TO PRODUCE OSCILLATORY MOTION

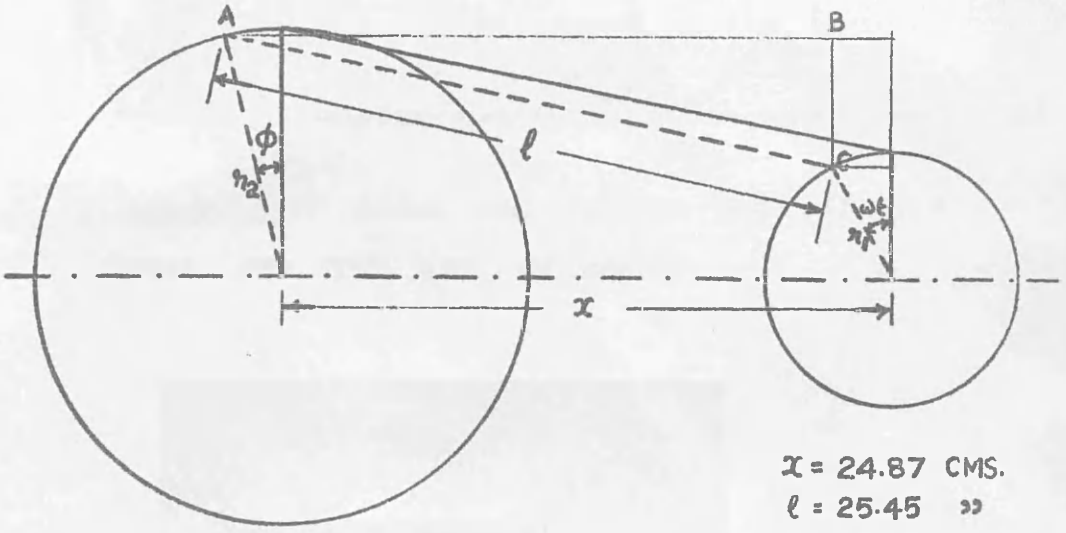

x = 24.87 CMS.
ℓ = 25.45 "
r_1 = 5.05 "
r_2 = 10.12 "

FIG. II.4. DESIGN DIMENSIONS OF THE LINK MECHANISM

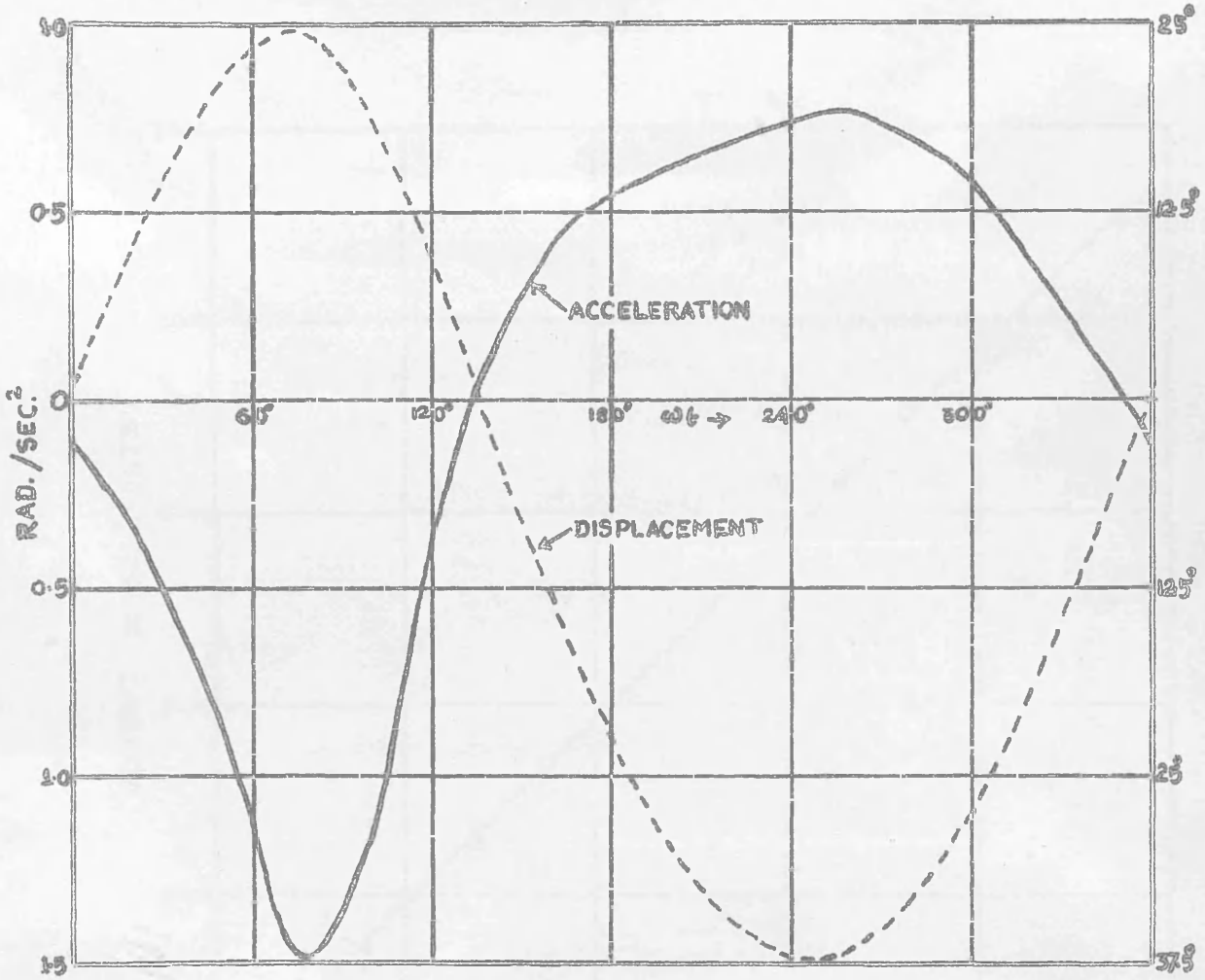

FIG. II. 5. DISPLACEMENT CURVE AND DERIVED ACCELERATION CURVE FOR THE LINK MECHANISM

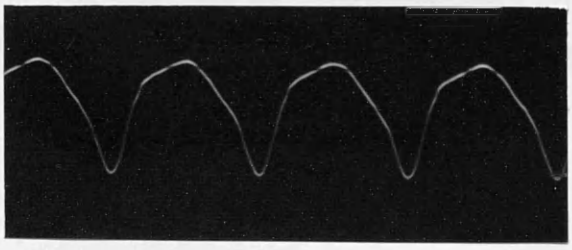

FIG. II 6. ACCELEROMETER OUTPUT WAVEFORM FOR THE LINK MECHANISM

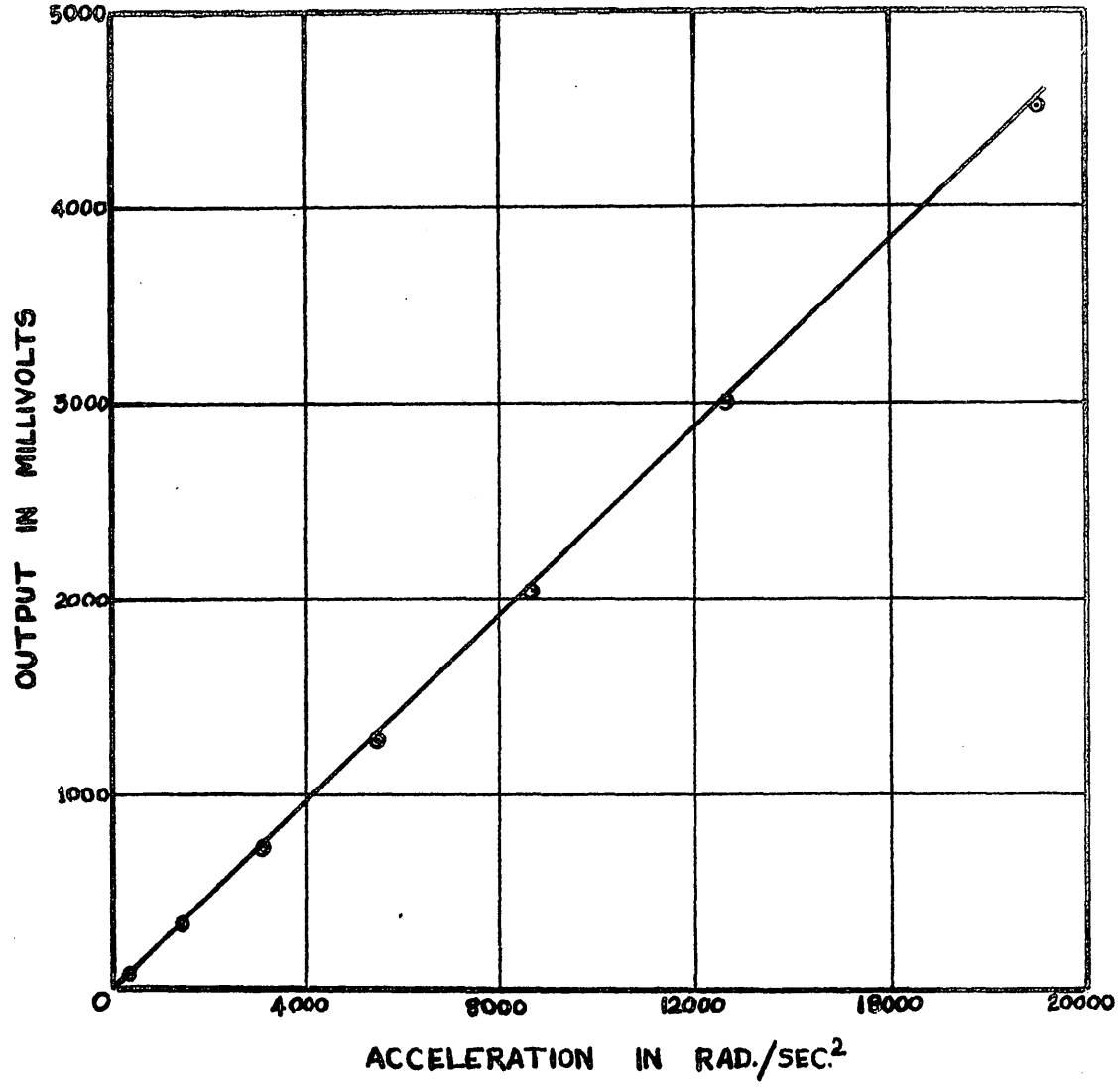

FIG. II. 7. CALIBRATION OF THE ACCELEROMETER USING LINK MECHANISM

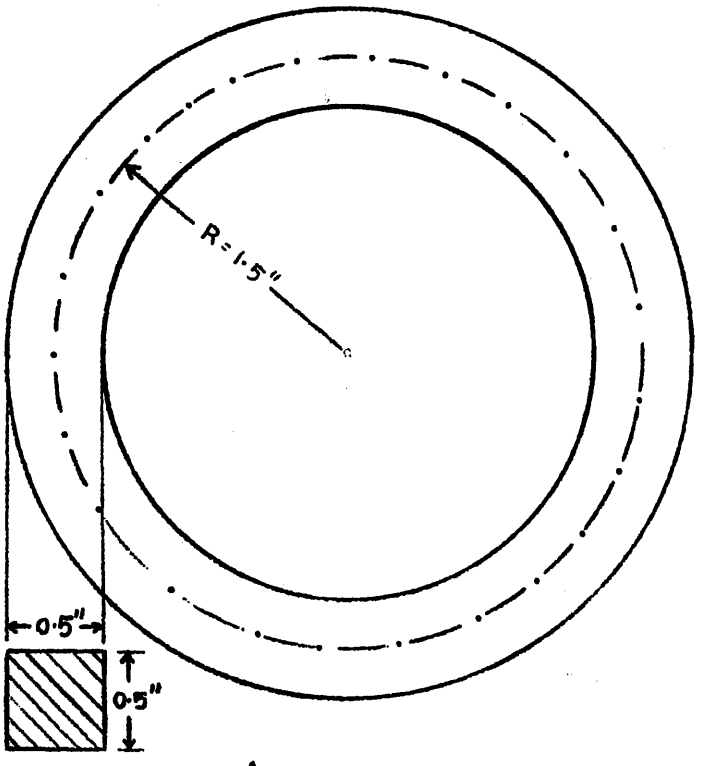

$$I = \frac{(0.5)^4}{12} = 52.08 \text{ INCH}^4$$

$$E = 30 \times 10^6 \text{ LBS/SQ. IN.}$$

FIG. III.1. DESIGN DIMENSIONS OF THE STIFFENING RING FOR THE STATOR REACTION DETECTING SCHEME

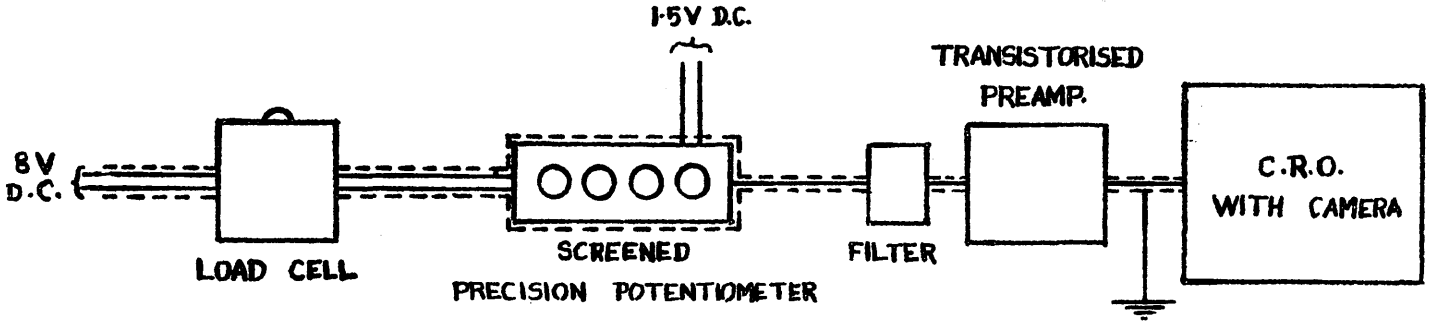

FIG. III.2. ELECTRICAL CONNECTIONS TO THE LOAD CELL